DISSERTATION

EFFECTS OF LUTEINIZING HORMONE RECEPTOR EXPRESSION LEVELS ON RECEPTOR AGGREGATION AND FUNCTION

Submitted by

Duaa Althumairy

Graduate Degree Program in Cell and Molecular Biology

In partial fulfillment of the requirements

For the Degree of Doctor of Philosophy

Colorado State University

Fort Collins, Colorado

Fall 2019

Doctoral Committee:

Advisor: B.George Barisas
Co-advisor: Deborah A. Roess

Debbie C. Crans
Charles W. Miller

ABSTRACT

EFFECTS OF LUTEINIZING HORMONE RECEPTOR EXPRESSION LEVEL ON RECEPTOR AGGREGATION AND FUNCTION

Luteinizing hormone receptors (LHR) are G protein-coupled receptors (GPCR) found primarily in female and male reproductive organs where they play a critical role in ovulation and sperm maturation, respectively, as well as maintenance of sex hormone production in both sexes. The role of oligomerization in LHR function is of considerable interest and not well understood. The oligomerization state of LHR has been suggested to have a significant role in signaling, desensitization and internalization of this receptor after activation by either luteinizing hormone (LH) or human chorionic gonadotropin (hCG) [2-8]. Overexpression of membrane proteins such as LHR may result in molecular crowding and may lead to increased protein oligomerization [10]. We hypothesize that LHR are present in the plasma membrane as constitutive small clusters or, alternatively, exist as dimers or mixture of monomers and dimers in the absence of hormone and then undergo varying degrees of aggregation after binding hCG. These differences in LHR organization depend on expression levels of LHR which may, in turn, affects LHR activity. In this project, we examined the effect of LHR expression levels on receptor oligomerization using polarized homo-transfer fluorescence resonance energy transfer (homo-FRET) methods to evaluate receptor interactions in cell lines stably expressing averages of 10,000 receptors per cell, 32,000 receptors per cell, 123,000 receptors per cell or 560,000 receptors per cell. In addition, we measured levels of cyclic adenosine monophosphate (cAMP), a second messenger involved in signal transduction which is produced in response to activation of LHR. This study demonstrated

that the oligomerization state of LHR depends on the expression level of LHR, *i.e.* the number of receptors per cell or the concentration of LHR per unit area. Although LHR appear as in dimers or oligomers in the plasma membrane when receptor expression levels are low, it is clear that, with increased expression levels, LHR are found in larger structures exhibiting lower values for initial anisotropy. The effect of hCG binding on LHR was dependent on the expression level of receptors in the absence of bound hormone. The greatest effect of hCG occurred in cells expressing low numbers of LHR per cell where receptors were able to undergo further aggregation in response to hormone binding. The effect of hCG on highly expressed LHR was negligible; LHR, when highly expressed, were already extensively aggregated and did not undergo measurable changes in their aggregation state. Deglycosylated human chorionic gonadotropin (DG-hCG) had modest effects on cells expressing comparatively few LHR per cell since these receptors were already present in small clusters. Depletion of plasma membrane cholesterol using MβCD caused a decrease in intracellular cAMP level accompanied by decrease in cluster size of LHR as expression level of LHR increased.

Together these results are important to our understanding of the roles that the expression levels of LHR, the oligomerization state of LHR and the plasma membrane play in LHR function. The organization of lipids in the bulk membrane and in membrane microdomains affects the ability of LHR to signal as does protein density, particularly when receptor crowding has occurred. These studies also suggest, more generally, that protein organization in the plasma membrane may function as an important pharmacological target that merits further exploration.

ACKNOWLEGEMENTS

First, I am very grateful to God for my wellbeing and good health which were essential to completing this doctoral dissertation. However, completing this doctoral dissertation would not have been possible without the support of several individuals.

I want to acknowledge and thank my co-advisors, Dr. Deborah Roess and Dr. George Barisas for supporting me throughout my research. Dr. Roess, with her immense knowledge, motivation and patience, supported me in difficult times especially while writing my dissertation. She shared her own dissertation despairs and provided a ray of hope in order to improve my knowledge and my overall wellbeing. She encouraged me, offered suggestions, motivated me and also provided valuable comments. Dr. George Barisas, also provided unwavering support together with his guidance on all the statistical and math areas. They helped me to realize that I can be as smart, knowledgeable, enthusiastic and energetic as they are. I could not have imagined having a better advisors and mentors for my Ph.D. studies. I would like to take this opportunity to thank my dissertation committee members, Dr. Crans and Dr. Miller, for their encouragement and insightful comments, as well as the tough questions that motivated me to broaden my study from different perspectives. I consider myself fortunate to have had such a team of smart, knowledgeable, helpful and kind people on my committee. I also thank the present and past laboratory members for the stimulating discussions and for enlightening me on my first glimpse of the research.

I would like to sincerely thank my family members, my parents, brothers and grandmother, for supporting me both spiritually while writing this dissertation and supporting my life in general.

I would not have made it this far without them. I want to give special thanks to my wonderful mother for her unconditional love and her support and prayers. In essence, she left everything behind and came to the United States to support and be close to me. Mum, you are the greatest woman I have ever known, and you will forever be in my heart. To my brother Abdullah, who came with me to America, I thank you for always being there for me. I cannot ask for a better brother. You stood with me through hard times, and for that, I will forever be grateful. I want to give heartfelt thanks to my wonderful father for believing in me and for his love, prayers and encouragement. I hope that I have made you proud. I want to express my gratitude to the four little stars in my family, Abdulaziz F, Abdulaziz A, Bander, and Amal. You are an inspiration to me. I love you to the moon and back. My sincere thanks also go to all my friends for always accepting nothing but the best from me. The memories that we share are phenomenal and I will cherish them forever.

Last, but not least, I wish to take this opportunity to express gratitude to the Saudi Arabian Cultural Mission (SACM) and King Faisal University. This work would not have been possible without their financial support. I also thank Colorado State University and Dr. Howard Lieber who admitted me to the Cell and Molecular Biology Program. I am also grateful for the kindness of the community of Fort Collins who helped ease my homesickness. And finally, my gratitude goes to all those who, either directly or indirectly, lent a hand in this entire project.

DEDICATION

To my parents and the soul of my grandmother Aljazi

TABLE OF CONTENTS

ABSTRACT ii

ACKNOWLEGEMENTS iv

DEDICATION vi

LIST OF TABLES x

LIST OF FIGURES xi

CHAPTER 1: PHYSIOLOGY OF LHR 1

1.1. Introduction 1

1.1.1. The G protein-coupled receptor superfamily 1

1.1.2. Biological action of the LHR 6

1.1.3. Clinical and pathological significance of the LHR function 11

1.1.2. Human LH (hLH) and hCG 17

1.1.3. DG-hCG is an hCG antagonist 22

1.1.4. Signal transduction by LHR 25

1.1.5. Crowding, oligomerization of LHR and receptor activity 32

1.1.6. The role of cholesterol in LHR function 37

CHAPTER 2: MEASURING THE SIZE OF PROTEIN CLUSTERS AND INTRACELLULAR cAMP 40

2.1. Measuring the size of protein clusters 40

2.1.1. Oligomerization of LHR 40

2.1.2. Fluorescence Resonance Energy Transfer (FRET) 44

2.1.3. Detection of homo-FRET using steady state anisotropy 45

2.2. Measurement of intracellular cAMP 50

2.2.1. Signal transduction and cAMP level are regulated by LHR 50

2.2.2. Measuring of cAMP 50

2.2.3. ICUE3, a FRET-based cAMP sensor 51

2.3. Hypothesis 56

2.4. Project Rationale 57

CHAPTER 3: METHODS AND MATERIALS 59
3.1. Introduction to methodological approach 59
3.2. Methods and Materials 61
3.2.1. Materials 61
3.2.2. Cell lines 62
3.2.3. Western immunoblotting for evaluation of plasma membrane expression of LHR 63
3.2.4. Sample preparation for flow cytometry sorting 64
3.2.5. Flow cytometry data analysis 65
3.2.6. Treatment of cells 67
3.2.7. Sample preparation for polarized homo-FRET experiments 67
3.2.8. Homo-FRET measurements 68
3.2.9. Experimental determination of the G factor 69
3.2.10. ICUE3 transient transfection for measurement of intracellular cAMP 70
3.2.11. Sample preparation for hetero-FRET studies of intracellular cAMP using ICUE3 70
3.2.12. Measurement of plasma membrane lipid order 71
3.2.13. Statistical analysis 72
CHAPTER 4: RESULTS AND DISCUSSION 73
4.1. The effect of expression level on cluster size of LHR. 73
4.1.1. Characterization of cell lines stably expressing LHR 73
4.1.2. Fluorescence anisotropy of LHR is dependent of receptor expression level 74
4.1.4. Effect of DG-hCG on LHR oligomerization 77
4.1.5. Effect of cholesterol depletion on receptor oligomerization 77
4.1.6. Effect of receptor oligomerization on cell plasma membrane lipid order 79
4.2. The effect of LHR expression levels as well as cluster size of LHR on receptor activity 80
4.2.1. High expression levels of LHR are associated with elevated intracellular cAMP 81
4.2.2. hCG promotes an increase in intracellular cAMP when receptor numbers per cell are low 82

4.2.3. DG-hCG alters LHR aggregation and reduces cAMP production..... 82
4.2.4. Effect of cholesterol depletion on cAMP production 83
CHAPTER 5: STUDY CONCLUSIONS AND FUTURE DIRECTIONS 111
REFERENCES 120
APPENDIX: DATA ANALYSIS FOR CALCULATING RECEPTOR NUMBER PER CELL 137
LIST OF ABBREVIATIONS..... 140

LIST OF TABLES

Table 1: hCG binding dissociation constatnt (K_D), binding capacity (B) and the number of LHR in per granulosa or luteal cells from different stages of the estrous cycle. 8
Table 2: Properties of fluorescent proteins used in these studies 55
Table 3: Summary of fluorescence parameters for FITC and eYFP excited at 488 nm. These quantities were used to convert the flow cytometer signal from FITC bead standards to numbers of eYFP and thus numbers of LHR-eYFP present on CHO cell lines. 100
Table 4: Summary of changes in fluorescence anisotropy upon fluorescence photobleaching for 15 minutes in unstimulated cells expressing different numbers of hLHR-eYFP per cell. 101
Table 5: Summary of change in initial anisotropy in cell lines expressing hLHR and treated with hCG. 102
Table 6: Summary of change in initial anisotropy in cell lines expressing hLHR and treated with DG-hCG. 103
Table 7: Summary of changes in intracellular cAMP as measured experimentally by changes in the CFP/YFPSE ratio. 110

LIST OF FIGURES

Figure 1: Generalized structure of GPCR. 4
Figure 2: Signal transduction pathways activated by GPCR. 5
Figure 3: RNA sequences for LHR found in 20 human tissues....9
Figure 4: Location and the biological role of LHR in the female and male reproductive systems 10
Figure 5: Amino acid sequence of human LHR. 15
Figure 6: Structure of hLHR showing three domains.. 16
Figure 7: Amino acid sequence of the common α-subunit and the unique β-subunit of hGC and hLH. 20
Figure 8: Interactions between LHR and hCG.. 21
Figure 9: LHR binding and cAMP production in response to DG-hCG.. 24
Figure 10: Sketches of differences in the interactions of hLH and hCG with the hinge region of LHR. 29
Figure 11: Schematic representation of *cis*-activation and *trans*-activation of LHR. 30
Figure 12: Signaling pathways regulated by activation of LHR....31
Figure 13: Binding assay and cAMP assay for WT FSHR and mutant FSHR (A189V). 35
Figure 14: cAMP level induced by hCG binding to cell populations expressing increasing numbers of receptors per cell. 36
Figure 15: Model of lipid organization in lipid raft microdomains including cholesterol's structure and relationship to the lipid bilayer. 39
Figure 16: Schematic representation of cis-activation and *trans*-activation leading to LHR clustering. 43
Figure 17: FRET diagram. The donor fluorophore is excited, *i.e.,* reaches the S1 state, and then relaxes to the lowest excitation level. 48
Figure 18: Principle of homo-FRET showing receptors excited with vertically polarized light…49
Figure 19: Excitation and emission spectra of a CFP-YFP FRET pair in ICUE3. 53
Figure 20: ICUE3 structure and function....54

Figure 21: Fluorescence anisotropy as function of time of fluorescence photobleaching for up to 5 minutes. 85
Figure 22: hLHR gene-containing plasmid used to generate stable hLHR-eYFP expressing cell lines. 86
Figure 23: Flow cytometry data.. 87
Figure 24: Schematic representation of the experimental setup used for homo-FRET measurements.. 88
Figure 25: Schematic representation of the experimental setup used for hetero-FRET measurements. 89
Figure 26: Experiments to confirm transfection of CHO cells with the hLHR-eYFP plasmid. 90
Figure 27: Simulated data for fluorescence anisotropy upon photobleaching. 91
Figure 28: Fluorescence anisotropy upon fluorescence photobleaching for 15 minutes for CHO cells with 10k hLHR per cell. 92
Figure 29: Correlation between initial anisotropy and initial fluorescence intensity for untreated cells. 93
Figure 30: Correlation between anisotropy value and fluorescence intensities during photobleaching for untreated cells 94
Figure 31: Fluorescence anisotropy during photobleaching for 15 minutes in cells that express hLHR at different levels. 95
Figure 32: Correlation between anisotropy values and fluorescence intensities during photobleach in cells treated with 100nM hCG. 96
Figure 33: Initial fluorescence anisotropy values for four cell lines in response to different hormone concentrations. 97
Figure 34: Initial fluorescence anisotropy for four cell lines in response to different DG-hCG concentrations. 98
Figure 35: Initial fluorescence anisotropy values for cells expressing various numbers of LHR per cell after treatment with MβCD. 99
Figure 36: Fluorescence emission of Di-4-ANEPPDHQ labeled CHO cell membranes. 104
Figure 37: Fluorescence emission of Di-4-ANEPPDHQ labeled the four groups of cells expressing various numbers of LHR per cell.). 105

Figure 38: Relationship between numbers of LHR per cell and levels of cAMP per cell in untreated cells. 106
Figure 39: Effect of hCG on intracellular cAMP 107
Figure 40: Effect of DG-hCG on production of cAMP in cells expressing different numbers of LHR per cell. 108
Figure 41: Effect of cholesterol depletion on production of cAMP in cells expressing different numbers of LHR per cell. 109
Figure 42: Relationship between the size of LHR clusters and production of cAMP in cells expressed low level of LHR. 116
Figure 43: Relationship between the size of LHR clusters and production of cAMP in cells expressing lower numbers of LHR per cell. 117
Figure 44: LHR expression levels affect the cluster size and activity of LHR in response to hCG. 118
Figure 45: LHR expression levels affect the cluster size and activity of LHR in response to DG-hCG. 119

1. CHAPTER 1: PHYSIOLOGY OF LHR

1.1. Introduction

1.1.1. The G protein-coupled receptor superfamily

GPCR, also known as seven transmembrane domain receptors, represent the largest family of membrane proteins in the mammalian genome [11, 12]. GPCR mediate cellular responses to diverse molecules such as hormones, neurotransmitters, peptides, tastants, odorants and other mediators [13]. The GPCR receptor superfamily contains about 800 members in humans [14-16]. GPCR are involved in the regulation of physiological processes and in transferring signals from cell exterior to the cell cytoplasm through common changes in the structure of their transmembrane domains [17]. Furthermore, GPCR have emerged as targets for the innovative drugs that are available today in clinical trials or that are under development for clinical applications [16, 18]. It estimated that 50% of clinically prescribed drugs are targeted to GPCR [19, 20]. Together, these reasons support the importance of studying GPCR structure and functional properties.

Human GPCR can be classified into six families; rhodopsin, secretin, adhesion, glutamate, frizzled and taste receptors (T2R), based on sequence homology and phylogenetic analysis [15, 21, 22]. They function as either peptide, carbohydrate, nucleotide, amino acid, neurotransmitter, ion channels, protein or lipid receptors, based on their endogenous ligand type [16]. The rhodopsin subfamily is the largest and most diverse group of GPCR [15, 21].

In general, the life cycle of GPCR includes synthesis in the nucleus, modifications in the endoplasmic reticulum, maturation in the Golgi Apparatus, delivery and insertion into the plasma

membrane. Upon ligand interaction and activation, signal transduction and then internalization is followed by recycling of GPCR back to the membrane or destruction through lysosomes [17].

Structurally, all the GPCR are composed of a single polypeptide chain with seven hydrophobic transmembrane (7TM) α-helices, an extracellular N-terminus and a cytoplasmic C-terminus **(**[13]; **Figure 1)**. However, they exhibit variations in size, in the structure of extracellular and intercellular loops [15], in receptor life cycle, the site of interaction with ligands, in the cluster size of the GPCR before and after binding to ligand and in the mechanism of signal transduction [17, 21].

As their name implies, GPCR interact with heterotrimeric G proteins. G proteins are members of the GTP-binding proteins family and have the ability to bind guanosine triphosphate (GTP) and guanosine diphosphate (GDP). A heterotrimeric G protein consists of three subunits α, β and γ. At least 16 different types of α subunits, 5 β subunits and 11 γ subunits in mammalian tissues have been identified in mammalian tissues. Each subunit leads to activation of different effectors downstream. Collectively, in an inactive state, heterotrimeric G proteins exist as a complex of α, β and γ subunits in which GDP is bound to α subunit at its guanine nucleotide binding site **(Figure 2A)**. When in an active state, GPCR have undergone a conformational change that drives exchange of GDP for GTP. This GDP-GTP exchange also results in the dissociation of the heterotrimeric G protein from its GPCR and separation of the G protein trimer into an α subunit and the β-γ dimer. Activated α subunits can trigger a variety of downstream effectors depending on the type of α subunit that has been stimulated. For instance, α_s activates adenylate cyclase (AC), the enzyme that convert adenosine triphosphate (ATP) to cAMP. cAMP, in turn, activates protein kinase A (PKA) which plays a role in phosphorylation and activation of downstream effectors [20, 23], as shown in **(Figure 2B)**. In contrast, α_i is an inhibitor of AC. The α_t subunit activates

phosphodiesterase (PDE) that catalyzes the breakdown of cyclic guanosine monophosphate (cGMP) to guanosine monophosphate (GMP) and leads to closure of a cGMP-dependent channel **(Figure 2C)**. Phospholipase C (PLC) is activated by α_q and breaks down to phospholipid phosphatidylinositol 4,5-bisphosphate (PIP_2) into diacylglycerol (DAG) which stimulate protein kinase C (PKC) and cytosolic inositol triphosphate (IP_3) leading to release of Ca^{+2}. Ca^{+2} has roles in the downstream signaling cascade (**Figure 2D)**. Activated β-γ subunits also have downstream effects on K^+ channels, different proteins kinases or the activity of AC or PLC [13, 21, 24].

GPCR have been shown to function, after binding ligand, as monomers, dimers or oligomers. Interestingly, ligand binding to the receptor can induce formation of larger receptor complexes, smaller receptor complexes or have no effect on oligomerization, depending on the receptors in question [25]. Therefore, no generalizations can be made regarding the effect of ligand on the oligomerization state of GPCR and, in practice, it is important to study the effect of ligand on GPCR oligomerization for each individual receptor.

The oligomerization state of GPCR is clearly an unresolved issue. Emerging results indicate that GPCR can form dimers or oligomers in an early stage after biosynthesis and this will subsequently play an important role in receptor's life cycle [26]. The concept of GPCR existence as dimers or oligomers may also be important in development of drugs targeting a specific receptor and its ability to undergo changes in its oligomerization [27].

Despite the importance of receptor oligomerization and its relevance to clinical areas, there are only a small number of all GPCR that have been studied in detail. That promotes interest in new GPCR that might have potential as drugs targets to treat diseases that are not successfully treated using current drug therapies. LHR, which are the focus of studies described in this dissertation, are examples of GPCR that are classified as members of the rhodopsin family [28]

and, in addition, belong to the glycoprotein hormone receptor subfamily [2]. LHR are of both physiologic interest and clinical interest as discussed later in this dissertation.

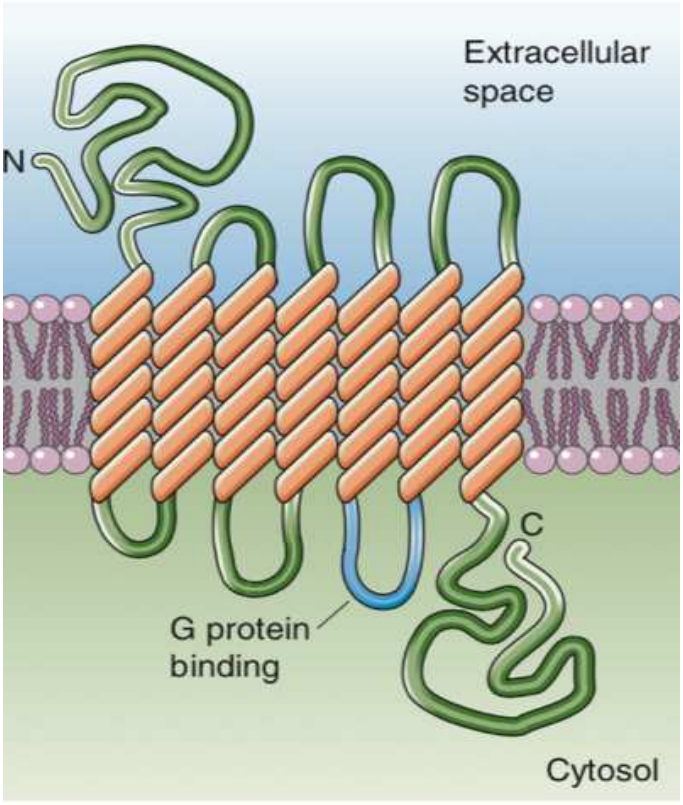

Figure 1: Generalized structure of GPCR [13].

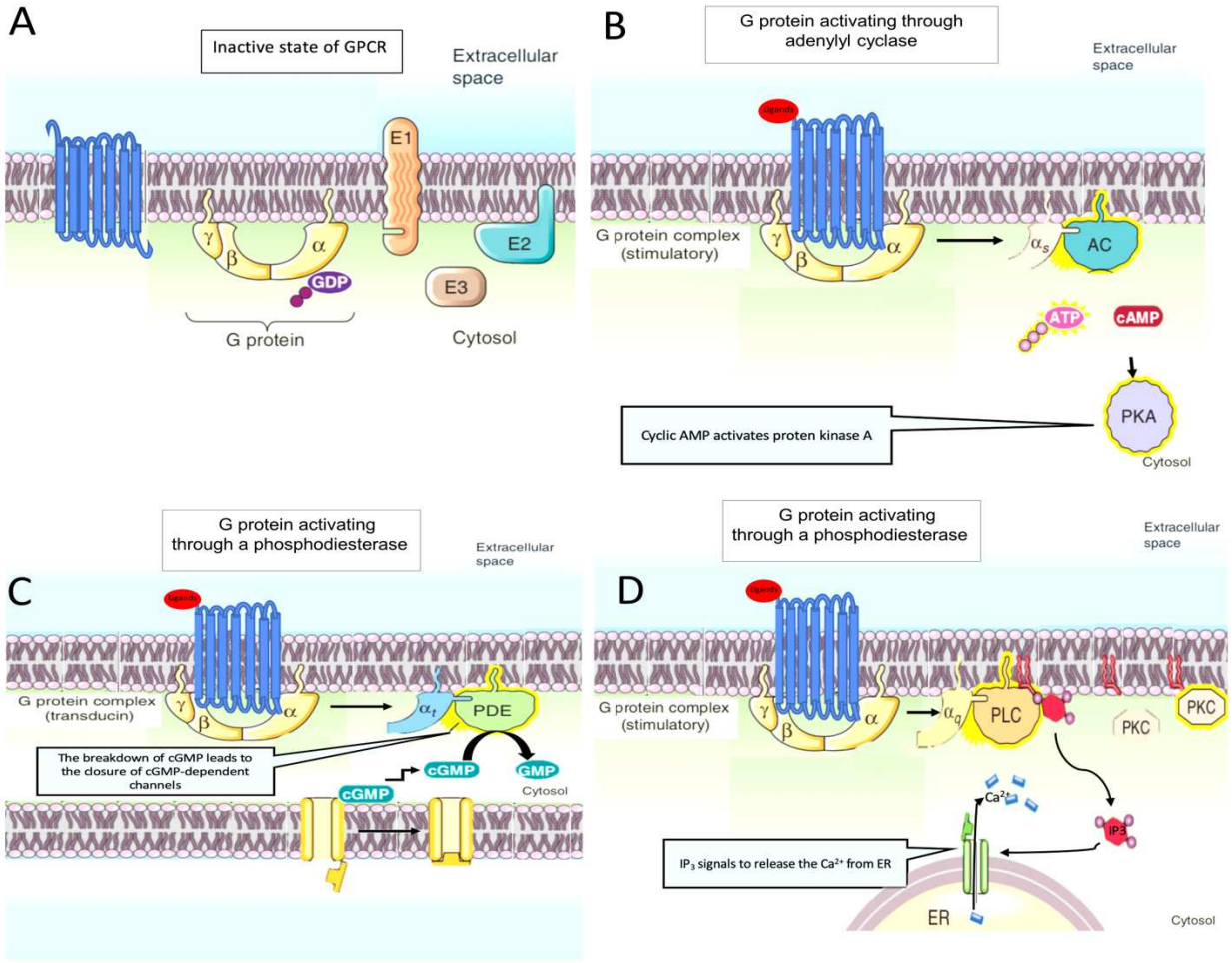

Figure 2: Signal transduction pathways activated by GPCR. Figure 2A shows an inactive receptor. No ligand is bound to the receptor and associated G proteins exist as a trimeric complex made up of an α, β and γ subunit. Figure 2B shows an active receptor in which the receptor has bound a ligand. α_s has been released from the G protein and is activating adenylate cyclase. Figure 2C shows an active receptor which has activated α_t which, in turn, activates PDE and hydrolyzes cGMP leading to closure of the cGMP-activated channel due to low concentrations of cGMP. Figure 2D shows an active receptor that activates α_q which in turn activates PLC, converting PIP_2 to IP_3 and DAG. IP_3 and DAG lead to release of Ca^{2+} and activation of PKC, respectively. Modified from W. Boron and E. Boulpaep [13].

1.1.2. Biological action of the LHR

LHR are critical to reproduction in both mammalian sexes [29]. The receptors are mainly present in gonadal cells including testicular Leydig cells and Sertoli cells in male and target cells in the female follicle and corpus luteum of the ovary [2, 28-31]. LHR are present more specifically in female in the theca, interstitial, and granulosa cells of the follicle [2] as shown in **Figure 4A**. LHR have also been identified in a number of non-gonadal cells such as cells from the prostate [32], breast [33], human uterus [4, 28], brain [2], human skin [34] and the adrenal cortex [33, 35, 36] as shown in **Figure 3**. The role of LHR in these extragonadal tissues is unclear.

The main biological role for the LHR in male puberty and the adult male is regulating the production and secretion of androgens that induce development of the secondary sex characteristics and stimulating sperm maturation [37, 38]. LHR in Leydig cells are also expressed during fetal life where they are critical to the development of the external male genitalia. The LHR in fetal Leydig cells are activated by maternal hCG. After puberty, testicular LHR are stimulated by pituitary LH [4, 38, 39].

In female, LHR are found in theca cells and differentiated granulosa cells in the follicle and on luteal cells in the corpus luteum [38]. The LHR on granulosa and theca cells can promote the development of the follicle, enhance steroidogenesis and trigger ovulation **(**[4, 40]; **Figure 4A)**. Active LHR on luteal cells can promote ovulation and induce formation of corpus luteum (CL) which maintains the secretions of estrogen and progesterone. During female fetal development, LHR are not detectable. Expression begins, and only at very low levels, in neonates [38]. In puberty, a pituitary LH surge causes initiation of the first ovarian cycle and menstruation [41].

Pituitary LH and follicle stimulating hormone (FSH) are secreted from the anterior lobe of the pituitary gland in response to activation of gonadotrophs expressing gonadotropin releasing hormone receptors (GnRHR) by GnRH from the hypothalamus. LH and FSH promote maturation of the follicle in the ovary and increase production of estrogen [39, 42]. Due to high levels of estrogen made during folliculogenesis, a surge of LH released from the anterior pituitary promotes the rupture of the pre-ovulatory follicle and ovulation, *i.e.*, release of the ovum [38, 39]. The follicle then forms a corpus luteum which maintains secretion of estrogen and progesterone, both of which stimulate endometrial growth. If there is a pregnancy, hCG synthesized by syncytiotrophoblast cells of the placenta will sustain corpus luteum function [43]. However, the non-pregnant corpus luteum rapidly reduces its production of estrogens and progesterone and this leads to the shedding of the endometrium in menstruation [44]. It is notable that the number of LHR are not constant during the ovarian cycle in follicular or luteal cells, as shown in **Table 1**. Thus, the number of LHR may provide information about the health of the reproduction system.

In summary, in males and normally cycling females, LHR bind LH, an anterior pituitary hormone, leading to synthesis of testosterone in males and hormone synthesis and ovulation in females. In addition, LHR bind hCG, a placental hormone, that helps maintain progesterone levels during the first trimester of pregnancy and stimulates fetal Leydig cell production of testosterone [45]. The normal function of the reproductive system in mammals is dependent on LHR and pulsatile release of LH, which act to regulate gonadal function in both sexes. Numerous mutations to inactivate or hyperactivate LHR have been identified and are associated with gonadal pathology related to reproductive disorders, endocrine-based diseases, metabolic changes or sex-dependent disease. Together these observations suggest that LHR plays an essential role in mammalian health. The significant of the LHR in clinical trials will be detailed in the following sections.

Table 1: hCG dissociation constants (K_D), binding capacity (B) and the number of LHR in per granulosa or luteal cells from different stages of the estrous cycle.

Cell type and oestrous phase	Binding affinity, K_D (10^{-10} mol l^{-1})	Binding capacity, B (pmol l^{-1})	Mean number of available receptors per viable steroidogenic cell
Granulosa cells late follicular phase ($n = 3$)	3.38 ± 0.53^{b}	68.9 ± 15.05^{d}	$76{,}600 \pm 13{,}420^{c}$
Luteal cells CL1 days 1–3 ($n = 3$)	1.46 ± 0.19^{a}	6.42 ± 1.35^{ab}	7300 ± 740^{a}
Luteal cells CL2 days 5–7 ($n = 3$)	1.66 ± 0.27^{a}	8.55 ± 0.44^{b}	$13{,}000 \pm 1080^{b}$
Luteal cells CL3 days 8–10 ($n = 3$)	1.79 ± 0.64^{a}	13.83 ± 1.87^{c}	$28{,}400 \pm 3530^{d}$
Luteal cells CL4 days 12–14 ($n = 3$)	1.44 ± 0.24^{a}	6.07 ± 1.04^{a}	$17{,}400 \pm 3150^{c}$

Data are presented as means ± SEM; means with different superscripts are significantly different ($p<0.05$) as shown by the analysis of variance followed by LSD (less significant difference analysis). These data were obtained from Dorota *et al*. [46].

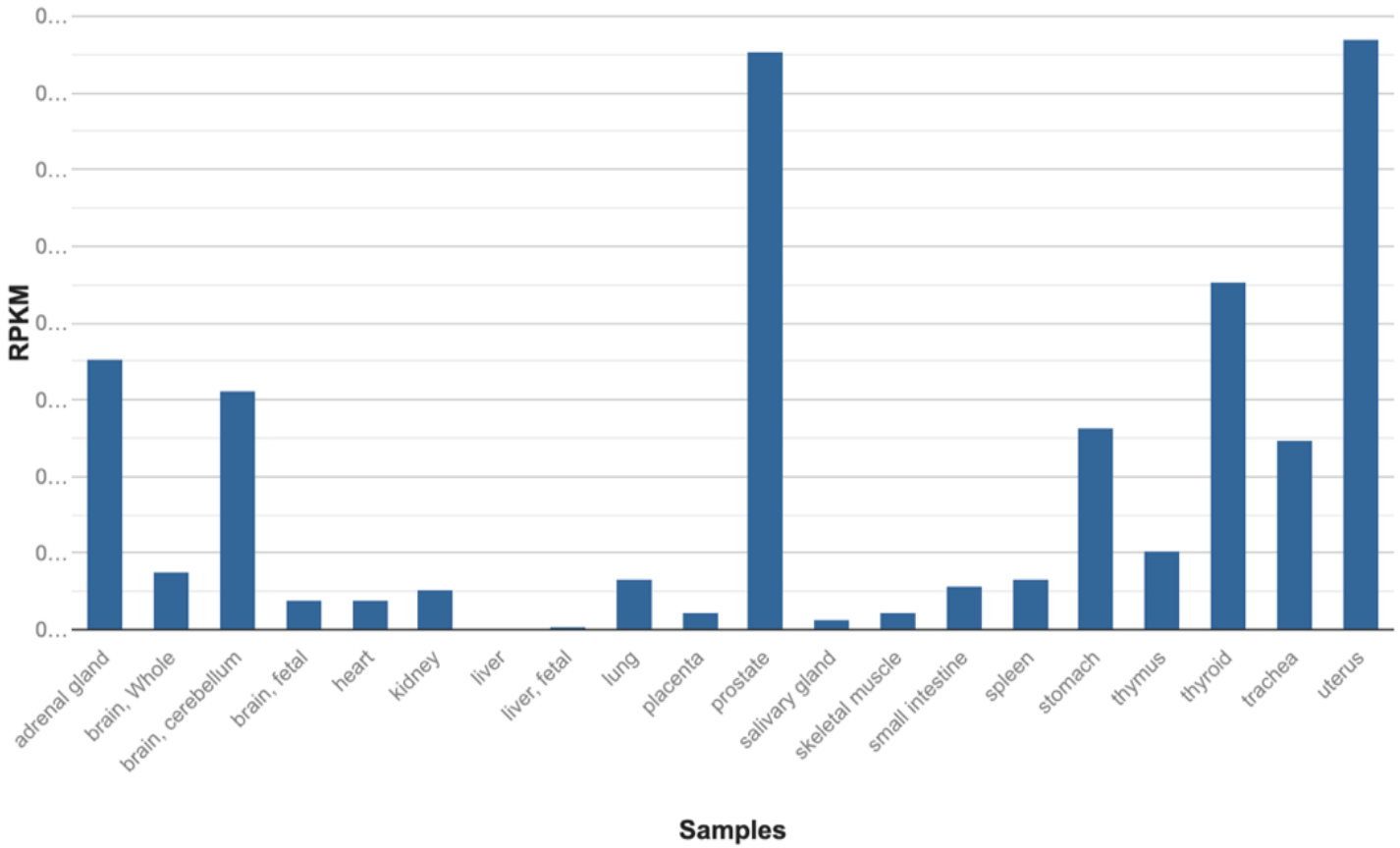

Figure 3: RNA sequences for LHR found in 20 human tissues [6]. The Y-axis label indicates “Reads Per Kilobase Million” .

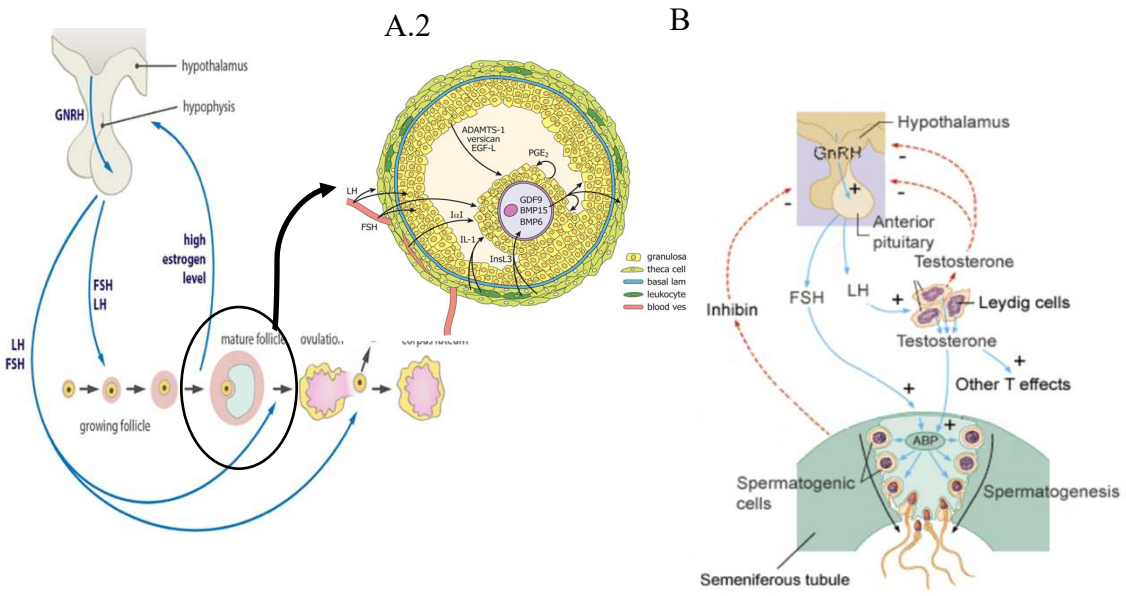

Figure 4: Location and the biological role of LHR in the female and male reproductive systems. In females, LH is secreted from the anterior lobe of pituitary gland in response to an increase in estrogen levels (left panel). Active LHR regulate the maturation of follicle, rupture of the follicle to release an oocyte and maintain the corpus luteum which synthesizes and releases progesterone [47]. A cross section through the follicle shows LHR expressed in theca cells, granulosa cells, and interstitial cells [48]. In males (panel on right), LH is secreted from the anterior lobe of pituitary leading to synthesis of testosterone and spermatogenesis [49]. LHR are expressed in Leydig and Sertoli cells in the testis.

1.1.3. Clinical and pathological significance of the LHR function

Signal transduction by LHR in both mammalian sexes is essential for successful reproduction. LHR have natural-occurring mutations and polymorphisms that cause disorders in sexual development and defects in reproductive function [50, 51]. In males, inactivating mutations within specific LHR domains result in failure of testicular Leydig cells to differentiate, leading to Leydig cell hypoplasia (LCH) [52, 53]. Likewise, inactivating mutations in specific LHR domains in females result in amenorrhea and anovulation [54]. In contrast, activating mutations in specific LHR domains can cause the receptor to be constitutively activated leading to familial male-limited precocious puberty (FMPP; [50, 55]). Clinically, patients with FMPP present with precocious puberty, Leydig cell hyperplasia, high levels of testosterone and low levels of gonadotropins [55].

In addition to effects of LHR mutations on gonads, there are a number of human diseases related to LHR including Alzheimer's disease (AD) [56-61], ovarian cancer [33, 62-64], breast cancer [65-68], prostate cancer [33, 69, 70], endometrial carcinomas [71-74], polycystic ovary syndrome [35, 40, 75, 76], uterus leiomyoma [33, 77], adrenocortical dysfunction [36], obesity [39] and Cushing's syndrome [78, 79]. Each has been associated with over-expression of LHR and high secretion of LH. Furthermore, endometriosis is associated with low-expression of LHR [33, 73].

Evidence obtained from several studies suggests that dysregulation of LHR may affect the pathogenesis of AD. An *in vivo* study used transgenic knockout LHR mice to provide evidence that ablation of LHR significantly reduces the β-amyloid peptide (Aβ) load found in AD [56-60]. Ovarian cancer and other cancers are associated with over-expression of LHR. This LHR overexpression and activation of LHR signaling may induce cell proliferation [80] leading to ovarian cancer or other cancers [33, 62-68]. Alternatively, ovarian cancer may be caused by

receptor overexpression leading to an increase in the cluster size of LHR. This may result in activated receptors, increased signaling by those receptors, increased cell proliferation and evasion of apoptosis by cancer cells. Thus, regulation of LHR expression may provide a new strategy for targeted cancer therapy. Finally, studies have found that skin changes in anovulatory and postmenopausal women can occur due to elevated of LH levels [34, 81, 82] which may result from an increase in expression of LHR in the skin of these women.

Therefore, studying and understanding LHR expression level, oligomerization, and the function of LHR may provide new pharmacological approaches for use in treatment of endocrine-related disorders. Furthermore, it is important to know the structure of intact LHR and to understand the human disorders related to LHR functions. Several mutations in LHR that naturally occur may lead to either loss or gain of function depend on how these mutations affect the conformation of receptors and LHR function [7, 31]. These mutations can lead to a lack of pubertal development and amenorrhea in females and impaired of spermatogenesis and infertility in males [2, 4, 39].

1.1.4. Structure of LHR

LHR are members of a superfamily of GPCR. LHR activate G proteins to initiate intracellular signaling as has been discussed above. LHR also belong to the subfamily of the glycoprotein hormone receptors (GPHRs). LHR bind glycoproteins hormones, LH and hCG, and are then activated [2, 28, 83].

The mature human LHR consists of 699 amino acids with a molecular mass about 85,000 Da [38, 84]. Human LHR are coded by a single copy gene that consists of 11 exons and 10 introns and is located on the short arm of chromosome 2 [85]. Exons 1-10 encode for extracellular domains and exon 11 encodes for the 7TM and the intercellular domain [4, 38, 76, 86].

LHR are synthesized as a single polypeptide chain that can be divided functionally into three domains as shown in **Figures 5** and **6** [2, 4, 28]. The large and divergent extracellular domain (ECD) is the glycosylated N-terminal domain with 340 amino acid residues. The ECD contains several leucine rich repeats (LRRs) flanked by cysteine-rich regions and a hinge region. LH or hCG bind LHR at the ECD with high affinity [2, 45]. The ECD is believed to be involved in hormone binding and hormone specificity via LRRs that initiate the interaction with its corresponding hormone [5, 7, 45, 84, 86-89]. Also, the hinge region that is located in the ECD at the juncture with the TM domains is responsible for initial signal transduction as it links to the TM domains [2].

A hinge region is coded by exon 10 and located in the ECD is crucial for differentiation of LHR signal transduction in response to hLH and hCG. The C-terminus of the hinge region sulfate tyrosine 331 is believed to be critical for hLH binding stability [5, 38] and plays a key role in differentiation of signaling transduction between hLH or hCG [5, 7]. Several studies suggested that deletion of exon 10 abolishes hLH, but not hCG, activity. Other studies have found distinct responses triggered by hLH or hCG binding to the extracellular domain [5, 7, 45, 86]. Although hLH and hCG bind the same receptor, they interact with different receptor sites and can cause different responses by target proteins in the intracellular pool.

The second domain is highly conserved and contains 7TM α helices connected by three extracellular loops (ECLs) and three intracellular loops (ICLs) [2, 4, 83, 90]. Each α helical segment has about 25 to 35 amino acids residues [2, 38]. This second domain has cysteine residues in the first and second extracellular loop that play a role in stabilizing the structure of seven transmembrane α helices by forming an intramolecular disulfide bridge [28]. Conformational changes occurring in the 7TM, after being activated by hormone, translate to interactions between

LHR and G proteins on the intracellular surface and generate the signal [5, 91]. Mutations in the 7TM segment cause LHR to be constitutively active, suggesting that it is essential for LHR activity [2].

In addition, the 3rd and 6th transmembrane α helix and carboxyl portion of ICL2-3 may have effects on activation of G proteins in the intracellular side [38, 84]. However, ICL2 is believed to have a fundamental role in maintaining the LHR in an inactive conformation and block the signaling cascade [4]. Conformational changes occurring in 7TM after being activated by hormone lead to interactions between receptors and G protein on the intracellular membrane surface and generates the signaling [5, 91].

The third domain is an intracellular C-terminal cytoplasmic tail (ICD) with 70 amino acids that initiates downstream signaling [2, 83]. This domain is the most divergent among the three domains and plays an important role in regulating the trafficking of receptors from endoplasmic reticulum to plasma membrane as well as receptor internalization [2]. It contains several threonines and serines that can be phosphorylated by PKA in the intracellular pool [28, 38]. The intracellular C-terminal region together with intracellular loops interacts with G proteins when LHR is activated by hormone [2, 4].

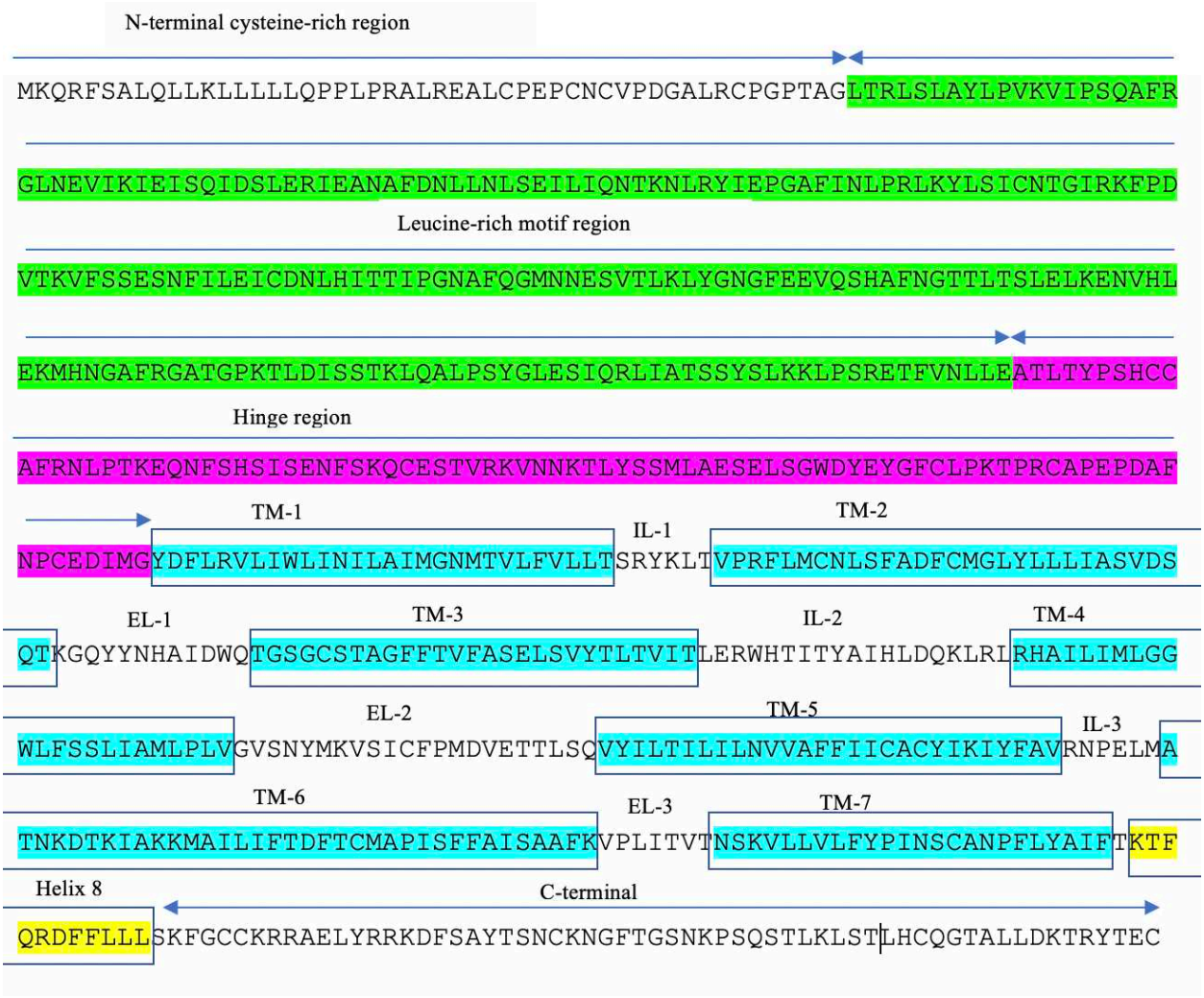

Figure 5: Amino acid sequence of human LHR. Different portions of the LHR are indicated, including the cysteine-rich N-terminus of the LRR and the hinge region in the extracellular domain. Also shown are the seven transmembrane helices connected by 3 intracellular loops and 3 extracellular loops and followed by the C-terminal tail [92].

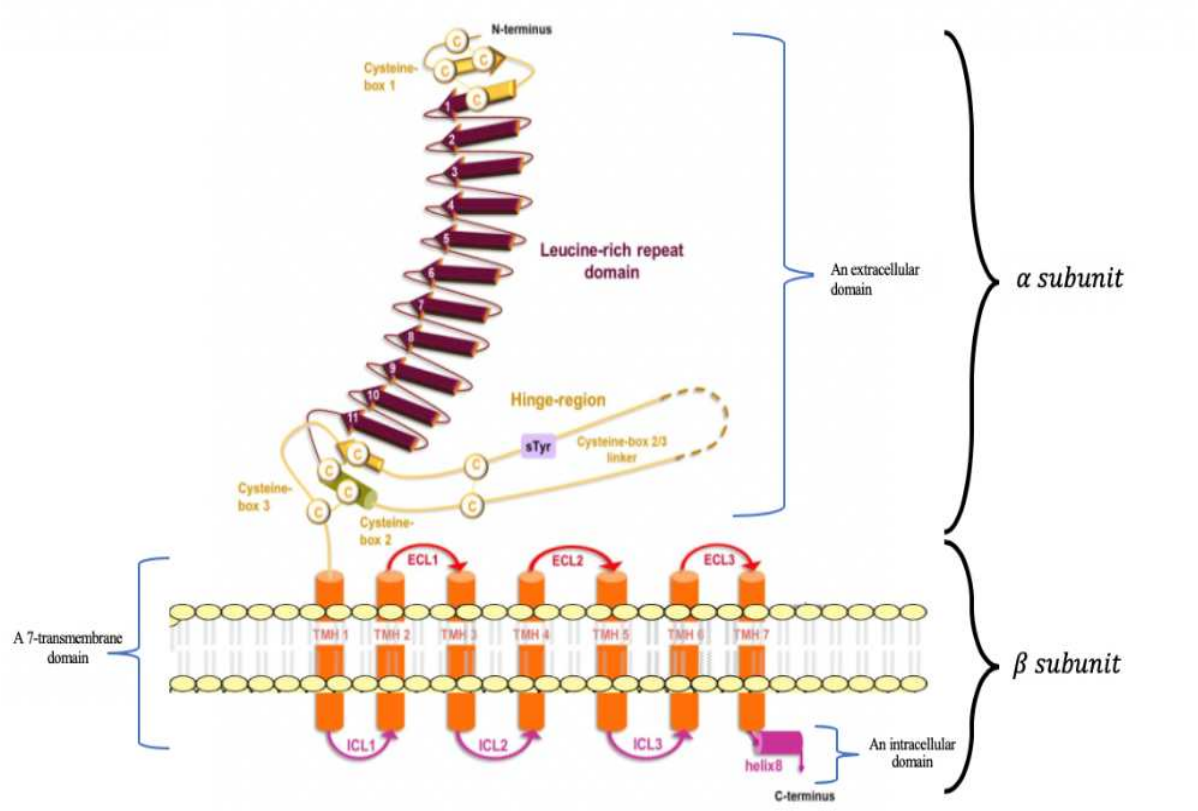

Figure 6: Structure of hLHR showing three domains. The large extracellular domain is a glycosylated N-terminal domain which contains the site for ligand binding. The transmembrane domain spans the phospholipid bilayer with seven segments connected by three extracellular loops and three intracellular loops. The intracellular domain is a C-terminal cytoplasmic tail which is involved in activating G proteins. Modified from [9, 93].

1.1.2. Human LH (hLH) and hCG

LHR are target receptors for the pituitary-produced hormone LH and a placenta-secreted hormone hCG [4, 94]. Both hormones are members of the glycoprotein hormone family and bind with high affinity to LHR found in the plasma membrane of target tissue cells ([95, 96]; **Figure 8A)**. Human LH (hLH) released during and after female puberty helps to convert androgens produced by theca cells in the follicle to estradiol. Estradiol plays a role in regulating the development of secondary sex characteristics in females as well as follicular development in preparation for ovulation. After fertilization, LHR bind hCG, a placental hormone, rather than hLH [13, 24, 38, 80, 95]. The maternal placental hCG produced during male fetal development plays a role in induction of androgen synthesis that, in turn, induces differentiation of the external male genitalia. In human males, hLH from the anterior pituitary stimulates testosterone production which increases during puberty and post-puberty [13, 39, 97, 98].

hCG has a molecular weight of 57,000 Da [24] and consists of an α-subunit and β-subunit which are connected together by noncovalent interactions [24]. The α-subunit has 92 amino acids and contains five disulfide bridges and two N-linked carbohydrate sites [99, 100] that are coded for by one gene located on chromosome 6 [24]. The β-subunit has 121 amino acids and contains six disulfide bridges, two N-linked carbohydrate sites, and four O-linked carbohydrate sites [99, 100] as shown in **Figure 7**. β-subunit is coded by six genes located in chromosome 19. The additional O-linked carbohydrate sites on hCG are present on the additional 24 amino acids found in hCG as compared to LH. Thus hCG has a larger molecular weight and additional carbohydrates when compared to hLH **(**[7, 24, 86, 96]: **Figure 8B)**. hLH has a molecular weight of 28,500 Da [24], the same α-subunit found in hCG and coded for by a gene located on chromosome 6, and a β-subunit coded by a single gene located on chromosome 19 [24, 101].

hLH and hCG are heterodimeric glycoproteins consisting of a species-specific common α-subunit non-covalently associated with a unique β-subunit that is stabilized by a β cysteine loop that forms a "seatbelt" around the two subunits [5, 28]. The β-subunit defines the hormone's individual biological properties. Both subunits, α and β, are required for full biological function [2]. Due to difference in the structures of hLH and hCG, LHR can qualitative discriminate between hLH and hCG through differences in hormone interactions with LHR [5, 95]. For instance, hLH has more hydrogen bond donors than hCG for interaction with sulfate tyrosine 331 in the hinge region of LHR [5]. Furthermore, it has believed that hLH and hCG can induce different signaling pathways in which hCG can activate the cAMP pathway to a greater extent than hLH, while hLH preferentially activates extracellular signal-regulated kinases (ERK) and protein kinase B (PKB) pathways [6, 94, 95, 102, 103]. In addition, studies suggest that hLH induces only *cis*-activation of LHR *in vitro* [5, 7, 45, 86] and induces *cis*-activation and *trans*-activation *in vivo* [104, 105] while hCG induces *cis*-activation and *trans*-activation of the receptor both *in vivo* and *in vitro* [5-7, 45, 86, 106-109]. Moreover hLH and hCG differ in their half-life, 60-120 minutes for hLH and several hours for hCG [95, 110], probably due to the extra carbohydrates on hCG. Taken together, the LHR-mediated signaling mechanisms may change from signaling pathways used during the ovarian cycle to be signaling pathways used during pregnancy.

In addition to structural differences in amino acid sequences, carbohydrates on both hormones are necessary for biological functions and hepatic clearance of the hormone from the body [111-113]. Most of the carbohydrates can be removed from hCG to generate DG-hCG [112] which can bind LHR with the same high affinity as hCG but with little or no function [114-116]. This antagonist has been found in serum from patients with chronic renal failure disease with accompanying hypogonadism [114].

In this study, hCG has been used for several reasons. Relative to LH, hCG has extra amino acids and these additional amino acids are believed to contribute to hCG association with LHR for longer times [4, 111, 117]. hCG binding to LHR appears to produce a larger molecular weight complex with multiple copies of the receptor. This leads to slower rotational diffusion rates for hCG-occupied receptors compared to LH-occupied receptors [116, 118] and higher levels of energy transfer between wild type LHR [118]. On a more practical level, hCG is more abundant, less expensive, more stable, has a longer half-life and is more readily available than hLH [38, 95, 111]. Finally, hCG is more active in terms of cAMP production than is hLH [6, 94, 95, 102, 119].

In summary, hLH and hCG have similar properties with respect to receptor binding and share a common α-subunit. Both hormones are important for reproduction in females. They do, however, differ in their β-subunits and this difference may causes activation of different signaling pathways (G_s versus G_q) through different mechanism mode of receptor interactions, *cis*-activation versus *trans*-activation, and different physiological responses [5-7, 45, 86, 117]. *Cis* activation versus *trans*-activation will be described in detail in section 1.1.7.

βhCG

MEMFQGLLLLLLLSMGGTWASREMLRPRCRPINATLAVEKEGCPVCITVNTTICAGYCPTMTRVLQGVLPALPQVVC

NYRDVRFESIRLPGCPRGVNPVVSYAVALSCQCALCRRSTTDCGGPKDHPLTCDDPRFQASSSSKAPPPSLPSPSRL

PGPSDTPILPQ

βhLH

MEMLQGLLLLLLLSMGGAWASREPLRPWCHPINAILAVEKEGCPVCITVNTTICAGYCPTMMRVLQAVLPPLPQVVC

TYRDVRFESIRLPGCPRGVDPVVSFPVALSCRCGPCRRSTSDCGGPKDHPLTCDHPQLSGLLFL

αhCG and αhLH

MDYYRKYAAIFLVTLSVFLHVLHSAPDVQETGFHHVAQAALKLLSSSNPPTKASQSARITDCPECTLQENPFFSQPG

APILQCMGCCFSRAYPTPLRSKKTMLVQKNVTSESTCCVAKSYNRVTVMGGFKVENHTACHCSTCYYHKS

Figure 7: Amino acid sequence of the common α-subunit and the unique β-subunit of hGC and hLH. hCG has additional amino acids that are believed to account for differences in hCG association with the LHR. Adapted from [92, 120, 121].

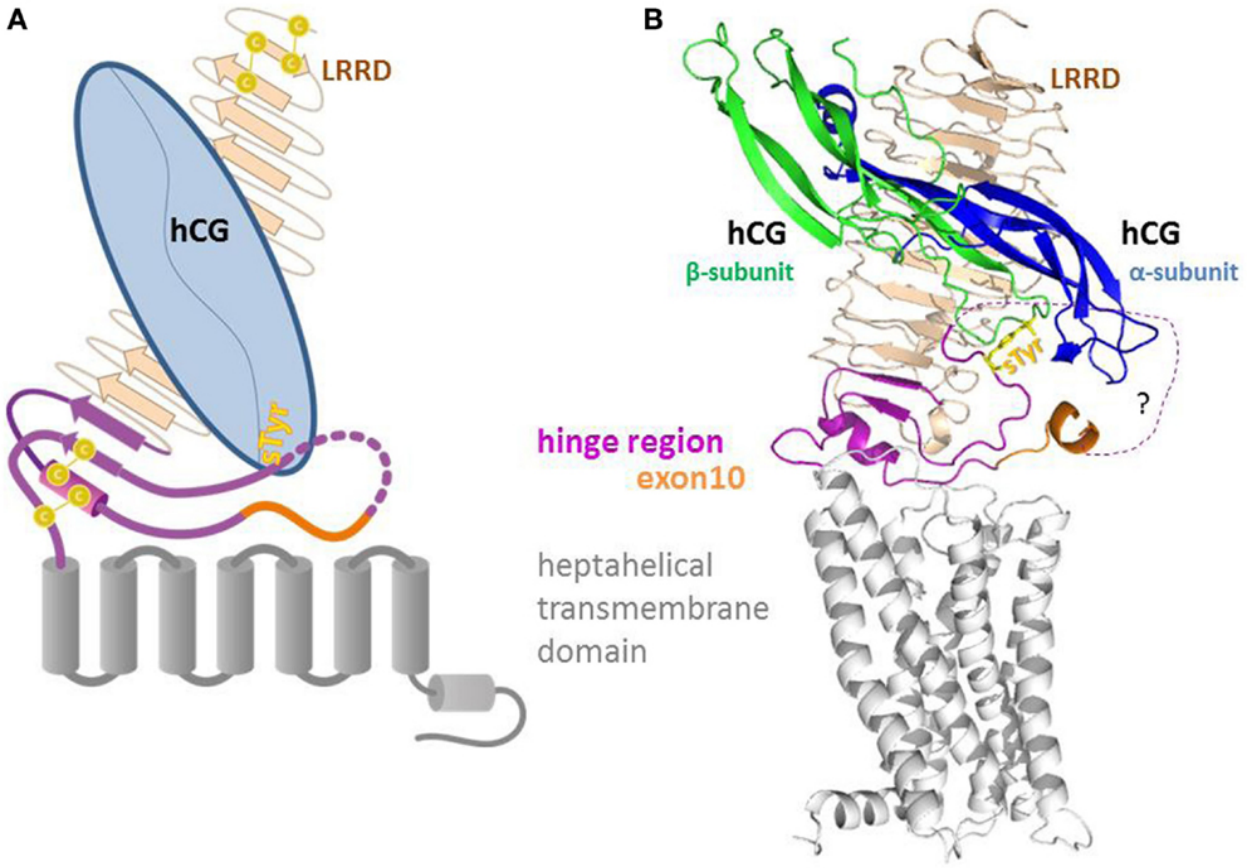

Figure 8: Interactions between LHR and hCG. Panel A is a sketch of hLHR interacting with hCG through the receptor's LRR domain and hinge region. Panel B is a homology model showing the ribbon diagram of hCG (α-subunit and β-subunit) and its interactions with hLHR [5].

1.1.3. DG-hCG is an hCG antagonist

Human CG contains an α-subunit with five disulfide bonds and two asparagine N-linked carbohydrate chains and a β-subunit with six disulfide bonds, two asparagine N-linked carbohydrate chains, and four O-linked oligosaccharide chains [122]. About 30% of hCG's molecular weight is due to glycosylation [112]. The carbohydrates are essential for biological function and control the rate of hepatic clearance from the body [111-113]. Approximately 85% of the carbohydrates can be removed from hCG by treating hCG with hydrogen fluoride (HF) for 3 hours. The deglycosylated molecule is referred to as DG-hCG [112, 123].

If the subunits of DG-hCG are examined in more detail, it appears that HF removes about 80% of carbohydrate from the α-subunit and 66% of carbohydrate from the β-subunit [112]. Alternatively, trifluoromethanesulfonic acid (TFMS) can be used for deglycosylation of hCG as has been done by Dr. George Bousfield at Wichita State University who prepared the DG-hCG used in this study [124, 125]. Alternatively, carbohydrate attachment sites, N-linked carbohydrate chains on either α-subunits or β-subunits, or O-linked carbohydrate chains, can be achieved by introducing mutations in the subunit genes [126, 127].

DG-hCG binds LHR with the same affinity as hCG, as shown in the binding affinity assay in **Figure 9A**, but has impaired ability to stimulate cAMP **(Figure 9B**; [112, 114, 122, 123, 127-129]**)**. Studies suggest that the carbohydrates removed from DG-hCG may, when present on intact hCG, interact with one or more "lectin-like" binding sites that are present on membrane sites near LHR causing activation of receptors and signaling via cAMP [112, 127]. Alternatively, there may be lectin-like binding sites present on LHR itself that interact with hCG's carbohydrates [127]. A third possibility is that carbohydrates on the β subunits may bind LHR and, via an unknown

mechanism, trigger production of cAMP [5]. In general, the question of how hCG's carbohydrates contribute to the function of LHR has not yet been answered.

DG-hCG causes a decrease in the ability of LHR to activate AC in a dose-dependent manner; in the presence of DG-hCG, cAMP production in response to hCG was impaired while the production of cAMP by forskolin activation of adenylate cyclase was not inhibited. Pre-incubation of LHR with DG-hCG prevents activation of the receptors by hCG for at least 46 h suggesting that binding of DG-hCG with LHR is slowly reversed [127]. Studies using human and monkey ovarian tissues, luteal cells, or granulosa cells treated with DG-hCG found some effect of DG-hCG on cAMP production and steroid production [130, 131]. However, it has been reported that DG-hCG can reduce production of cAMP in the presence of hCG or hLH but not inhibit testosterone production to the same extent [128]. Interestingly, DG-hCG does not interfere with steroidogenesis in the presence of hCG [132, 133] although the mechanism for this lack of response is unknown; a low concentration of DG-hCG, an abbreviated incubation time, and the presence of either hCG or hLH may account for this lack of effect.

There remains interest in DG-hCG's properties as an LH/hCG antagonist. Although several antagonists have been designed to block LHR activity and reduce the progression of certain LHR-associated cancers [134], DG-hCG may be a better antagonist since it exists naturally. DG-hCG has been found in serum from male patients with chronic renal failure disease who were suffering with hypogonadism [114]. LHR function is inhibited by DG-hCG with no production of cAMP and impaired testosterone production [114, 135, 136], both attributed directly to the hormone [114, 135].

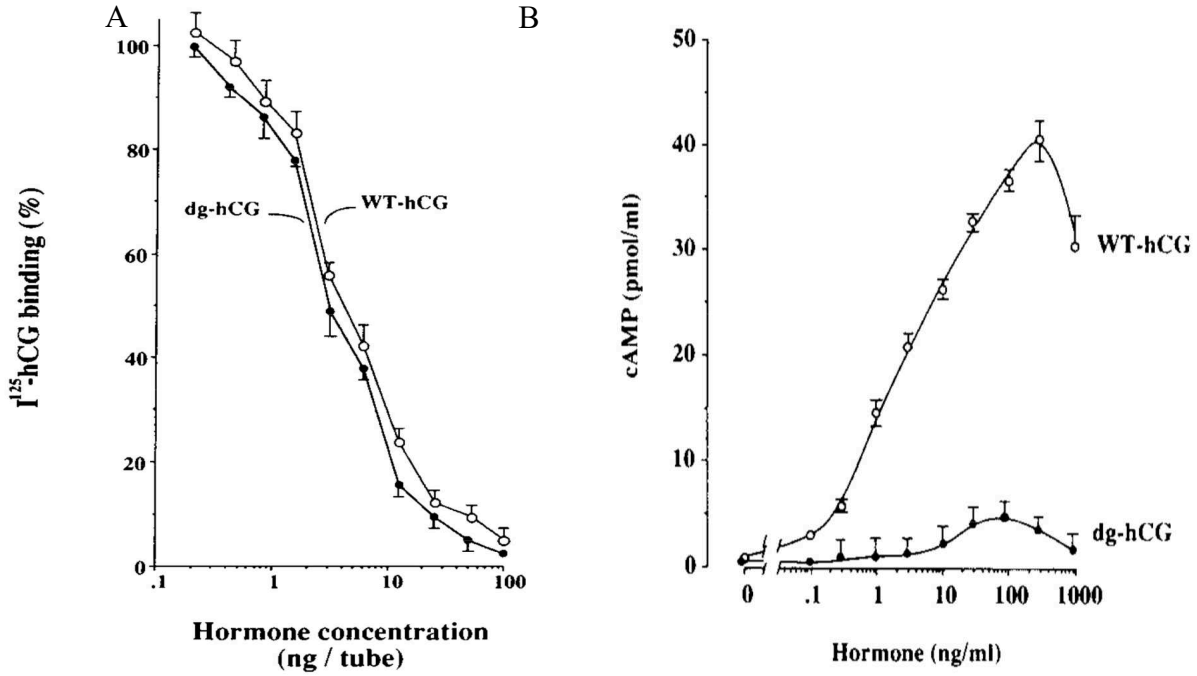

Figure 9: LHR binding and cAMP production in response to DG-hCG. Panel A shows that displacement of I^{125}-hCG by hCG and DG-hCG were equally effective. Panel B shows dose-dependent cAMP responses by cells expressing LHR and treated with hCG or DG-hCG [127].

1.1.4. Signal transduction by LHR

LHR can be activated by high affinity binding of hLH or hCG although these hormones interact differently with the extracellular domain of LHR. The segment of hinge region that is encoded by exon 10 is particularly important in signaling by hLH [5, 7, 38, 86]. This region creates a non-specific spacer element that adjusts the position of the sulfated tyrosine 331 residue in the receptor to favor hydrogen-bound interactions with hLH. Interactions between hCG and LHR also depend on this region encoded by exon 10 region which serves as a structural interface with hCG. If exon 10 is deleted, interactions with the adjacent helix can compensate [5] as shown in **Figure 10**.

Once the hormone binds to LHR, conformational changes in the 7TM of the LHR are induced leading to either *cis*-activation or *trans*-activation. These distinct mechanisms lead to different signaling pathways. In *cis*-activation, either hLH or hCG binds to an extracellular domain of LHR leading to activation of the same LHR that originally bound hormone [6, 7, 106-109]. In *trans*-activation, the ligand, hCG in *in vitro* experiments [6, 7, 106-109] or hLH in *in vivo* experiments [104, 105], binds to the extracellular domain of first LHR and then causes *trans*-activation of an adjacent receptor that has not bound ligand [6, 107-109] **(Figure 11)**. Studies using mutated hLHR which are unable to signal (LHR^{cAMP-}), combined with muted hLHR that cannot bind hormone, (LHR^{LH-}) have suggested that hLH can activate hLHR only through *cis*-activation. In contrast, hCG has ability to initiate both *cis*-activation and *trans*-activation [6, 7, 106-109]. In contrast, studies using male mice with knockout LHR and co-expressing the two mutant LHR, $LHR^{cAMP-}$and LHR $^{LH-}$, demonstrated complete rescue, *i.e*., the wild-type phenotype, in the presence of high levels of LH. This could happen only through receptor *trans*-activation and

provides support for this mechanism of receptor activation by both hLH and hCG [104, 105, 137].

Once activated, LHR triggers the activation of a G protein, a heterotrimeric protein consisting of α, β and γ subunits. The G protein is associated with the cytoplasmic C-terminus of the LHR. LHR independently activate two distinct G protein-dependent signaling pathways via G_s and G_q. For both G proteins, the activated α subunit undergoes an allosteric change and swaps GTP for GDP leading to the dissociation of α subunit from the membrane-anchored βγ subunits. It then binds to an effector downstream, either AC for G_s or PLC for G_q **(Figure 12)**

In the G_S-activated pathway, the α subunit activates AC which converts ATP to cAMP [5, 38, 45, 138]. cAMP then activates PKA and an exchange protein directly activated by cAMP, EPAC. This results in the phosphorylation of transcription factors such as a cAMP-response element-binding protein (CREB) which regulates expression of target genes like P38 mitogen-activated protein kinases (P38 MAPK) which is responsible for a pro-apoptotic event. In addition, CREB can activate the steroidogenic acute regulatory protein (STAR) gene to produce the STAR protein. STAR regulates steroidogenesis [4, 45, 80, 84, 94, 102, 139] by controlling the transport of cholesterol to the mitochondria for synthesis of steroid hormones. The first enzyme participating in steroidogenesis is a cytochrome P450 cholesterol side chain cleavage enzyme (P450scc) needed for synthesis of pregnenolone and further modifications to produce steroid hormones [13, 139].

Although the G_s pathway is the major signaling cascade regulating steroidogenesis, additional pathways are involved in steroidogenesis such as the G_q pathway [5, 38, 140, 141]. In this pathway, the α subunit activates PLC leading to formation of DAG and cytosolic IP_3 from PIP2. IP3 triggers release of Ca^{+2} from the endoplasmic reticulum and activates rapamycin complex 1 (mTORC1) which is involved in proliferation and cell survival [2, 4]. An increase in

the Ca^{+2} in the cytoplasm from intracellular stores affects potassium channels and activity of a variety of target proteins that play important roles in steroidogenesis including progesterone synthesis [111, 139, 142]. DAG in turn activates PKC, protein kinase B (PKB) and Akt signaling pathways that have roles in regulating cell proliferation and cell survival and induce several enzymes involved in steroid synthesis [2, 4, 39, 141, 143-145].

Activated LHR can participate in crosstalk with other receptors such as epidermal growth factor receptors (EGFRs) or insulin-like growth factor 1 receptors (IGF-I) [146], both tyrosine kinase receptors. Activation of tyrosine kinase receptors leads to activation of Rap/Raf/Ras proteins that, in turn, activate extracellular signal-regulated kinases 1 and 2 (ERK1/2) to trigger phosphorylation and activation of transcription factors involved in cell cycle regulation, cumulus expansion, and cell growth. In addition, transcription factors involved in tumor progression, proliferation, and steroidogenesis may also be activated by cAMP and PKC [2, 147]. Activated ERK can activate EPAC which triggers an anti-apoptotic response [4, 80, 102, 139, 143]. Activation of the ERK cascade might involve other signaling molecules such as the Src family of kinases (SFKs) that induce expression of genes important in regulating Leydig cell and corpus luteum function [80]. IGF-I has been shown to increase the expression level of LHR mRNA [139]. Collectively, multiple pathways interact with each other to stimulate steroid biosynthesis in LHR-dependent pathways.

LHR also undergo receptor desensitization following hormone binding to the receptor and activation. Phosphorylated hLHR causes activation of an Arf nucleotide binding site opener (ARNO) which in turn activates ADP ribosylation factor 6 (ARF6), a guanine nucleotide exchange factor, via exchange of GDP by GTP. Active ARF6 promotes the disassociation of β-arrestin from a membrane docking site in ARF6. Arrestin is then available to bind to active LHR to terminate

their activity. Subsequently, hydrolysis of GTP to GDP in G_α leads to inactivation of the G protein and re-association of α with the γβ dimer to restore the G-protein heterotrimer [84, 148, 149]. β-arrestin is directly activated by ERK1/2 slowly [4]. Interestingly, recruitment of β-arrestin to inactivated receptors is detrimental to expression levels of the receptors. A decrease in receptor density in cell membranes can regulate and induce β-arrestin-dependent signaling [150] suggesting that there is a balance between active and inactive receptors that depends on receptor numbers. However, other studies have suggested that phosphorylation of LHR is not required for desensitization [151-153]. Therefore, LHR desensitization is expected to use other mechanisms such as interaction between LHR and β-arrestins without requiring LHR phosphorylation [154] In alternatively, desensitization of LHR have been reported to be dependent upon GTP mechanisms [155] and studies using mutated LHR in candidate amino acids involved in phosphorylation of LHR, have found that the phosphorylation is needed but not sufficient for desensitization of LHR [156, 157]

As have been described, there are slight differences between hLH and hCG structures that lead to differences in association with hLHR and which may affect LHR activation and signaling pathways. hCG can activate G_{α_s} to produce more intracellular cAMP and pro-apoptotic potential while hLH can activate G_{α_q}. In addition, hLH appears responsible for crosstalk with tyrosine kinase receptors leading to more ERK and PKB production and greater anti-apoptotic potential [6, 94, 95, 102, 119, 143]. Signaling effects of LH and hCG are complicated by hormone effects on *cis*-activation and *trans*-activation of hLHR *in vitro* [5, 7, 45, 86] which can lead to different receptor-mediated pathways and different physiological responses [5-7, 45, 86, 117].

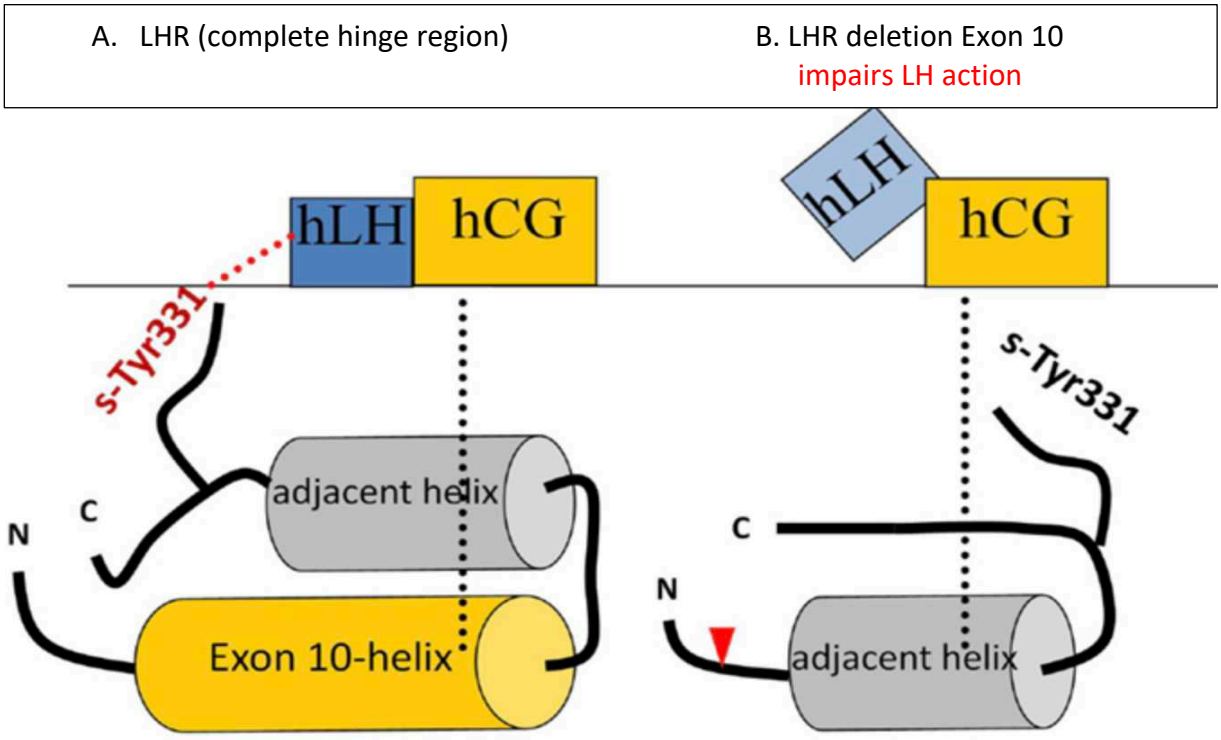

Figure 10: Sketches of differences in the interactions of hLH and hCG with the hinge region of LHR. Panel A shows that the wild-type LHR has an exon 10-derived helix that shifts the s-Tyr331 to an appropriate position near an adjacent helix to interact with hLH. For hCG, the exon 10-derived helix functions as a structural interface. Panel B shows that deletion of exon 10 in LHR causes the adjacent helix to move to an appropriate position to interact with hCG. There is an accompanying loss of interaction with hLH [5].

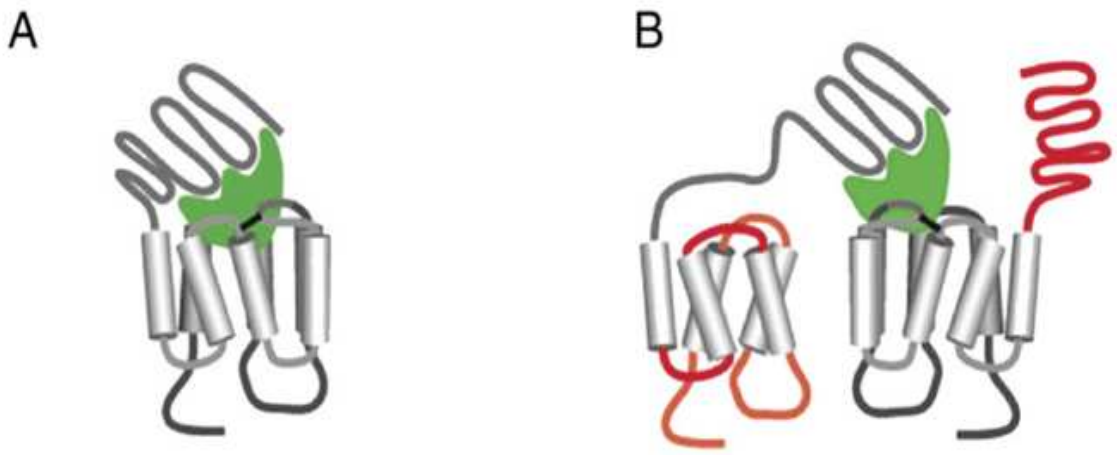

Figure 11: Schematic representation of *cis*-activation and *trans*-activation of LHR. Adapted from Rivero-Muller *et al*. [104].

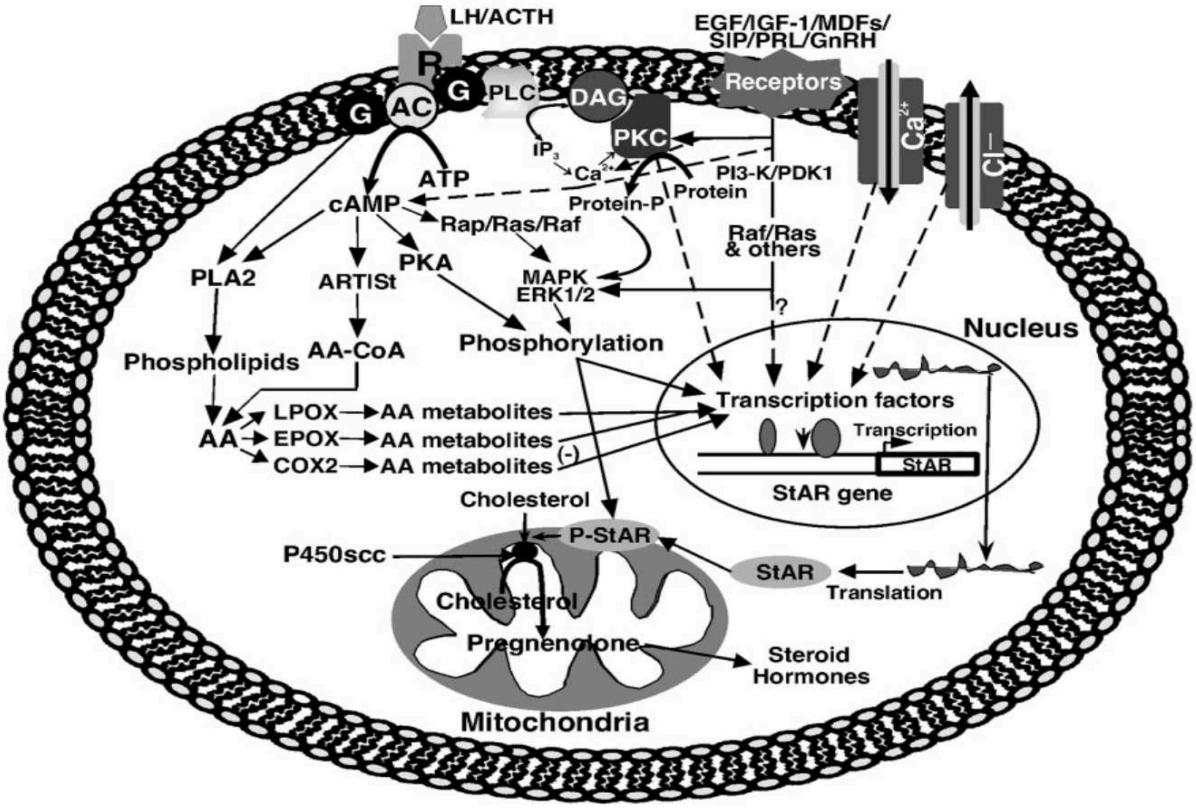

Figure 12: Signaling pathways regulated by activation of LHR. AC can be activated by LHR to induce its downstream pathway. Similarly, PLC can be activated by LHR to induce its downstream pathway. Also, LHR can participate in crosstalk with other receptors such as EGFR and IGFR, activating their respective downstream signaling pathways [139].

1.1.5. Crowding, oligomerization of LHR and receptor activity

The oligomerization of membrane proteins increases in response to increasing molecule crowding [149, 158]. In addition, the activation of receptors also occurs in response to increased receptor density in cell membranes [7, 150, 159]. Macromolecular crowding is considered to be a high concentration of proteins or high density of proteins in a given area. High protein concentrations in membranes tends drive formation of oligomeric structures or nonfunctional aggregates [160].

Crowding of molecules strongly depends on the relative number of molecules, size of molecules, shape of molecules and dilution of molecular reactants [158, 160]. Molecular crowding is important because of its effects on cell membrane molecular structures including folding, shape, conformational stability, molecule diffusion and behavior including binding of other molecules, enzymatic activity, and downstream signaling. Thus, molecular crowding plays an important role in signal transduction and cell function [119, 149, 158-160]. It has been found that many proteins can become activated in the oligomerized state. Other studies found that many proteins exist as dimers or oligomers even when they are inactive. Thus, the oligomerization state of proteins and their activity can be affected by crowded environments with variable effects on protein activation [119, 149, 158-160].

A crowded environment can affect the aggregation of LHR and may have effects on LHR activity [119, 149, 150, 159, 161]. The density of follicle stimulating hormone receptor (FSHR), a structurally-related glycoprotein receptor, in the plasma membrane can control receptor signal transduction including cAMP production in response to hormone. However, a mutant FSHR (A189Va) mimics the hormone-response of wild type FSHRs when expressed at low levels of receptors **(Figure 13)**. cAMP production can be rescued when A189Va-mutated FSHRs are

expressed in higher numbers [150]. Therefore, controlling the expression level of receptors has potential use as a therapeutic approach to treat this type of mutation. Furthermore, when cells are co-transfected with LHR that are signaling-deficient (LHR^{-cAMP}) and binding-deficient (LHR^{-LH}), increased expression levels of these mutant LHR in plasma membranes increases intracellular levels of cAMP in the presence of hormone [7]. Increasing the expression levels of wild type LHR from 600 to 125,000 LHR/cell and co-expressing these wild type receptors with mutant receptors (LHR^{-cAMP}, LHR^{-LH}) leads to increased cAMP production in response to hormone in an expression-dependent manner **(Figure 14**; [159]).

Therefore, it is necessary to consider the potential impacts of molecular crowding on oligomerization state of proteins when evaluating receptor or protein activation, particularly for those proteins that naturally exist at low concentrations such as LHR [46, 160]. The overexpression of proteins can lead to a crowded environment and increase protein oligomerization. As an example, neurokinin-1 receptors overexpressed in cells were present in larger clusters when compared to cluster sizes in cells expressing physiological levels of neurokinin-1 receptors [10].

These various effects of receptor crowding suggest that it is important to carry out experiments under physiological conditions with an expression levels of proteins that are similar to naturally-occurring receptor numbers. Interestingly, when proteins are expressed in live cells via transient transfection processes, there is a higher chance of obtaining higher expression levels [149] and concerns about changes in protein structure, oligomerization and function.

In conclusion, the crowded environment of proteins including LHR may lead to effects on protein structure, protein oligomerization and activity. Furthermore, aggregation of LHR may result from high expression levels. This may contribute to many human diseases such as AD [56-61], ovarian cancer [33, 62-64], breast cancer [65-68], prostate cancer [33, 69, 70, 162],

endometrial carcinomas [71-74], polycystic ovary syndrome [35, 40, 75, 76], uterus leiomyoma [33, 77], adrenocortical dysfunction[36], obesity [39] and Cushing's syndrome [78, 79]. One goal of studies described in this dissertation is to provide a foundation for new pharmacological approaches to diseases associated with receptor overexpression.

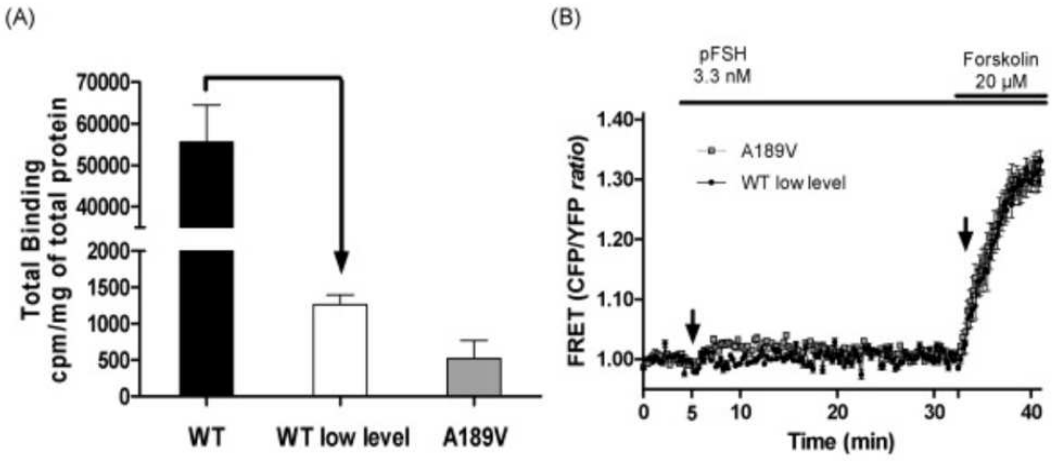

Figure 13: Binding assay and cAMP assay for WT FSHR and mutant FSHR (A189V). Panel A shows results of a binding assay to determine the total number of FSHR expressed. Panel B shows results of expressing low levels of wild type FSHR or mutant FSHR, Both receptors failed to produce cAMP in presence of hormone [150].

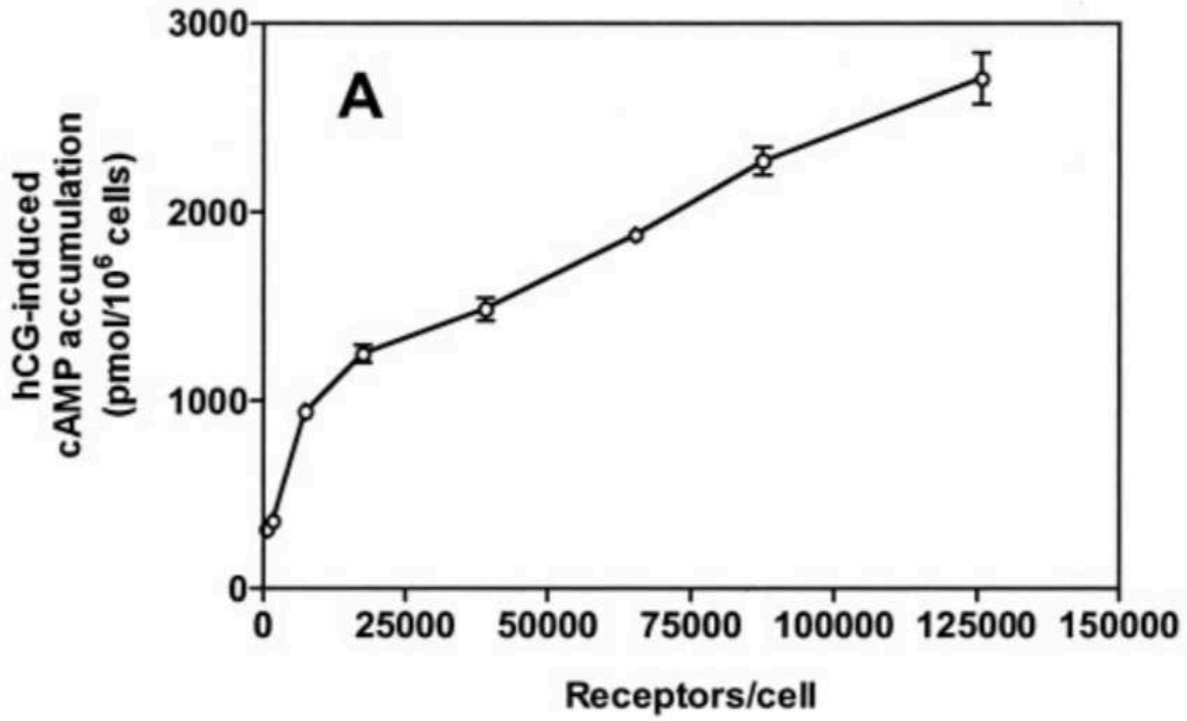

Figure 14: cAMP level induced by hCG binding to cell populations expressing increasing numbers of receptors per cell. Intracellular levels of cAMP increased as the average numbers of wild type LHR per cell increased [159].

1.1.6. The role of cholesterol in LHR function

Cholesterol is major component of eukaryotic plasma membranes and plays an essential role in membrane organization, dynamics and function [1, 163, 164]. Cholesterol is a lipid that contains four fused hydrocarbon rings with a flexible hydrocarbon tail. The tail interacts with the plasma membrane as does the hydroxyl group on the first fused ring **(**[1, 165]; **Figure 15)**. Cholesterol, together with sphingolipids, is distributed in plasma membrane domains called lipid raft microdomains [164]. Membrane cholesterol also modulates the function, dynamics, and stability of many membrane proteins [1, 166-173]. Although the depletion of membrane cholesterol has detrimental effects on many proteins [1, 166-168, 174, 175], the presence of cholesterol inhibits the function of rhodopsin [176]. Therefore, cholesterol-mediated effects in protein function appear to be protein specific.

Despite the importance of membrane cholesterol in protein function, the mechanistic basis for cholesterol's effects is still under investigation. Recent studies have shown that membrane cholesterol can directly or indirectly interact with membrane proteins [1, 164, 172, 177, 178]. Membrane cholesterol may interact directly with a cholesterol binding motif in membrane proteins. This interaction could induce a conformational change, help to stimulate oligomerization, or improve the stability of the membrane protein. Specific cholesterol binding motifs in different membrane proteins are of intense interest [179, 180]. Conversely, membrane cholesterol may indirectly affect a membrane protein by altering the physical properties of lipid membranes.

The localization of LHR in rafts containing cholesterol may be important in LHR function. Functional LHR treated with hCG and constitutively active LHR exist in lipid rafts while non-functional LHR are found in the bulk membrane [181, 182]. These studies indicated that membrane cholesterol and raft domains are important in LHR signal transduction and that cholesterol

depletion using methyl-β-cyclodextrin (MβCD) [183-186] leads to a decrease in intracellular cAMP [181]. Studies of adenosine A_{2A} receptors have shown that cholesterol depletion inhibits the activity of these receptors and reduces cAMP production [187]. In addition, MβCD reduces the cluster size of the serotonin1A receptors and decreases signal transduction in response to ligand [166, 171, 173, 188]. Similarly, reducing membrane cholesterol leads to a decrease in the cluster size of μ-opioid receptors and glycosyl phosphatidyl inositol (GPI) anchored proteins [189] and decreased signaling transduction [190]. In this study, the effect of expression level of receptors on the degree of change in LHR oligomerization, on receptor activity upon depletion of plasma membrane cholesterol, and extent of lipid packing was evaluated.

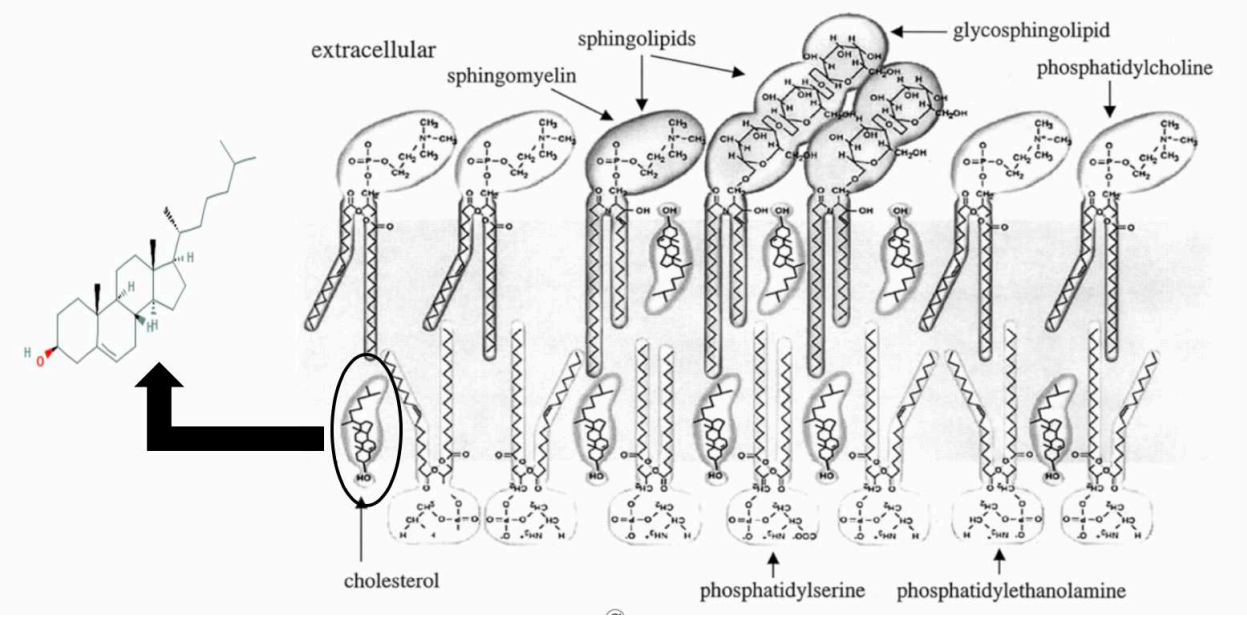

Figure 15: Model of lipid organization in lipid raft microdomains including cholesterol's structure and relationship to the lipid bilayer (from [1]). Cholesterol's structure is shown on the left [9].

2. CHAPTER 2: MEASURING THE SIZE OF PROTEIN CLUSTERS AND INTRACELLULAR cAMP

2.1. Measuring the size of protein clusters

2.1.1. Oligomerization of LHR

The view that most GPCR, including LHR, function as monomers is changing. More recent studies of GPCR support the concept that receptor oligomerization is a fundamental process required for receptor activation [191]. LHR, in particular, have been found clustered as dimers or oligomers in the plasma membrane using techniques based on fluorescence resonance energy transfer (homo-FRET, BRET) [149, 192], fluorescence cross-correlation spectroscopy (FCCS) [7] dual-color photoactivatable dyes and localization microscopy (PD-PALM) [140] or co-immunoprecipitation [193].

Activated LHR, after binding to hLH or hCG, are involved in two distinct mechanisms for receptor activation, *cis*-activation and *trans*-activation [5-7, 45, 86, 117]. Both activation mechanisms are accompanied by receptor clustering in the plasma membrane **(Figure 16)**. Oligomerization of LHR in the plasma membrane after activation has been shown using fluorescence photobleaching recovery (FPR) [8, 194], techniques based on florescence resonance energy transfer such as homo-FRET and hetero-FRET [3, 8, 118, 149, 182], electron microscopy studies with ferritin-labeled LH [195] and co-immunoprecipitation of epitope-tagged LHR [193]. It has been found that the cluster size of hLHR increases upon hormone binding in a concentration-dependent manner [196]. The clustering of LHR is suggested to play an important role in signaling, desensitization and internalization of LHR after activation by hormone [2-8].

Dimerization or oligomerization of LHR may also occur, to some extent, early in receptor biosynthesis in the endoplasmic reticulum and is unrelated to receptor activation [2, 27, 192]. As a result, inactive LHR may be inserted in the plasma membrane as dimers. Studies using mutated hLHR that do not signal (LHR $^{cAMP-}$) combined with mutated hLHR that do not bind hormone (LHR $^{LH-}$) have shown that *trans*-activation and the association between these muted receptors occurs in the plasma membrane [104, 106, 137].

A number of biochemical and biophysical methodologies have been used during the last decade to study the cluster size of proteins in general and LHR in particular. The most common biochemical approaches that have been used to study oligomerization of LHR are co-immunoprecipitation and SDS-PAGE with cross-linking [3, 66, 104, 109, 193, 197, 198]. The drawback to these approaches is that they require lysis of the cell and solubilizing the cell membrane which can lead to artificial protein-protein interactions or destroy existing interactions. In addition, these methods are not suited to monitoring protein oligomerization in live cells. On the other hand, common biophysical approaches that have been used to study oligomerization in live cells include FRP [8, 194], BRET [192, 199], hetero-FRET, FCCS [7, 200, 201] and bimolecular fluorescence complementation (BiFC) [202, 203]. Nevertheless, each of these methods has drawbacks. For instance BRET requires long integration time and the emission intensity is very low [17, 204]. FCCS does not provide spatial information so it cannot distinguish signals from the plasma membrane from those of intracellular molecules and is limited by interactions where diffusion is rapid. FCCS is not ideal for studying membrane proteins that have slow diffusion and do not transit the interrogation volume frequently enough to provide reliable fluctuations over experimental times [204]. In hetero-FRET, it is hard to control the expression

level of two fluorophores at equivalent levels [205]. BiFC cannot distinguish between dimer and oligomer formation [202, 203].

In this study, homo-FRET [149, 196] was used to evaluate the cluster size of LHR on the nanometer scale **(Table 4-6)**. Homo-FRET measurements are the best choice for quantitative assays because they can measure clusters of proteins in live cells, are sensitive to changes in molecule formation or molecule abundance, have high spatial resolution, and are convenient for use with commercial florescence microscopes with FRET accessories and software [19]. Observation of cluster size of proteins within live cells will greatly help is better understand biological mechanisms, movement, interaction, and any changes in these parameters.

.

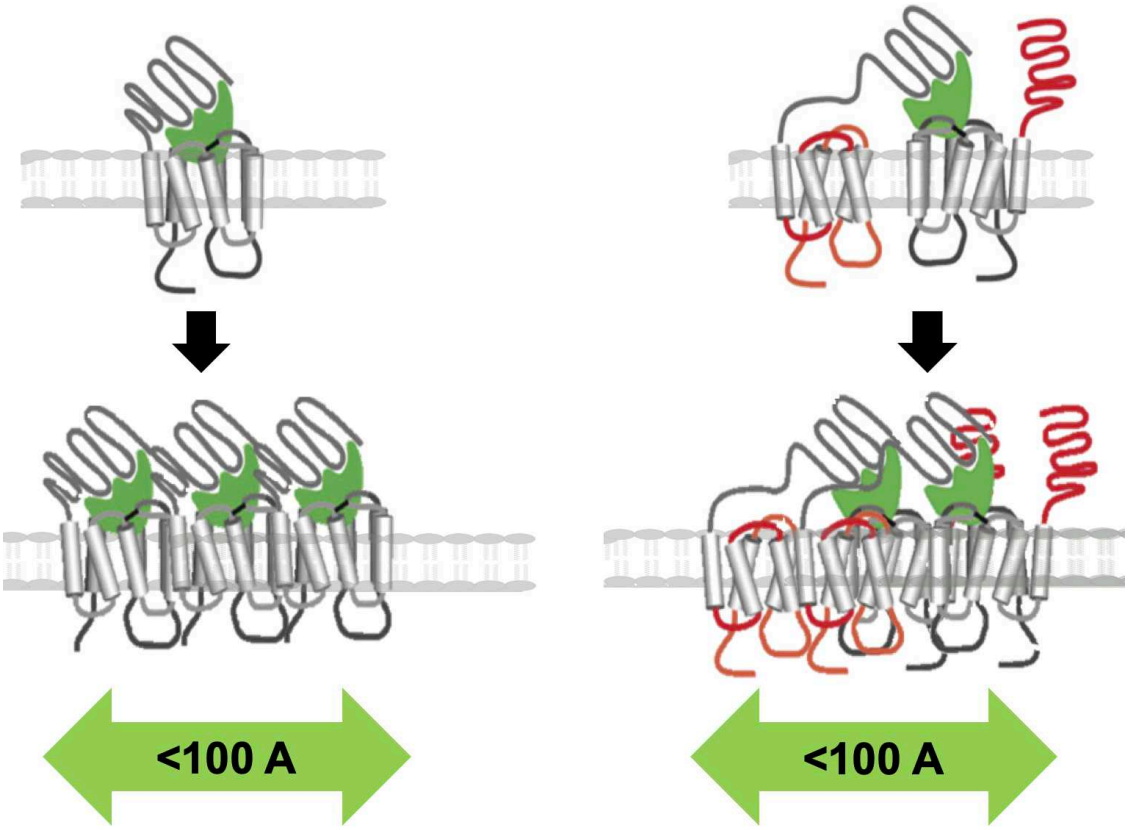

Figure 16: Schematic representation of cis-activation and *trans*-activation leading to LHR clustering. This cluster of LHR dimers or oligomers exists in the plasma membrane of cells as individual receptors separated from one another by distances of less than 100 Angstroms.

2.1.2. Fluorescence Resonance Energy Transfer (FRET)

Fluorescence resonance energy transfer (FRET), first described by Theodor Förster in 1946, is a physical phenomenon in which an excited donor fluorophore non-radiatively transfers energy to a neighboring acceptor fluorophore. Subsequently the acceptor fluorophore emits its characteristic fluorescence ([206], **Figure 17)**. FRET has become a popular technique used in cell biology, biochemistry and biophysics for studying molecular aggregation, interactions, conformation and dynamics in live cells [171, 207-211].

There are three requirements for FRET. First, the emission spectrum of the donor should overlap with the absorption spectrum of the acceptor. Second, the emission of donor and absorption of acceptor transition dipole moments are not perpendicularly oriented. Third, the donor and acceptor should be close together. FRET can be an accurate measurement of molecular proximity at distances between 2-10 nm (10–100 Å) and reaches the highest efficiency when the donor and acceptor are positioned within this range [19, 206, 207, 210]. The Förster distance r_0 is the distance at which 50% the excitation energy of the donor is transferred to the acceptor. If the distance between donor and acceptor is more than 10 nm, FRET does not occur. The efficiency of FRET (E) as showed in **Equation 1** is depends on the inverse sixth power of the intermolecular distance (r) between the donor and acceptor which FRET efficiency sensitive to small changes in distance [19, 212-216].

$$E=1/(1+r/ r_0^6) \quad (1)$$

In general, there are two types of FRET. The first type of energy transfer is between different donor and acceptor molecules and is called hetero-FRET. In the second type, energy transfer occurs between identical molecules which is called homo-FRET. In hetero-FRET, the emission from donor is quenched and emission from the acceptor is enhanced so the efficiency of

FRET can be determined by measuring the donor/acceptor intensity ratio [161, 213]. Homo-FRET can be measured by steady state anisotropy or time-resolved fluorescence anisotropy [217-219]. To evaluate FRET, confocal microscope or wide-field fluorescence microscope is used with a laser or an arc lamp source with appropriate filters as an excitation source [215, 217, 220, 221]. Both steady state anisotropy and time-resolved fluorescence anisotropy can detect the oligomerization state of proteins based on measuring the transfer between the fluorophores. Since only steady state anisotropy was used to detect the cluster size of LHR, it will be the only FRET method discussed here.

2.1.3. Detection of homo-FRET using steady state anisotropy

Homo-FRET is a powerful tool that has been used to determine the aggregation state of proteins such as neurokinin-1 receptor, serotonin1A receptor [19, 171, 211], GPI [208, 217], EGFRs [197, 208, 215, 222, 223], band 3 protein [224], melittin [209], and herpes simplex virus (HSV-1), thymidine kinase (TK) [218] as well as other GPCR [208].

Homo-FRET, also called polarized FRET, excites a single fluorophore with polarized light [225]. Homo-FRET, as illustrated in **Figure 18**, is based on energy transfer between two identical fluorescent molecules such as enhanced yellow fluorescent protein (eYFP). Fluorescent molecules appropriate for use in homo-FRET should have a small Stokes shift between their absorption and emission spectra peaks, significant overlap between the excitation and emission spectra as is the case for eYFP, high quantum yields and large extinction coefficients, **(Table 2)** [19, 188, 204, 209, 226]. Homo-FRET is accompanied by changes in the polarization of emitted fluorescence [225].

Homo-FRET can be measured by steady state anisotropy which is evaluating the loss of the polarization of emitted fluorescence with respect to polarized excitation light [212, 217]. The

polarization of emitted fluorescence can be monitored by examining differences in polarization that occur. In steady-state anisotropy, as more energy is transferred between molecules, there is an accompanying increase in the depolarization of emission fluorescence. Steady-state anisotropy r is calculated from emitted fluorescence intensities I_{vv} and I_{vh}, parallel and perpendicular to the polarization of vertically exciting light, respectively, as in **Equation 2**

$$r = \frac{(I_{vv} - GI_{vh})}{(I_{vv} + 2GI_{vh})} \quad (2)$$

where I_{vv} is the intensity of emission that is vertically oriented and I_{vh} is the intensity of emission that is horizontally oriented with respect to vertically polarized excitation light. I_{vv} and I_{vh} are measured in separate channels [161, 171, 215, 216, 220, 227] . The G factor (G) is a correction factor for different detection sensitivities of vertical and horizontal polarized fluorescence in the instrumental setup. It acts as a normalization factor to compensate for optical properties such as reflections from mirrors that may change the polarization angle of excitation light. In an ideal setup, G would be equal to 1 [215, 216, 220]. Methods used to determine the instrumental G factor are discussed in methods.

Experimentally, a sample is illuminated with vertically polarized light and photo-selection occurs. Those fluorophores that are oriented parallel to the vertically polarized light are preferentially excited while fluorophores that have horizontally-oriented transition dipoles relative to vertically polarized light are not excited. The excited fluorophores that exist in this anisotropic distribution will transfer energy to randomly oriented nearby fluorophores. As a result, the emitted light will be partially depolarized because the emission dipoles are oriented randomly relative to the polarized excitation light **(Figure 18)**. If there is no energy transfer between fluorophores because the distance between fluorophores is more than 10 nm, the emission will be polarized

(Figure 18) [161, 217, 220, 227-229]. Anisotropy decreases as a result of transfer of energy between fluorophores.

Anisotropy, however, can decrease by other means such as rotational movement of the fluorophore molecule which increases the depolarization of anisotropy [171, 207, 218]. To distinguish between the rotation effects and homo-FRET effects on fluorescence anisotropy, fluorescence anisotropy can be measured during progressive fluorescence photobleaching under conditions where steady state anisotropy can be recorded [171, 207, 208]. Basically, photobleaching effectively decreases the number of intact fluorophores in a cluster over time. This leads to an increase in fluorescence anisotropy as the number of fluorophores available for energy transfer decreases. Important to these studies, which used eYFP as a fluorophore, is that rotational movement of the fluorophore molecule can be neglected. This is because the rotation correlation time of eYFP is θ ~16 ns [230] which is slower than its fluorescence lifetime of τ_D ~3.5 ([171], **Table 2)**. This means, in practice, that any observed depolarization of emission occur by transferring energy since the rotational movement of eYFP is very slow and can be ignored [171, 208].

The steady state anisotropy or the degree of polarization has been demonstrated to be inversely proportional to the oligomerization state of fluorophores [209, 227]. The number of fluorophores in clusters can be revealed by comparing anisotropy of experimental data with a simulation of different cluster sizes as have been described by Yeow and Clayton [171, 223].

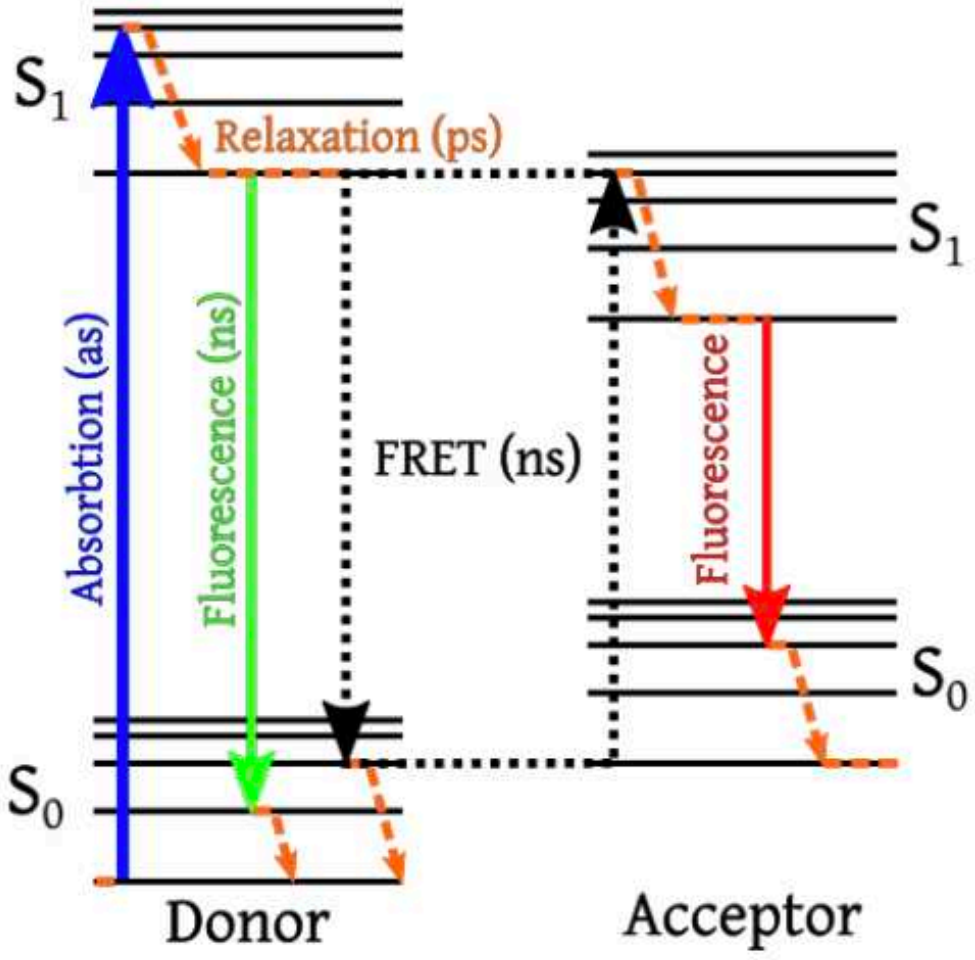

Figure 17: FRET diagram. The donor fluorophore is excited, *i.e.,* reaches the S1 state, and then relaxes to the lowest excitation level. During relaxation, it transfers its energy to a neighboring fluorophore that serves as an energy acceptor. After that, the acceptor fluorophore drops back to the ground state and emits a photon [216].

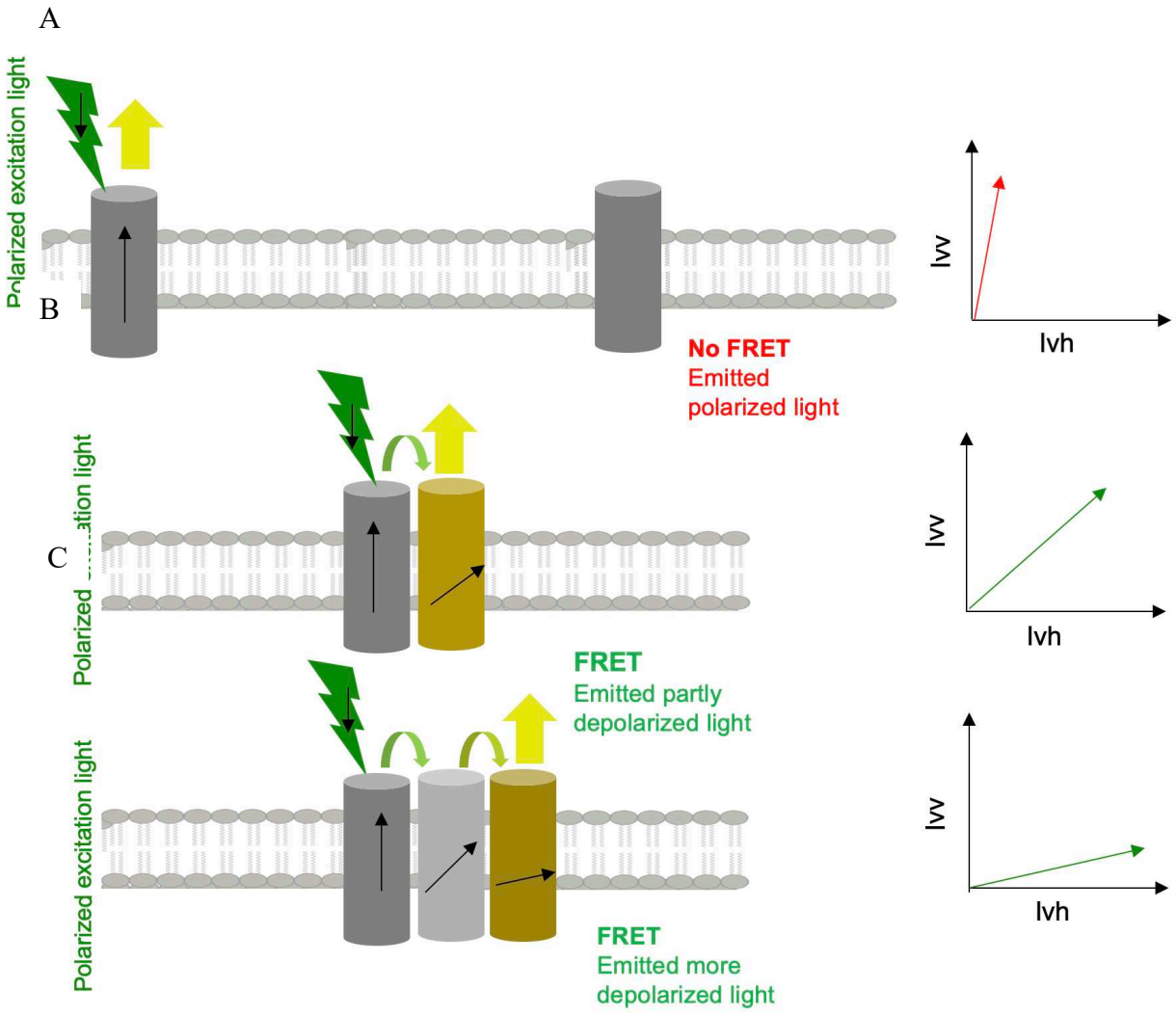

Figure 18: Principle of homo-FRET showing receptors excited with vertically polarized light. Upper panel: In the case of no homo-FRET, receptors tagged with eYFP are separated by distances greater than 10nM and fluorescence emission is relatively polarized. Middle and lower panels: When receptors are comparatively close together, there is transfer of energy between two like fluorophores. This energy transfer results in depolarized fluorescence emission from the acceptor fluorophore and lower anisotropy values. The depolarized fluorescence emission can be used to estimate the cluster size since depolarization is increased when the cluster size is increased, and homo-FRET has occurred. I_{vv} is the intensity of emission that is vertically oriented and I_{vh} is the intensity of emission that is horizontally oriented with respect to vertically polarized excitation light.

2.2. Measurement of intracellular cAMP

2.2.1. Signal transduction and cAMP level are regulated by LHR

cAMP is a ubiquitous second messenger that plays an important role in many cellular processes [231-233]. Increased cAMP levels in the cytoplasm are generated by activation of GPCR that lead, in turn, to activation of the G_{α_s} subunit and AC, an enzyme that converts ATP to cAMP [5, 38, 45]. cAMP can trigger cellular responses through activation of effector proteins such as PKA and EPAC [4, 45, 80, 84, 94, 102, 139].

When LHR bind hLH or hCG, a signaling cascade is activated. Due the minor differences between the two hormones, the signaling pathways used will differ slightly. hCG can activate G_{α_s} which produces more intracellular cAMP than does hLH [6, 94, 95, 102, 119, 143]. Despite the differences, binding of either hormone leads to increases in intracellular cAMP [5, 38, 45]. Thus, the increase in cAMP production in cells reflects receptor activity [234] and can be measured by biochemical and biophysical assays [94, 231, 232, 234].

2.2.2. Measuring of cAMP

The traditional biochemical technique used to measure cAMP *in vitro* is radioimmunoassay (RIA), a method that has been available for decades. This technique requires lysis of cells to obtain a small amount of soluble cAMP. This cAMP can be quantified using cAMP antibodies and ^{125}I-labeled cAMP. The drawbacks to RIA and other biochemical techniques such as electrochemiluminescence immunoassays (ECLIA) and enzyme-linked immunosorbent assays (ELISA; [234]) is that information is obtained from many cells but cannot be obtained from a single cell. In addition, temporal changes in intracellular cAMP are difficult to measure [232, 233]. This has led to the development of methods using FRET-based sensors that provide information on cAMP levels in individual living cells with high spatial resolution [94, 231-236]. FRET-based

sensors have regulatory and catalytic subunits of a cAMP-dependent protein kinase, Epac, or a single cAMP-binding domain from a cyclic nucleotide-gated channel that has been fused to two fluorescent proteins used as donor and acceptor fluorophores. FRET donor and acceptor pairs must have overlap between the emission spectrum of the donor and the absorption spectrum of the acceptor [231, 233, 236-238]. These FRET-based sensors can be transfected into a cell as, for example, Epac-based cAMP sensors, or do not require cell transfection as is the case for homogeneous time-resolved fluorescence (HTRF) assays available in kit from Cisbio [94, 202, 235, 236, 239].

Multiple studies have measured intracellular levels of cAMP in cells expressing LHR in response to hCG via RIA or ELISA assays that are commercially available [80, 86, 108, 159, 194, 234]. More recent studies have used Epac-based cAMP sensors to measure cAMP in individual cells. FRET-based sensors like the "indicator of cAMP using Epac" sensor (ICUE), the mTurquoise sensor, or a BRET-based cAMP sensor using YFP-Epac-RLuc (CAMYEL sensor), have been used to measure intracellular level of cAMP in cells expressing LHR that have been treated with hCG [94, 234, 236, 239-242].

2.2.3. ICUE3, a FRET-based cAMP sensor

Several FRET-based sensors derived from Epac are called ICUE. They have been used to measure in real time cAMP in live cells [231, 236-238]. The ICUE3 molecule is targeted to the plasma membrane and provides dynamic detection of cAMP. ICUE3, illustrated in **Figure 20**, has a palmitoylation site from Lyn kinase for membrane targeting, allowing measurement of cAMP close to the plasma membrane. ICUE3 has an N-terminally truncated Epac1 protein fused at its N-terminus with an enhanced cyan fluorescence protein (eCFP) donor and a circularly permuted Venus at lysine 194 of eYFP (cpV-L194) acceptor, an improved version of eYFP [231, 236, 243],

(Table 2). In the absence of bound cAMP, ICUE3 folds so that the distance between eCFP and eYFP is 5 nm or less FRET occurs from the CFP to the eYFP moiety **(**[244]; **Figure 19)**. In presence of cAMP, ICUE3 undergoes a conformation change resulting in separation of eCFP and eYFP and a decrease in FRET. Calculating the change in the emission intensity ratio of CFP to YFP is used to monitor changes in intracellular cAMP levels [231, 233, 236-238, 243].

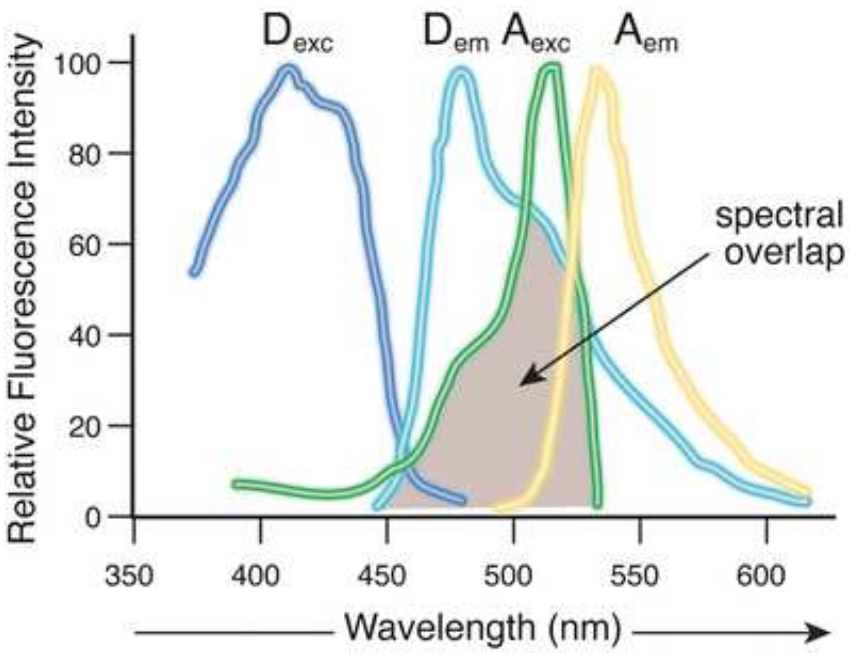

Figure 19: Excitation and emission spectra of a CFP-YFP FRET pair in ICUE3. This figure shows donor (CFP) excitation and emission spectra and acceptor (YFP) excitation and emission spectra. The shaded region is the overlapping between CFP and YFP spectra which is required for FRET [205].

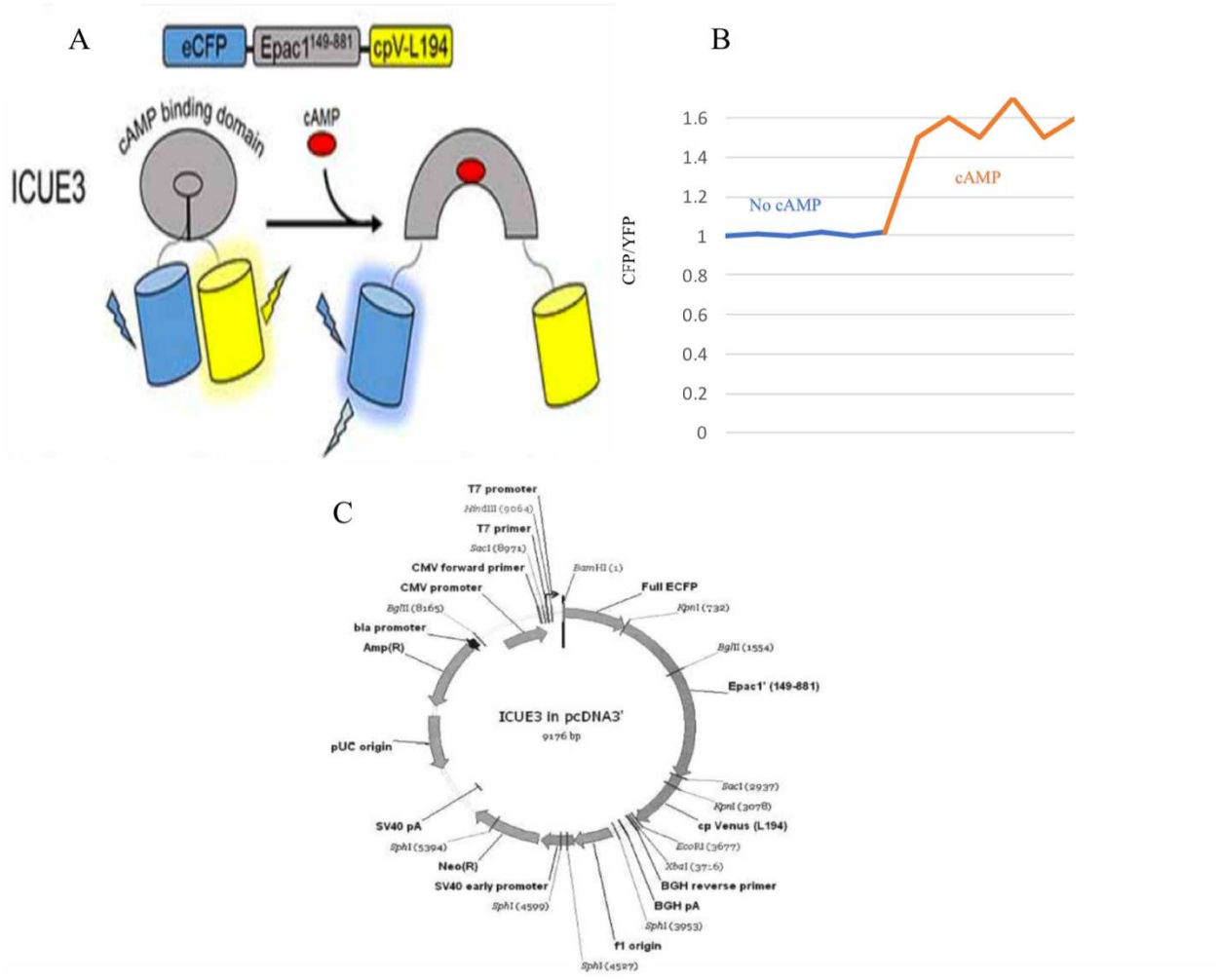

Figure 20: ICUE3 structure and function. Panel A illustrates the structure of ICUE3 which consists of Epac1 flanked by ECFP and cpV-L194. When there is no cAMP, ICUE3 is folded in such a way to allow FRET to occur. Upon binding cAMP, the ICUE3 undergoes a conformational change that results in a decrease in the FRET signal [236]. Panel B shows that upon binding cAMP, the CFP:YFP ratio increases as result of reduced FRET. Panel C shows a map of the ICUE3 plasmid [240].

Table 2: Properties of fluorescent proteins used in these studies

Experiment	FRET	Fluorophore	Excitation (nm)	Emission (nm)	donor quantum yield	donor Lifetime (ns)	Förster distance (nm)	Reference
measure cluster size	homo-FRET	eYFP	495	540	0.61	2.9	4.45	[219, 245, 246]
measure cAMP	hetero-FRET	eCFP-eYFP pair in ICUE3	435	540	0.4	3	4.9	[205, 244, 245, 247, 248]

2.3. Hypothesis

When large numbers of LHR are expressed in individual cells, LHR exist in a crowded environment [119, 149, 150, 159, 161]. As discussed previously, an increase in expression of LHR may lead to increased protein density and drive oligomerization of these proteins [149, 160, 196]. Oligomerization of LHR, either in response to binding of hCG or over-expression of the receptor, increases intracellular levels of cAMP [7, 150, 159]. Many studies have found that hormone binding to LHR increases oligomerization of LHR [3, 5-7, 45, 86, 117, 149, 196] and increased intracellular levels of cAMP [80, 86, 94, 108, 159, 194, 234, 240, 241, 249]. Importantly, overexpression of LHR may induce molecular crowding that can lead to changes in proteins structure, protein oligomerization and protein function, all of which may lead to misinterpretation of experimental results. Therefore, it is essential to consider the potential effects of LHR expression levels, *i.e.*, receptor number per cell, on the oligomerization state and activation of LHR. **We hypothesize that, in unstimulated cells, the size and activity of LHR clusters have strong positive correlation with expression levels of LHR, as indicated by measured anisotropy and intracellular levels of cAMP, respectively. However, in hCG-treated cells with low numbers of LHR, there are increased cluster sizes and activity of LHR. In cells expressing high numbers of LHR per cell, receptors unable to under further aggregation upon binding hCG. In addition, we hypothesize that cells treated with an hCG antagonist DG-hCG or with MβCD have reduced cluster sizes and reduced activity at all expression levels of LHR. However, effects are more pronounced where cells express higher numbers of LHR per cell.**

2.4. Project Rationale

LHR are GPCR that are critical in the maturation of cells within the gonads and in reproductive function in both mammalian sexes [22]. Notwithstanding progress in studying LHR, we still do not know the effect of expression levels of hLHR on the size of clusters containing those receptors. Also, we do not know if the expression level of LHR can play a role in changing the response of LHR to hormone agonists or antagonists and receptor activity. Understanding these questions may provide new strategies for developing therapies to treat LHR-related diseases. As examples, Alzheimer's disease [56-61], ovarian cancer [33, 62-64], breast cancer [65-68], prostate cancer [33, 69, 70], endometrial carcinomas [71-74], polycystic ovary syndrome [35, 40, 75, 76], uterine leiomyoma [33, 77], adrenocortical dysfunction [36] obesity [39] and Cushing's syndrome [78, 79] may be associated with over expression of LHR. These diseases may in fact be caused by an increase in receptor cluster size and abnormal signal transduction leading to cell proliferation and protection from apoptosis, particularly in cancer cells.

When developing cell lines used in these studies, it was also important to consider that the expression levels of LHR in the human ovary varies depending on the stage of follicular development or the age of the corpus luteum formed after ovulation. Expression levels of LHR are positively correlated with oocyte maturation stage. However, when LHR were expressed in in high numbers, the fertilization rate was decreased [40, 250]. Thus, it is very important to consider threshold levels of LHR at each stage of the follicular phase or luteal phase of the ovarian cycle and to examine a range of receptor numbers that include naturally occurring numbers of LHR per cell **(Table 1)**. This study also provides novel information about the role of expression levels of LHR on receptor clustering and function. Such information will have utility in *vitro* fertilization (IVF) and *in vitro* maturation (IVM) protocols given the observation

that circulating LH levels in IVF patients affect implantation of the embryo [251]. There are also diagnostic implications of these results for patients with endometrial cancer. In uveal melanoma cell lines, expression levels of LHR could be used for cancer diagnostic purposes since LHR play a role in growth and invasion of cancer cells. The inactivation of LHR has the potential to reduce the growth rate of cancer cells [71, 252].

3. CHAPTER 3: METHODS AND MATERIALS

3.1. Introduction to methodological approach

LHR are members of the superfamily of GPCR and are mainly present in gonadal cells such as Leydig cells and Sertoli cells in males and in theca, interstitial, cumulus and granulosa cells in the follicle and luteal cells in the corpus luteum in females. LHR in these structures are critical to the maturation and function of reproductive systems in both mammalian sexes [2, 28-31, 85]. LHR are also found in a number of non-gonadal cells such as prostate [32], breast [33], human uterus [4, 28], brain [2, 57], human skin [34, 253] retina [253, 254], and adrenal cortex [33, 35, 36] although the role of LHR in these tissues remains unclear.

Recently it has become clear that many unstimulated GPCR including LHR exist in the plasma membrane as dimers or oligomers. Dimerization or oligomerization of GPCR seems to occur early in receptor biosynthesis in the endoplasmic reticulum and, at this point in the receptor life cycle, is unrelated to receptor activation [2, 27, 192]. However, once inserted in the plasma membrane, ligand binding to the receptor can increase, decrease or no effect on oligomerization of GPCR depending on the type of receptor being examined. For LHR, receptors appear to be inserted in the plasma membrane as dimers or small oligomers [2, 27, 192] and undergo further oligomerization after binding of hormone.

LHR have been found to be clustered in dimers or oligomers in the plasma membrane using florescence resonance energy transfer methods such as homo-FRET and BRET [149, 192], FCCS [7], PD-PALM [140] and co- immunoprecipitation [193]. Activated LHR that have bound hLH or hCG appear to be clustered in the plasma membrane. This has been suggested in fluorescence

recovery after photobleaching studies [8, 194], experiments using FRET methods such as homo-FRET and hetero-FRET [3, 8, 118, 149, 182], electron microscopy with ferritin-labeled LH [195], or co- immunoprecipitation of tagged receptors [193]. There are some studies, however, using hetero-transfer FRET, that suggest that LHR stably expressed in Chinese hamster ovary (CHO) cells exist as monomers in the absence of hormone [182]. This may depend on low receptor expression levels that favor membrane expression of LHR as monomers instead of dimers or oligomers [2, 7, 27, 140, 149, 192, 193, 255].

Several studies have found a number of human diseases related to LHR expression. AD [56-61], ovarian cancer [33, 62-64], breast cancer [65-68], prostate cancer [33, 69, 70], endometrial carcinomas [71-74], polycystic ovary syndrome [35, 40, 75, 76], uterine leiomyoma [33, 77], adrenocortical dysfunction [36] obesity [39] and Cushing's syndrome [78, 79] are associated with over-expression of LHR and high secretion of LH. Endometriosis is associated with low expression of LHR [33, 73].

Increased expression of membrane proteins including LHR leads to molecular crowding in the membrane [158, 160]. Molecular crowding can affect molecule structure including folding, shape, conformational stability, molecule diffusion and molecular behavior including the ability to bind other molecules, enzymatic activity, and downstream signaling. Thus, molecular crowding affects protein and, more generally, cell function [119, 149, 158-160]. Changes in LHR expression levels might alter or affect oligomerization of the receptor as well as its function. This prediction derives from observations that overexpression of proteins leads to a crowded membrane environment and an increase in protein oligomerization [10]. Thus, oligomerization of LHR resulting from high expression levels may also contribute to these human diseases. It is therefore prudent to consider the potential influence of protein expression levels on the oligomerization state

of proteins, particularly for those proteins like LHR that are expressed in low numbers under physiologic conditions [46, 160].

Our initial studies **(Figure 21)** used homo-FRET techniques to show that 37,000 LHR per cell stably expressed in CHO cells were more likely to exist as dimers, a result in agreement with results obtained using other methods suggesting that LHR exist as constitutive dimers [2, 7, 27, 140, 149, 192, 193, 255]. In addition, when cells were treated with 100 nM hGC, LHR appeared to form high order oligomers [196]. To investigate how the expression level of LHR impacts the receptor-containing clusters, we assessed the effect of LHR expression levels on the oligomerization states of unbound receptors and of receptors on cells treated with hCG or DG-hCG. We also examined the effects of cholesterol depletion on receptor oligomerization and the receptor's ability to signal productively. Four stable cell lines that differed in expression levels of LHR were generated. We measured changes in receptor cluster size in each cell line using homo-FRET techniques and then explored the effect of LHR numbers and the receptor oligomerization state on intracellular cAMP levels using the ICUE3 probe.

3.2. Methods and Materials

3.2.1. Materials

CHO-K1 cells were kindly provided by Dr. Takamitsu Kato in Department of Environmental and Radiological Health Sciences at Colorado State University. These cells were purchased originally from American Type Culture Collection (Manassas, VA). Dulbecco's Modified Eagle medium (DMEM) and geneticin were purchased from Corning Cellgro (Visalia, CA). Penicillin/streptomycin (P/S) and L-glutamine solution were purchased from Gemini Bio-Products (West Sacramento, CA). Fetal bovine serum (FBS) was purchased from Atlas Biologicals (Fort Collins, CO). 100 x MEM non-essential amino acid solution, bovine albumin and

ethylenediaminetetraacetic acid (EDTA) were purchased form Sigma-Aldrich (St. Louis, MO). Trypsin-EDTA (0.25%) was purchased form Fisher Scientific Co (Pittsburgh, PA). Rhodamine 6G was purchased from Eastman Kodak (Rochester, New York). Lipofectamine 3000 was purchased from Life Technologies (Carlsbad, CA). Quantum FITC MESF (molecules of equivalent soluble fluorophore) beads were purchased from Bangs Laboratories, lnc. (Fishers, IN). Optimal-MEM™ was purchased form Life Technologies (Carlsbad, CA). hCG was purchased from Fitzgerald Industries (Acton, MA). DG-hCG was kindly provided by Dr. George R. Bousfield, Department of Biological Sciences at Wichita State University. WillCo glass bottom cell culture dishes with 35 mm diameter wells were purchased from *In Vitro* Scientific (Sunnyvale, CA). A plasmid containing the entire coding region of the human LHR sub-cloned into pEYFP-N1 was kindly prepared by Dr.Ying Lei **(Figure 22)**. For western blots, the primary antibody used was a Chp grade anti-GFP antibody. The secondary antibody was a HRP-conjugated anti-rabbit antibody that was kindly provided by Dr. Claudia Wiese in the Department of Environmental and Radiological Health Sciences at Colorado State University. For cAMP measurements, the ICUE3 plasmid was provided by Dr. Jin Zhang. Forskolin was purchased from Enzo Life Sciences (New York, NY). MDL-12,330a hydrochloride was purchased form Sigma-Aldrich (St. Louis, MO). For lipid fluidity measurement, the phase-sensitive aminonaphthyl ethenylpyridinium-based dye, Di-4-ANEPPDHQ was purchased from Invitrogen (Carlsbad, CA).

3.2.2. Cell lines

CHO cells stably expressing LHR were prepared with 0.5 µg/µL of hLHR-eYFP plasmid using Lipofectamine 3000 in accordance with Manufacturer's instructions. Contents of a microcentrifuge tube containing 125 µL of optimal-MEM™ Media and 7.5 µL Lipofectamine 3000 reagent were mixed with contents of a second microcentrifuge tube containing 250 µL of

optimal-MEM medium, 2.5 µg/µL of hLHR-eYFP and 2 µL/µg DNA of Lipofectamine 3000 and incubated at room temperature for 10-15 minutes. The mixture was then added to cells in one well of a 6-well plate. Transfection of the cells progressed for 24 - 48 hours.

For stable cell line selection, optimal-MEM medium was replaced with medium containing G418 and cells were fed every 2-3 days with fresh medium. After 2-3 weeks post-transfection, cells were selected that stably incorporated the hLHR-eYFP plasmid into their genomic DNA. Negative and positive controls for transfection were included. In one negative control, cells incubated without hLHR-eYFP or pEGFP plasmids and without G418 were expected to be alive in the end of selection process. In a second negative control, cells without hLHR- eYFP or pEGFP plasmid and with media containing G418, were expected to have died by the end the selection process.

Stable cell lines were maintained in DMEM with 10% FBS, 1% P/S, 1% L-glutamine, 1% 1x non-essential amino acids and 200 µg/mL of geneticin. Untransfected CHO cells were maintained in DMEM with 10% FBS, 1% P/S, 1% L-glutamine, 1% 1x non-essential amino acids but without 200 µg/mL of geneticin. These two cell populations were maintained in 5% CO_2 at 37°C.

3.2.3. Western immunoblotting for evaluation of plasma membrane expression of LHR

Cells plated in 35 mm dishes were lysed in lysis buffer (pH 6.8) containing 150 mM NaCl, 100 mM Tris-buffered saline (pH 8), 1% Tween 20, 50 mM diethyldithiocarbamate, 1 mM EDTA, and 1 mM phenylmethylsulfonyl fluoride. A protease inhibitor was added together with the lysis buffer. Cell were sonicated 5 times for 1 sec on ice. Then, supernatants of centrifuge lysates that had been centrifuged at 12,000 rpm at 4 °C for 30 min were transferred to new tubes. The protein concentration of each tube was determined using a BCA protein assay kit. Approximately, 50 µg

of protein containing hLHR and 5x sample buffer was incubated at 100 °C for 5 min. Samples were run on 10% SDS-polyacrylamide gels and transferred to polyvinylidene fluoride or polyvinylidene difluoride (PVDF) membranes. The membranes were blocked overnight in 5% non-fat dry milk in TBST and incubated for one hour at 4 °C with anti-GFP antibody diluted 1:10000 in 5% non- fat dry milk in Tris-buffered saline with Tween (TBST). Membranes were then washed with PBS two times for 5 min. HRP-conjugated anti-rabbit antibodies were added for 60 min at room temperature followed by washing with PBS and detection using enhanced luminol-based chemiluminescent substrate kit as described by the Manufacturer. As a loading control, α-tubulin primary antibody was incubated for 60 min at a 1:1000 dilution in 5% non-fat dry milk in TBST followed by a 60 min incubation with HRP-conjugated anti-rabbit antibodies.

3.2.4. Sample preparation for flow cytometry sorting

Cells were grown to 80-90% confluence in a 25 cm^2 culture flask and then incubated with 1.0 ml trypsin-EDTA (0.25%) for 3 min. The flask was lightly washed with 3 mL of 1xPBS and the 3 mL effluent containing cells was placed into a 5 mL VWR polypropylene tube for flow cytometric analysis. Cells number needed to be between 10^5 and 10^6 cells per mL. The Moflo Astrios EQ flow cytometer located in the Molecular and Radiation Biology Building at Colorado State University was used in these experiments. Fluorescence intensity was collected using a 488 nm argon ion laser as an excitation source and a 525/40 nm emission filter. Moflo Astrios EQ software was used to obtain fluorescence signal intensities from individual cells or from Quantum FITC molecules of equivalent soluble fluorophores (MESF) bead standards.

3.2.5. Flow cytometry data analysis

To quantify LHR numbers expressed on stably transfected cells, Quantum FITC MESF bead standards were used. In a Quantum MESF kit, each microsphere population had a MESF value that was equivalent to the number of FITC molecules in solution. The MESF values for the blank, bead standard 1, bead standard 2, bead standard 3, bead standard 4 and bead standard 5 were zero, 2003, 11639, 43155, 179437 and 527664 fluorescein equivalents, respectively. The intensity values for the bead standards in flow cytometry are shown in **Figure 23**. The signals measured for hLHR-eYFP on the cell surface required that those signals be related to signals from the Quantum FITC-MESF beads. The beads needed to be analyzed for signal on the same day, in the same buffer used for hLHR-eYFP cell samples and using the same instrument settings such as amplifier gain, compensation and PMT voltage.

Since there are no bead standards for eYFP, the measurements for FITC standard beads was converted to eYFP fluorophore signals obtained from cell samples using the following calculations. The relative fluorescence signal R_B for one bead molecule measured in the cytometer was obtained using the **Equation 3**

$$R_B = A\varepsilon_B(\lambda_{max,B})\left(\frac{a_B(\lambda_{exc,B})}{a_B(\lambda_{max,B})}\right)\Phi_B \frac{\int_{\lambda_{c,B}-w_B/2}^{\lambda_{c,B}+w_B/2} f_B(\lambda)\,e(\lambda)d\lambda}{\int_0^{\infty} f_B(\lambda)d\lambda} \quad (3)$$

where ε_B ($\lambda_{max,B}$) is the molar absorptivity coefficient of the given bead dye molecule. at its maximum absorption wavelength $\lambda_{max,\mathbf{B}}$, Φ_B is fluorescence quantum yield, a($\lambda_{exc,B}$) is the fractional absorbance for the bead dye molecule at the excitation wavelength $\lambda_{exc,B}$. a($\lambda_{max,\mathbf{B}}$) is the fractional absorbance for the bead dye molecule at the maximum absorbance value. The upper integral in Eq. 3 is the integral of the bead fluorophore corrected emission intensity $f_B(\lambda)$ times the detector quantum efficiency e(λ) across the bead fluorophore filter bandwidth. The lower integral

is the corresponding integral over all wavelength spectra from 250 nm to 650 nm. The constant A, **Equation 4** , essentially unimportant here, involves the exciting light wavelength λ, the intensity I on the chromophore of exciting light, the efficiency e of delivery of fluorescence photons to the detector and subsequent detection of primary photoelectrons, Avogadro's number N_A, Planck's constant h and the speed of light c.

$$A = \frac{2303 \lambda I e}{N_A h c} \tag{4}$$

The detected fluorescence signal R_P for one fluorescent protein molecule (eYFP) on a cell is given by **Equation 3** but with all subscript "B" changed to "P" to indicate quantities for the fluorescent protein instead of beads. The ratio R_B / R_P can thus be calculated for a pair of bead and protein fluorophores from photophysical data.

Cytometric measurements of beads using emission filters appropriate to the target protein provided calibration curves of the Manufacturer's numbers N_B of FITC per bead versus measured mean fluorescence intensity S_B of FITC per bead. The slope N_B//S_B of such a curve is the number of bead fluorophores per unit bead fluorescence detected under conditions used to measure the protein of interest. Measurements of protein fluorescence S_P were then obtained for cells using the same emission filters. Finally, the number of fluorescent hLHR-eYFP molecules N_P expressed on each cell is given by **Equation 5**

$$N_p = \left(\frac{N_B}{S_B}\right) * \left(\frac{R_B}{R_p}\right) * S_P \tag{5}$$

where S_B is fluorescence signal for beads containing N_B number of dye molecules and S_P is the fluorescence signal of a particular cell. The ratio R_B / R_P as described above.

To calculate YFP numbers from measurements on FITC beads [256], we used the peak molar absorptivity of FITC, 75,800 L $mol^{-1}cm^{-1}$ at 498 nm, the fraction of maximum molar

absorptivity, 0.77 at an excitation wavelength of 488 nm, and the YFP fluorescence quantum yield of 0.48. The (upper) integral over the filter bandwidth is 778 nm, and the total emission (lower) integral is 5010 nm. **Equation 3** then gives R_b as A*4373 s^{-1}. In addition, it is known that YFP has a peak molar absorptivity of 84,000 L mol^{-1} cm^{-1} at 514 nm, that the fraction of that maximum molar absorptivity is 0.38 at an excitation wavelength of 488 nm, that the fluorescence quantum yield is 0.61. the (upper) integral over the filter bandwidth is 626 nm, and the total emission (lower) integral is 3808 nm. From **Equation 3**, R_P is A*3212 s^{-1}. Thus, the ratio RB /RP is 1.36, consequently, the number of YFP per cell is 1.36 times the number that would be inferred from FITC bead standards assuming the cells bore FITC-tagged molecules. **Table 3** summarizes the numbers used in this calculation.

3.2.6. Treatment of cells

Stock solutions of 10 µM of hCG, 10 µM DG-hCG, 100 mM MβCD, 100µM forskolin, and 10 µM of *cis*-N-(2-Phenylcyclopentyl)-azacyclotridec-1-en-2-amine hydrochloride (MDL-12,330a hydrochloride) were made by dissolving these compounds in phosphate-buffered saline (PBS) containing 1mM $CaCl_2$ and 0.5 mM $MgCl_2$ and adjusting the pH to 7.4. For experimental measurements, the final concentrations of hCG and DG-hCG used experimentally were 100 nM, 30 nM, 10 nM, 1 nM and 0.1 nM. 10mM MβCD was used for cholesterol depletion. 50µM forskolin was used as cAMP positive control, and 10 µM MDL-12,330a hydrochloride was used as cAMP negative control.

3.2.7. Sample preparation for polarized homo-FRET experiments

Four populations of stable cell lines expressing averages of 10,000, 32,000, 123,000 or 560,000 LHR per cell were established. Cells were grown to 80-90% confluence in 25 cm^2 culture

flask and then incubated with 1.0 ml trypsin-EDTA (0.25%) for 3 min. Cells (0.5 mL) were plated in a 35 mm glass bottom petri dish and, after 6-12 hours, were washed twice with 1xPBS (pH 7.3) and suspended with solutions of PBS alone or with MβCD for 1hr or various concentrations of hCG, or DG-hCG for 1 hr. One hr was sufficient for hCG to activate LHR and for hormone effects on the formation of LHR clusters. It has previously been shown that clustering of LHR receptors occurs within minutes and these clusters do not dissociate for several hours [8, 194]. After taking the dishes from the incubator, cells were washed once, resuspended in 1x PBS and immediately imaged with a Zeiss Axiovert 200M inverted microscope. For untreated cells, the cell pellet was resuspended in PBS alone.

3.2.8. Homo-FRET measurements

Energy transfer between chromophores such as eYFP molecules occurs only when donor eYFP and acceptor eYFP are within 2-10 nm of one another [257]. To measure homo-FRET, a Zeiss Axiovert 200M inverted microscope with an Andor DU897E EMCCD camera was used. Images were acquired using an arc lamp for fluorescence excitation together with a polarized excitation filter. Fluorescence emission was collected using eYFP emission filter and a 63x water objective for observing cells. All filters were from Chroma Technology. **Figure 24** showed the experimental setup that used in this measurement. Cells were photobleached for 15 minutes. One image was obtained each minute using a 15 second exposure time. Parallel and perpendicular fluorescence emission images were obtained simultaneously using a Photometrics Dual View image dissector. These images were oriented with respect to the polarization of the exciting light. The microscope focus was adjusted so that the cell membrane appeared as a ring-like shape. Background was subtracted from fluorescence emission images. MetaMorph software allowed us to acquire and visualize cells during individual experiments.

Image J software was used for the calculation of the fluorescence anisotropy by obtaining the parallel and perpendicular fluorescence intensities from cell measurements and rejecting out fluorescence intensities from cell cytoplasmic. These intensities were used to calculate anisotropy. The fundamental anisotropy (r_0) of eYFP fluorophore is 0.38 [171, 230] and we assumed that the fundamental anisotropy of LHR tagged with eYFP was close to ~0.38 which represents an immobile monomer receptor. The intrinsic anisotropy was adjusted to 0.38. For each petri dish, 5-7 cells were recorded for a total of at least 30 cells for each treatment. To avoid internalization of LHR, images were acquired within 30 minutes for each petri dish used [241].

3.2.9. Experimental determination of the G factor

The G factor was calculated using rhodamine 6G dye to correct for efficiency differences in instrument optics. The G factor in **Equation 6** is the correction factor for differences in vertical and horizontal polarized fluorescence detection sensitivity in our instrumental setup. The G factor compensates for optical properties such as reflections from mirrors, objective or lenses that may change the polarization of excitation light. The G factor can be estimated from a reference aqueous solution with a known anisotropy value near zero such as rhodamine 6G. Rhodamine 6G has an anisotropy value of about 0.012 and emits completely depolarized light because it can rotate freely and quickly. During measurement of the G factor, the polarization excitation filter is removed and rhodamine 6G (R6G) is excited by a depolarized light source. Since the anisotropy of rhodamine 6G is expected to be zero, The G factor can simply be calculated by the following equations

$$G = I_v / I_h \tag{6}$$

where I_v is the intensity of emission that is vertically oriented and I_h is the intensity of emission that is horizontally oriented with respect to the non-polarized excitation light.

A background was measured using water and under the same conditions used to examine R6G. This background was subtraced from Rhodamine 6G signal before calculating the G factor using Image J. In an ideal setup, G would be equal to one. However, in our instrument the G factor ranged from 1.27 to 1.34. This means that the detection sensitivity in our instrument was higher for parallel polarization measurements than it was for perpendicular polarization measurements. The G factor was then used to calculate the fluorescence anisotropy r.

3.2.10. ICUE3 transient transfection for measurement of intracellular cAMP

The four stable cells lines with an average of 10K, 32K, 122K or 560K hLHR- eYFP per cell were transiently transfected with 0.4 μg of cAMP level reporter ICUE3 plasmid provided by Dr. Jin Zhang using Lipofectamine 3000 in accordance with the Manufacturer's instructions. The contents of two sterilized microcentrifuge tubes, one containing 125 μL of optimal-MEM™ Media and 7.5 μL Lipofectamine 3000 and the other containing 250 μL of optimal-MEM Medium, 0.4 μg of ICUE3 and 5 μL Lipofectamine 3000, were mixed and incubated at room temperature for 10-15 minutes. This mixture was then added to the cells in a 35 mm petri dish containing 1mL optimal-MEM™ Media. Transfection took approximately 24-48 hrs. Cells were maintained in 5% CO_2 at 37°C during ICUE3 transfection.

3.2.11. Sample preparation for hetero-FRET studies of intracellular cAMP using ICUE3

Following transient transfection with ICUE3, cells were washed twice with 1xPBS, pH 7.3, and suspended in PBS, hCG, DG-hCG, 50nM forskolin or 100 μM MDL-12,330a hydrochloride. Forskolin was used as a positive control to activate adenylate cyclase. MDL-12,330a hydrochloride inhibits adenylate cyclase and serves as a negative control. After taking dishes from the incubator, cells were washed once, resuspended in PBS and immediately imaged. Seven

images of untreated cells were acquired every minute for 6 minutes beginning at time zero. Treatments were then added with 15 min incubation and then 10 images were acquired every minute. All images were acquired using a 63x 1.2 NA water objective and a Zeiss Axiovert 200M inverted microscope with an Andor DU897E EMCCD camera. Images were acquired using an arc lamp with a 436DF20 excitation filter and two emission filters, 480DF40 for CFP and 535DF30 for YFP and YFP sensitized emission (YFPSE) due to energy transfer from CFP. All filters were from Chroma Technology. **Figure 25** shows the experimental set up that used in this measurement. MetaFluor software was used to observe and image cells during experiments. Images were acquired at 60s intervals. Backgrounds were subtracted from fluorescence images and data were analyzed using Image J software to calculate the emission intensity ratios CFP/YFPSE. For each petri dish, 2-5 cells were observed and data were collected from a total of 15 cells in various dishes for each treatment [256].

3.2.12. Measurement of plasma membrane lipid order

Four stable cell lines (10K, 32K, 122K, and 560K LHR per cell) and untransfected CHO cells were grown to 80-90% confluence in 25 cm2 culture flasks and then incubated with 1.0 mL trypsin-EDTA (0.25%) for 3 min. Cells (0.5 mL) were seeded into a 35 mm glass-bottom petri dish. After 12 hours, cells were washed twice with 1x PBS (pH 7.3) and labeled and suspended in 200 µL of 1.5 µM the environmentally-sensitive dye di-4-ANEPPDHQ for 15 min, washed and immersed in 1x PBS buffer for imaging using a Zeiss Axiovert 200M inverted microscope equipped with a 63x 1.2 NA water objective and an Andor Du897E EMCCD camera Cell samples were illuminated with an arc lamp with a 480/30x or 495/20x excitation filter. Fluorescence emission was collected simultaneously in channel 1 using a 535/40nm filter and in channel 2 using a 620/40 nm filter. MetaFluor software was used to observe and image cells during experiments.

Background correction for each image and fluorescence intensity ratio of 620nm/535nm calculation were performed using Image J. Images of control cells not labeled with di-4-ANEPPDHQ were subtracted from the four population groups to remove fluorescence from eYFP-LHR.

3.2.13. Statistical analysis

Data are expressed as the mean ± SEM. Statistical evaluation of mean differences between untreated groups and treatment groups were analyzed by one-way ANOVA followed by the Tukey multiple comparison test and Student's t-test to compare between two groups using R version 3.3.1. P values of less than 0.05 were considered statistically significant.

4. CHAPTER 4: RESULTS AND DISCUSSION

4.1. The effect of expression level on cluster size of LHR.

Changes in expression level might alter and affect the oligomerization state and function of LHR since it has been found that the overexpression of proteins leads to a crowded environment and can increase the likelihood of protein oligomerization [10]. Our initial data using homo-FRET suggested that LHR might exist mainly as dimers, a result in agreement with results suggesting that LHR exist as constitutive dimers [2, 7, 27, 140, 149, 192, 193, 255]. However, other studies suggest that LHR exist as monomers in the absence of hormone [182]. The conflict may raise from the differences in expression level, high values of which might drive aggregation of LHR monomers into dimers or oligomers as seen by others [2, 7, 27, 140, 149, 192, 193, 255]. To investigate how the expression level of LHR impacts the cluster size of LHR, we assessed the effect of LHR numbers on the oligomerization state of unstimulated cells and cells treated with hCG, DG-hCG and MβCD. Thus, four cell lines that differ in expression levels of LHR were generated. We then measured the cluster size in each of them using homo-FRET techniques. The oligomerization of LHR that might result from high expression levels may also contribute to human diseases related to LHR aggregation. Therefore, the potential influence of expression level on oligomerization state of proteins specially those proteins that naturally exist at low expression level as do LHR [46, 160], must be considered.

4.1.1. Characterization of cell lines stably expressing LHR

Stable CHO cell lines expressing LHR-eYFP were generated as shown in **Figure 26A**. Images of membrane-associated fluorescence from LHR-eYFP were obtained with a Zeiss Axiovert 200M inverted microscope and expression was confirmed using western blot analysis as

shown in **Figure 26 B**. Lanes 2 and 3 in **Figure 26 B2** are stable cell lines expressing LHR-eYFP with different loading concentrations.

After confirming expression of functional LHR-eYFP, we used flow cytometry to sort four populations of these cells based on the number of LHR per cell as established using FITC bead standards **(Figure 23)**. Cell populations expressing an average of 10,000 LHR per cell, 32,000 LHR per cell, 122,000LHR per cell or 560,000 LHR per cell were obtained. Calibration curve for conversion of the receptors number per cell in flow cytometry to numbers of receptor per cell in fluorescence is shown in Appendix I.

4.1.2. Fluorescence anisotropy of LHR is dependent of receptor expression level

The oligomerization of membrane proteins such as LHR is often necessary for function. The oligomerization state of LHR in live cells was observed using polarized homo-FRET measurements and was manifest as a decrease in fluorescence anisotropy with increasing cluster sizes. Experimentally, homo-FRET results were quantitated from an increase in fluorescence anisotropy upon fluorescence photobleaching, *i.e.*, steady state anisotropy. The enhancement of florescence anisotropy upon photobleaching was used to distinguish between protein rotational effects and homo-FRET effects on anisotropy [171, 207, 208]. Photobleaching effectively reduced the number of fluorophores in a cluster over time. This led to an increase in fluorescence anisotropy and reduced transfer of energy between eYFP molecules due to the reduced numbers of fluorescence acceptors. Therefore, increases in anisotropy resulted from decreased energy transfer in response to fluorophore photobleaching.

A simulation of fluorescence anisotropy enhancement upon photobleaching is shown in **Figure 27**. This shows simulated anisotropy curves for photobleaching of homogeneous populations of monomers, dimers, and higher-order oligomers. Photobleaching of a homogeneous

population of monomers does not change the fluorescence anisotropy values while higher order oligomers demonstrate an upward, curved increase in anisotropy with photobleaching.

Examination of cell lines expressing LHR showed initial fluorescence anisotropy significantly lower than predicted for monomeric proteins, 0.38. This indicates that LHR are likely to exist as mixtures of monomers and dimers or some high aggregate, (**Figure 28)**. With increased expression of LHR as shown in **Figure 29-31**, it appears that receptors exist in a more crowded environments with increased numbers of dimers and larger oligomers. This is a reasonable result based on previous observations that receptors such as neurokinin-1 receptors, when over-expressed in cells, are more extensively clustered than when the same receptors are expressed in lower numbers in the same cell type [10]. In contrast, the oligomerization state of serotonin1A receptors in cells is independent of expression levels [171] as has also been reported for GPI-anchored proteins [161]. This suggests that there is no single model for the relationship between protein oligomerization and protein expression levels. Thus, it is very important to study the relationship between oligomerization and expression levels for each protein on an individual basis.

Figures 29 examines in more detail the relationship between initial fluorescence anisotropy and LHR expression levels. These results suggest that the oligomerization state of LHR is highly dependent on the number of LHR expressed per cell. With increased expression, LHR become more clustered and fluorescence anisotropy decreases. These data are summarized in **Table 4**.

The curvature found in **Figure 29** for initial anisotropy for the four expression groups and **Figure 30** for anisotropy during photobleaching for the four expression groups indicate that the cluster size of LHR is increased as LHR expression increased. Moreover, the correlation between anisotropy and receptors number per μm^2 during photobleaching is shown in Appendix I.

4.1.3. Effects of hCG on LHR oligomerization

GPCR can function as monomers, dimers or oligomers after binding ligand. Such ligation can either increase, decrease or have no effect on the GPCR oligomerization state depending on receptor type [25]. Therefore, there are no general rules governing the effect of ligand binding on the degree of receptor oligomerization.

LHR, upon binding hormone, exist as dimers or oligomers at the plasma membrane as suggested by fluorescence recovery after photobleaching studies [8, 194], use of fluorescence resonance energy transfer techniques such as homo-FRET or hetero-FRET [3, 8, 118, 149, 182], electron microscopic analysis of LHR using ferritin-labeled LH [195] and co-immunoprecipitation studies [193]. Moreover, we have found that the cluster size of hLHR increases in a hormone concentration-dependent manner [196]. Nevertheless, the effect of hCG on LHR oligomerization has not been studied using cells with well-defined numbers of receptors per cell.

As shown in **Figure 32**, fluorescence anisotropy during photobleaching, serving as a readout for LHR oligomerization state was dependent on receptor expression levels. Treating cells that expressed low numbers of LHR per cell with 100 nM hCG produced a significant decrease (0.101±0.005) in anisotropy indicating that hormone binding increased LHR cluster size. When cells expressed higher numbers of LHR per cell and were treated with 100 nM hCG, there is no change in fluorescence anisotropy indicating that LHR are already aggregated and hormone binding does not drive further protein-protein interactions.

Values for initial fluorescence anisotropies in hCG-treated cells as a function of LHR expression are shown in **Table 5**. The effect of hCG on the cluster size of LHR was concentration-dependent when cells expressed low numbers of LHR per cell (**Figure 33**). As the number of LHR

per cell increased, the effect of hormone on oligomerization of LHR was negligible, presumably because these receptors are aggregated already (**Figure 33**).

4.1.4. Effect of DG-hCG on LHR oligomerization

DG-hCG has been found in serum from male patients with chronic renal failure and suffering with hypogonadism [114]. The DG-hCG used in these studies was prepared using TFMS to remove carbohydrate groups [124, 125]. Chemically-modified DG-hCG binds LHR with the same affinity as hCG but exhibits little or no ability to stimulate cAMP levels within cells [112, 114, 122, 123, 127-129]. Because DG-hCG also competes with hCG for binding to LHR DG-hCG is described as an hCG antagonist.

The effect of DG-hCG on the oligomerization of LHR has not been extensively characterized, particular in cells where the number of LHR per cell is well characterized. In experiments described here, concentration-dependent effects of DG-hCG on LHR oligomerization were evaluated as shown in **Figure 34**. DG-hCG treatment increased fluorescence anisotropy in cells expressing an average of 10K LHR per cell indicating that it is likely that cluster size is reduced in response to DG-hCG. Effects of DG-hCG were more pronounced with increases in the expression level of LHR per cell. The values for initial fluorescence anisotropies of DG-hCG-treated cells with different concentration are shown in **Table 6.**

4.1.5. Effect of cholesterol depletion on receptor oligomerization

Membrane cholesterol has important roles in the function and organization of many membrane proteins [1, 166-173] and can modulate the stability of membrane protein dimers [173, 179, 189, 190]. Depletion of cholesterol by MβCD affects the function of many proteins [1, 166-168] although mechanistic details are not known. Membrane cholesterol may interact directly or

indirectly with membrane proteins to induce conformational changes in proteins or alter the physical properties of lipid membranes. Both of these cholesterol effects could, in turn, modulate formation of protein oligomers or alter the stability of protein oligomers [1, 164, 172, 177, 178]. Previous studies have suggested that membrane cholesterol is important in the formation of GPI-anchored protein clusters [189], μ-opioid receptor clusters [190] and serotonin 1A receptor clusters [166, 171, 173, 188, 258].

In this study we found that membrane cholesterol depletion affects LHR clusters in cells expressing both high and low receptor numbers. Thus, LHR clusters in the plasma membrane are associated with cholesterol-containing membrane microdomains and this association is independent of receptor expression levels (**Figure 35**). However, depletion of membrane cholesterol by MβCD had greater affects in cluster sizes in cell lines expressing higher numbers of LHR per cell (**Figure 35**). Given the number of GPCR and other membrane proteins that utilize cholesterol-enriched microdomains in signaling mechanisms, membrane microdomains may provide a drug target for reducing the effects of receptor over-expression in some disease processes by effectively increasing receptor monomers and limiting formation of dimers or higher order oligomers [259].

hCG treatment of cells pre-treated with MβCD reduced the effect of MβCD on cluster size. This suggested that presence of hCG, after cells were treated with MβCD, might recruit cholesterol into association with LHR leading to a decreased effect of MβCD **(Figure 35)**. The actual mechanism involved in hCG effects on cells pre-treated with MβCD remains unknown and its elucidation will require additional work.

Other investigators have found that hCG effects on the production of endogenous testosterone could restore normal reproductive function in cells exposed to vanadium compounds

[260]. This observation agrees with our results from experiments where hCG treatment of cells pretreated with MβCD where hCG reduced effects of vanadium compounds. Interestingly, vanadium compounds were found to decrease cell-surface plasma membrane lipid order as assessed using di-4-ANEPPDHQ [261] in a manner similar to MβCD **(Figure 36).** Di-4-ANEPPDHQ has been reported to be a useful tool for probing membrane lipid order in live cells. [261-264]. In cells treated with di-4-ANEPPDHQ, the spectral properties of the dye are altered in response to lipid packing.

4.1.6. Effect of receptor oligomerization on cell plasma membrane lipid order

Previous work has shown that the oligomerization state of LHR is dependent on the number of LHR expressed per cell. When cells express higher numbers of LHR, receptors become clustered. This may be due to cholesterol stabilizing membrane protein dimers [173, 179, 189, 190]. However, we found that cholesterol depletion affects LHR clusters. Thus, how the number of LHR per cell is related to LHR interactions in the plasma membrane was investigated by examining the changes in membrane lipid order using di-4ANEPPDHQ as previously described [261-263]. As shown in **Figure 37,** cells expressing 122K and 560K LHR per cell have 640nm/545nm fluorescence emission ratios of 2.22±0.03 and 2.23±0.02, values that are significantly less than from ratios measured in cell lines expressing 10K or 32K LHR per cell. This indicates that tighter lipid packing occurs in cells expressing high number of LHR per cell and also explains why depletion of membrane cholesterol has greater effects on the oligomerization state of LHR in cells expressing 122K and 560K LHR per cell **(Figure 35).** This result also suggests that increased numbers of LHR per cell can lead to greater receptor association with cholesterol and that oligomers become more stable. Depletion of cholesterol in these cells may lead to a decrease in the cluster size **(Figure 35)**. Thus, the role of cholesterol in forming and

stabilizing the oligomerization of membrane proteins may be a promising area of research. Modulating that the concentration of cholesterol in the plasma membrane and, as a result, the oligomerization state of membrane proteins, might prove to be a helpful pharmacologic strategy [259]

4.2. The effect of LHR expression levels as well as cluster size of LHR on receptor activity

Molecular crowding resulting from high protein expression levels has effects on cell membrane molecular structure. These effects include change in folding, shape, conformational stability, diffusion, ligand binding, enzymatic activity, and downstream signaling [119, 149, 158-160]. It also appears that the clustering of LHR plays an important role in signaling, desensitization and internalization of the receptors after activation by hormone [2-8]. Thus, the effect of the oligomerization state on receptor function is important.

The overexpression of neurokinin-1 receptors leads to a crowded membrane environment and increases the receptor's oligomerization state [138]. This may lead to increased intracellular cAMP. Also, it has been reported that the basal level of cAMP rises as the expression level of β_2-adrenergic receptors increases [265]. Based on our finding that increased expression levels of LHR lead to aggregation of LHR, the relationship between the expression level of LHR, cluster size and intracellular cAMP were assessed experimentally.

To investigate how the expression level of LHR and cluster size of LHR are related, we evaluated the effects of LHR number and receptor oligomerization state on intracellular cAMP levels in unstimulated cells and cells stimulated with hCG, DG-hCG and MβCD. The ICUE3 cAMP sensor was used to measure changes in intracellular cAMP in four population of cells with different expression levels of LHR.

4.2.1. High expression levels of LHR are associated with elevated intracellular cAMP

Previous studies have shown that a change in the expression level of wild type LHR from 600 to 125,000 LHR/cell increases cAMP production in response to hormone as illustrated in **Figure 14** [159]. In addition, studies using FSHR demonstrated that low expression levels of FSHR mimic the activity of a mutated FSHR (A189V) that is unable to produce cAMP even in present of hormone **(Figure 13**; [150]**)**. However, there have been no studies evaluating the effect of LHR expression levels on production of cAMP when receptor numbers are well characterized. In this project, the impact of expression levels of LHR on intracellular cAMP was evaluated using ICUE3 (**Figure 20**). This cAMP sensor has an N-terminally truncated Epac1 protein fused to an eCFP donor and a cpV-L194 (Venus) acceptor. Venus is an improved version of eYFP [231, 236, 243] and is referred to as eYFP in this dissertation. In the absence of cAMP, ICUE3 folds in such a way that the distance between eCFP and eYFP is less than 10 nm. When eCFP is excited with 440 nm light, energy transfer from eCFP to eYFP occurs due the close proximity of these molecules so that donor emission overlaps with acceptor excitation wavelengths. As a result, there is a low level of eCFP emission. In the presence of cAMP, cAMP binds to ICUE3 which undergoes a conformation change causing separation of eCFP and EYFP. This is accompanied by reduced FRET. Thus, an increase in the emission intensity ratio of eCFP to eYFP reflects cAMP presence. This permits monitoring relative changes in intracellular cAMP levels in response of LHR activity.

As discussed above, the cluster size of LHR is dependent of receptor expression levels. Therefore, it is important to examine the effect of receptor expression on intracellular cAMP levels in unstimulated cells. Therefore, we evaluated the basal levels of intracellular cAMP in four cell populations with different LHR expression levels. The data illustrated in **Figure 38** indicate that

there is a positive relationship between LHR numbers per cell and receptor activity. This positive relationship was also found between LHR numbers per cell and receptor oligomerization **(Figure 31)**.

4.2.2. hCG promotes an increase in intracellular cAMP when receptor numbers per cell are low

hCG was used to evaluate effects of hormone binding on intracellular cAMP as a function of LHR number. hCG treatment increased production of cAMP in cells that expressed comparatively fewer LHR per cell **(Figure 39)**. However, cells with highly expressed LHR (32k and 560k LHR per cell) had no significant change in cAMP levels suggesting that these LHR were maximally active even in the absence of hormone.

4.2.3. DG-hCG alters LHR aggregation and reduces cAMP production

Carbohydrate residues on hCG are essential for hormone function as well as for slowing of hCG clearance from the body [111-113]. When carbohydrates in hCG are removed by TFMS, DG-hCG results [124, 125]. DG-hCG binds LHR with the same affinity as hCG **(Figure 9A)** but results in little or no activation of AC to increase cAMP **(Figure 9B**; [112, 114, 122, 123, 127-129]**)**. Effects of DG-hCG are concentration-dependent [127] and, when the hormone is present in excess, can reduce the production of cAMP in cells treated with hCG or hLH [128, 132, 133]. This suggests that DG-hCG competes with these hormones for binding sites on LHR.

In this study, the effect of LHR expression level on the impact of DG-hCG on intracellular cAMP was explored. The ICUE3 sensor was used to measure changes in intracellular cAMP in four population of cells with different expression levels of LHR. Results showed that DG-hCG effects were dependent on LHR expression level. As shown in **Figure 40** and **Table 6**, the largest

effects of DG-hCG occurred when cells stably expressed higher numbers of LHR. At the lowest expression level of LHR, 10k LHR per cell, these was only a modest difference in cAMP levels between untreated cells having low basal levels of intracellular cAMP and cells treated with 100 nM DG-hCG. Cell lines expressing either 122k LHR per cell or 560k LHR per cell exhibited reduced intracellular cAMP levels with DG-hCG treatment more than lowest expression level of LHR. Both of these cell lines have high basal levels of intracellular cAMP in the absence of hormone and their LHR are constitutively active.

4.2.4. Effect of cholesterol depletion on cAMP production

Membrane cholesterol plays an important role in the function and dynamics of many membrane proteins [1, 166-173]. In particular, it modulates formation of membrane protein dimers [173, 179, 189, 190]. Previous studies found that both functional LHR exposed to hCG and constitutively active LHR are present in membrane microdomains enriched with cholesterol while unliganded LHR are located in the bulk membrane [181, 182]. Thus, membrane cholesterol affects the activity of LHR which require intact, cholesterol-containing microdomains for function. Depletion of plasma membrane cholesterol using MβCD reduces the ability of LHR to signal in response to hormone binding and lowers intracellular cAMP [181]. As shown in **Figure 40**, MβCD reduces the level of intracellular cAMP as the expression level of LHR increased. MβCD treatment also reduces the size of receptor clusters, particularly when LHR are expressed at higher numbers of receptors per cell. Nonetheless, it is not clear precisely how cholesterol affects LHR function. Cholesterol may interact directly or indirectly with membrane proteins, *e.g.* LHR. Direct interactions could alter the structure and function of the membrane protein in question while indirect effects on physical properties of membrane lipids could alter protein-protein interactions

and improve the stability of protein oligomers [1, 164, 172, 177, 178]. Measurements of cAMP levels in cells treated in the above ways are summarized in **Table 7.**

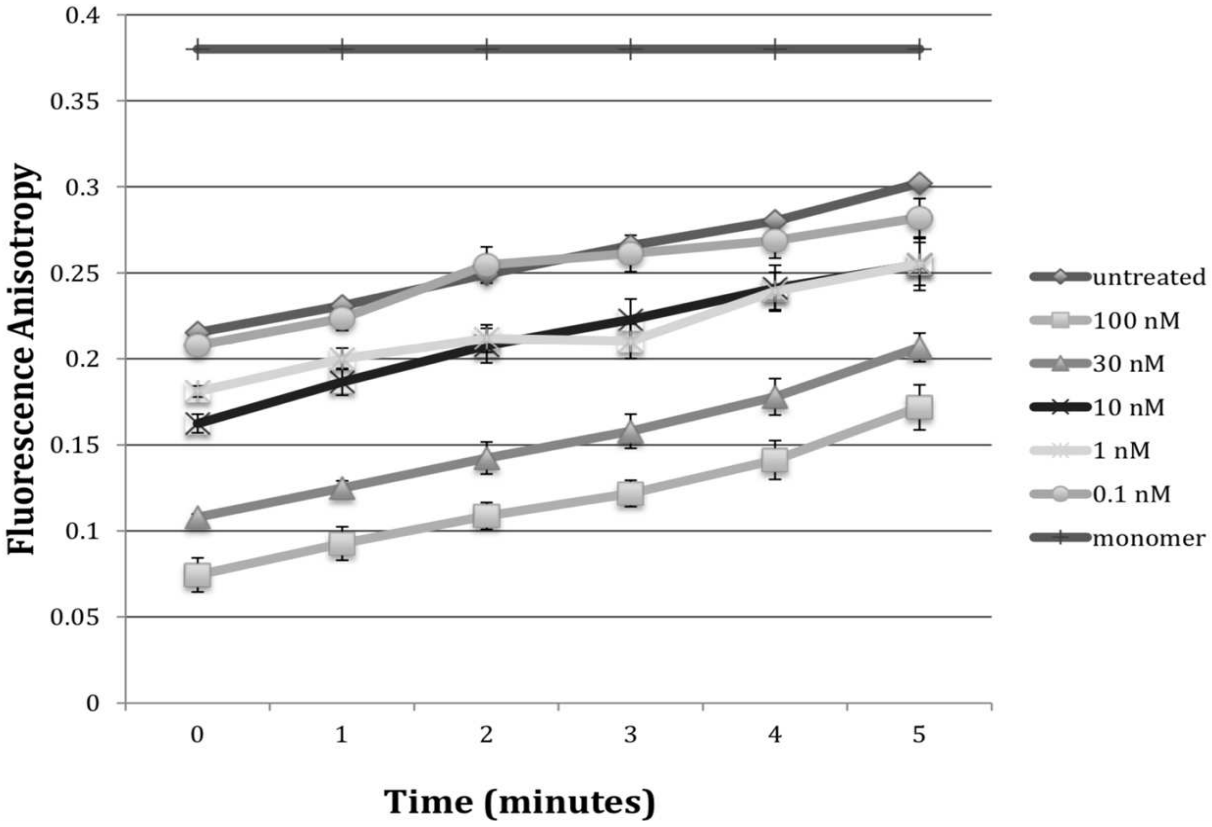

Figure 21: Fluorescence anisotropy as function of time during fluorescence photobleaching for up to 5 minutes. Cells expressed 37k LHR per cell.

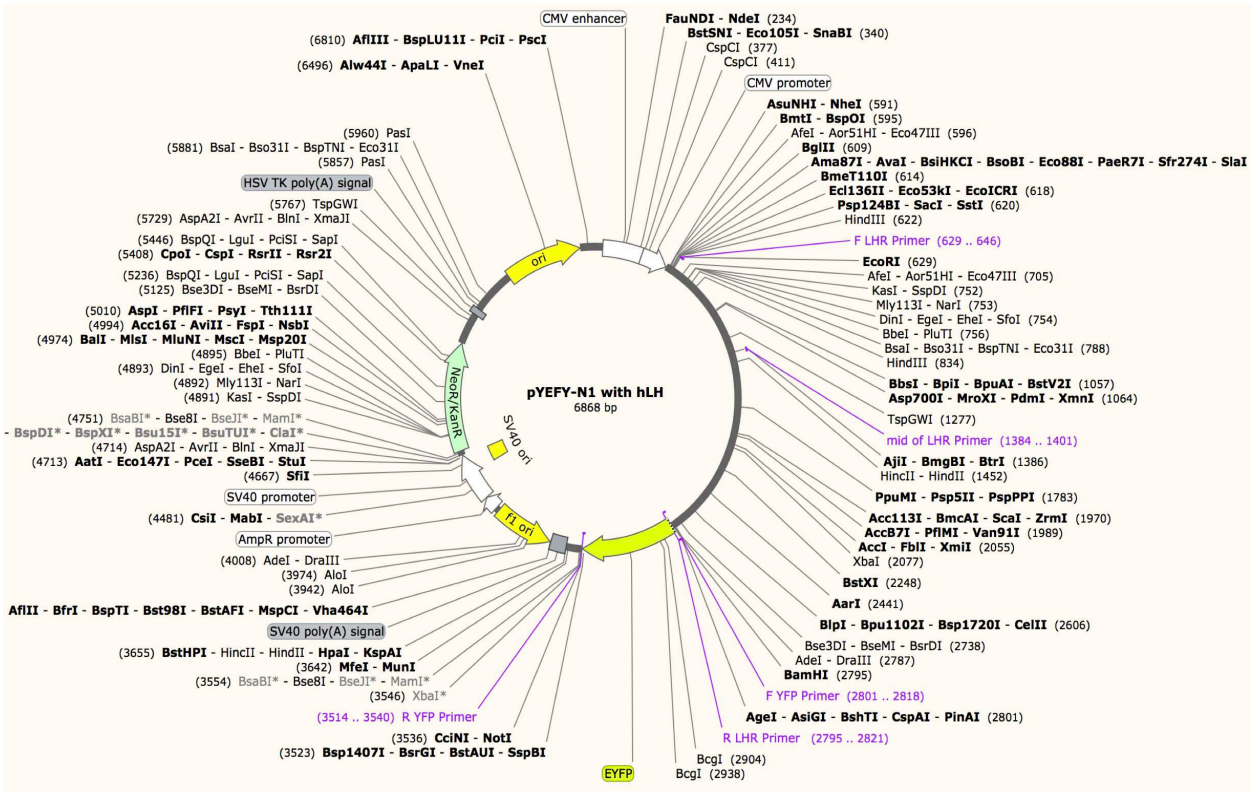

Figure 22: hLHR gene-containing plasmid used to generate stable hLHR-eYFP expressing cell lines. This plasmid contains the entire coding region of the hLHR sub-cloned into pEYFP-N1.

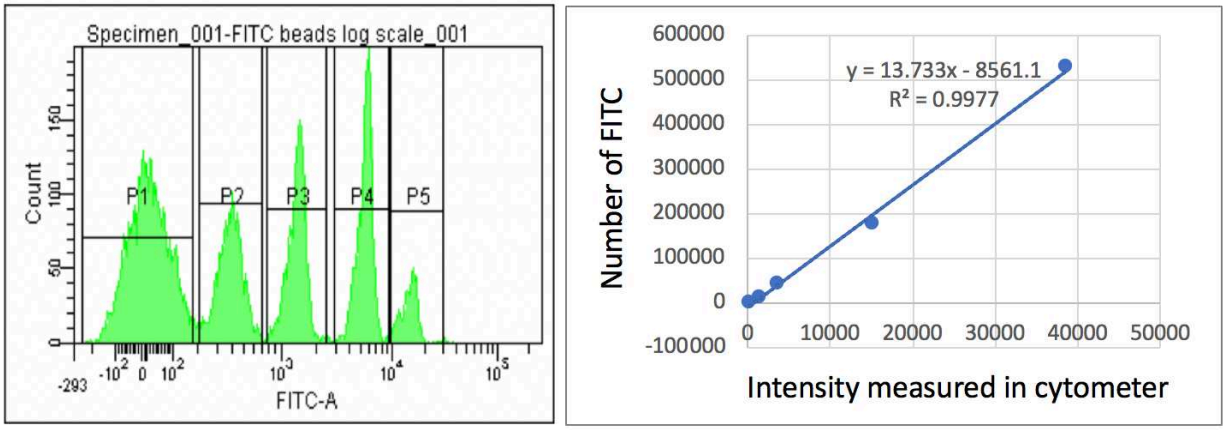

Figure 23: Flow cytometry data. The panel on the left shows the intensity histogram of the four Quantum FITC bead standards showing the number of beads (y-axis) detected in various fluorescence intensity channels (x-axis). The panel on the right is the calibration curve for the Quantum FITC bead standards relating Manufacturer's numbers of fluorescein (FITC) molecules per bead with the measurement mean intensity for that bead group as detected in the cytometer.

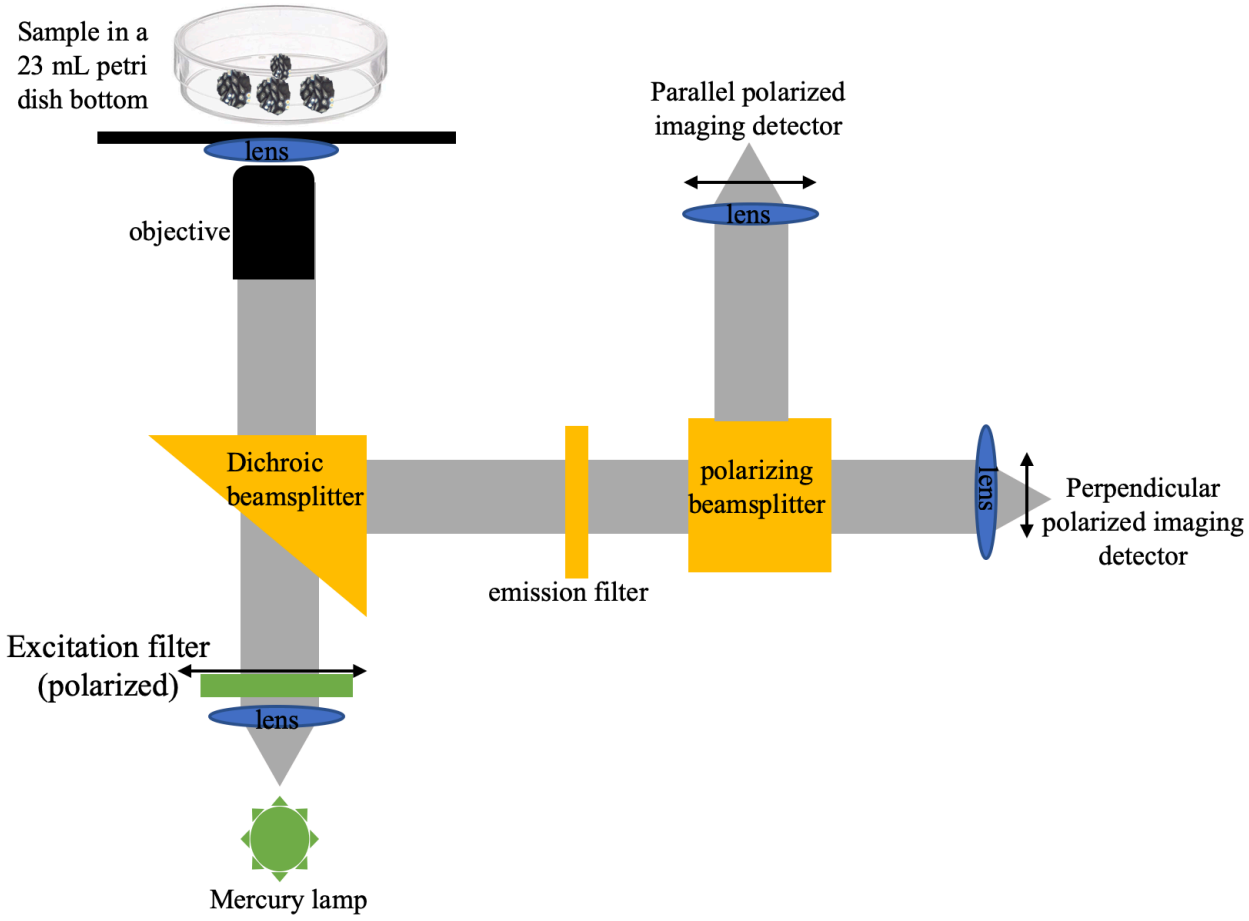

Figure 24: Schematic representation of the experimental setup used for homo-FRET measurements. The excitation filter and the parallel polarized detector are polarized vertically while the perpendicular polarized detector is polarized horizontally in the plane of the optical table. Sample images from the parallel- and perpendicular-polarized detectors are actually recorded side-by-side at the same time on the camera chip.

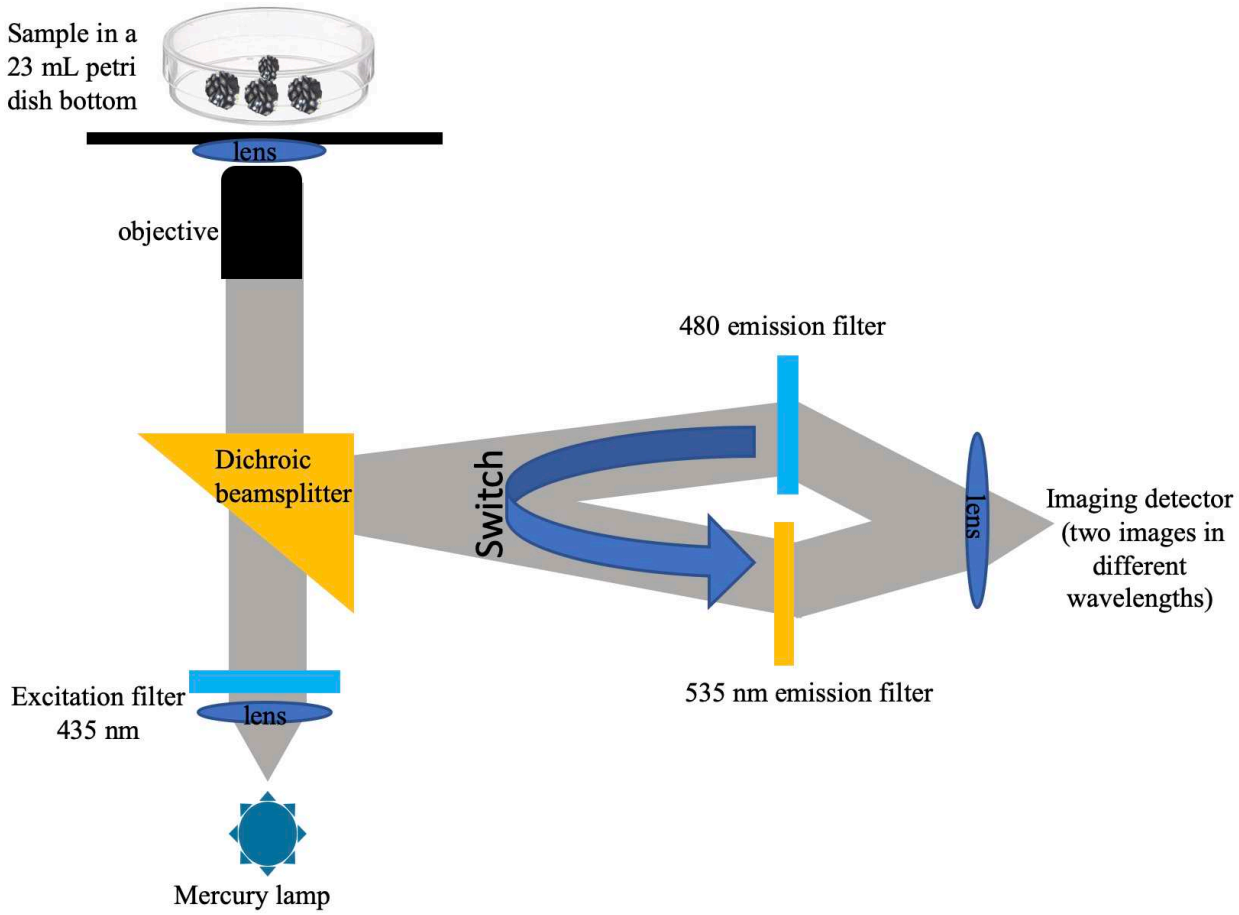

Figure 25: Schematic representation of the experimental setup used for hetero-FRET measurements. This instrumental setup was used in ICUE3 experiments measuring intracellular cAMP. Emission filters were changed manually to select emission wavelengths.

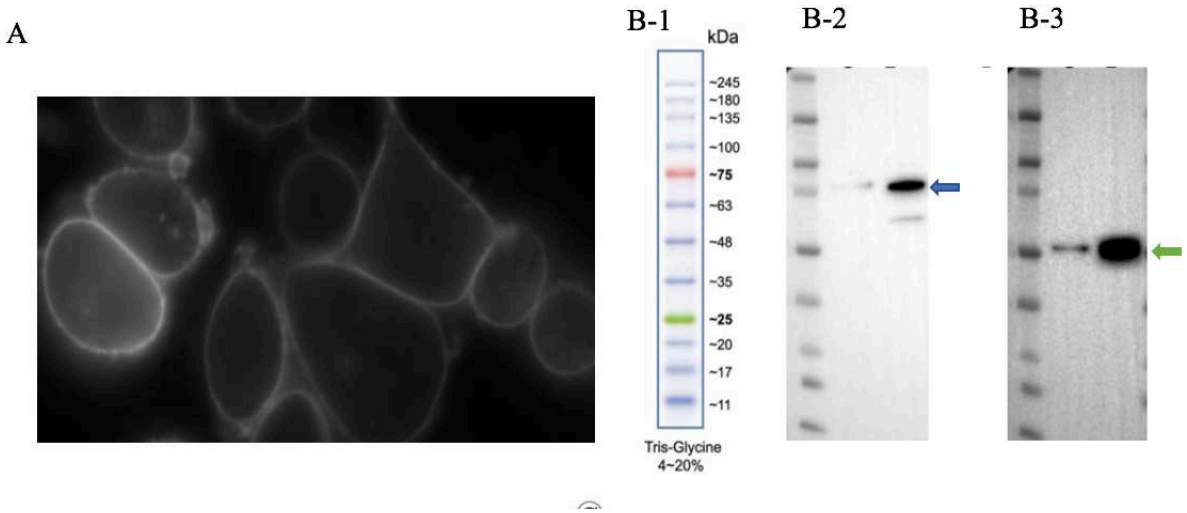

Figure 26: Experiments to confirm transfection of CHO cells with the hLHR-eYFP plasmid. The panel on the left shows CHO cells expressing hLHR-eYFP. These images were acquired using a Zeiss Axiovert 200M inverted fluorescence microscope and show excellent membrane localization of the transfected receptor. Panels on the right show western blots of molecular weight markers beside a blot showing a 105.6 kDa band that is hLHR-eYFP (blue arrows). The western blot on the far right includes α-tubulin as a loading control (green arrows).

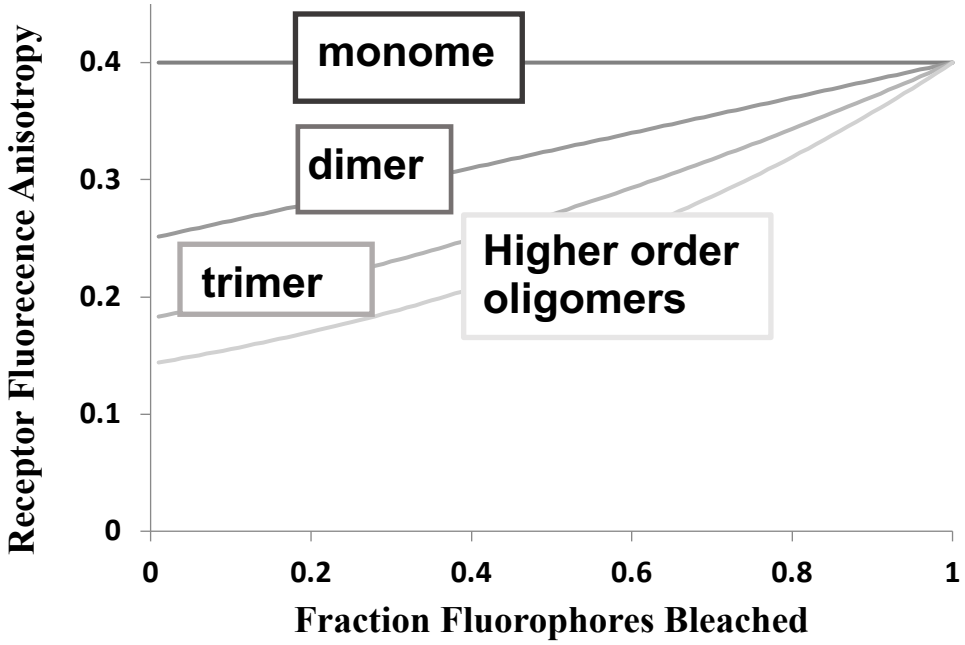

Figure 27: Simulated data for fluorescence anisotropy upon photobleaching. This graph indicates differences in initial anisotropy values and anisotropy values upon photobleaching for receptor monomers, dimers, trimers and higher-order oligomers.

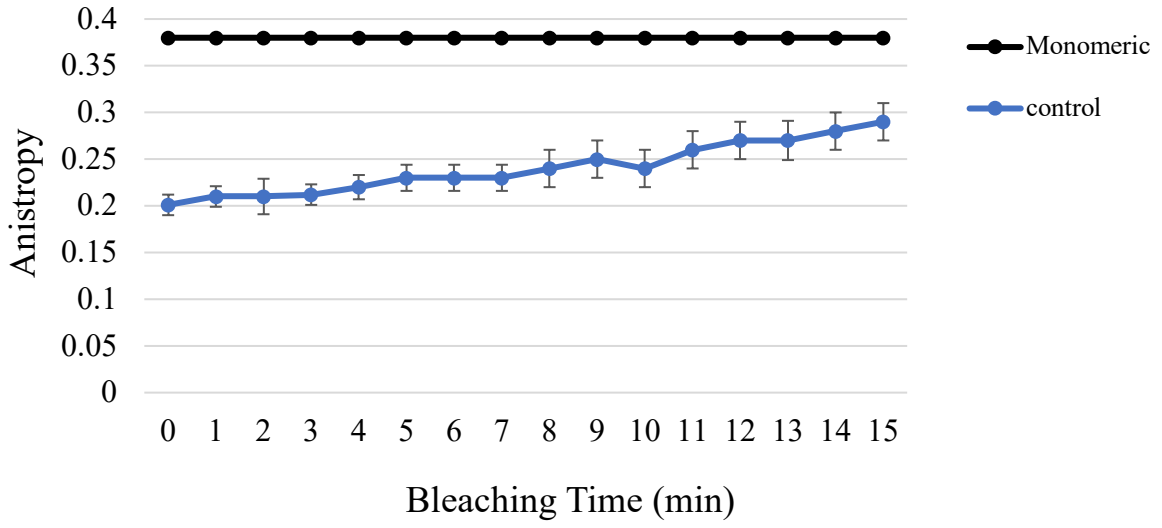

Figure 28: Fluorescence anisotropy upon fluorescence photobleaching for 15 minutes for CHO cells with 10k hLHR per cell. The difference between the predicted anisotropy values for receptor monomers and extrapolated anisotropy in cells with less than 10k LHR per cell provides information on the cluster size of LHR. Data are presented as means ± SEM for n = 30 measurements. The two lines are significantly different in one-way ANOVAs and Tukey's multiple comparisons tests ($p < 0.05$).

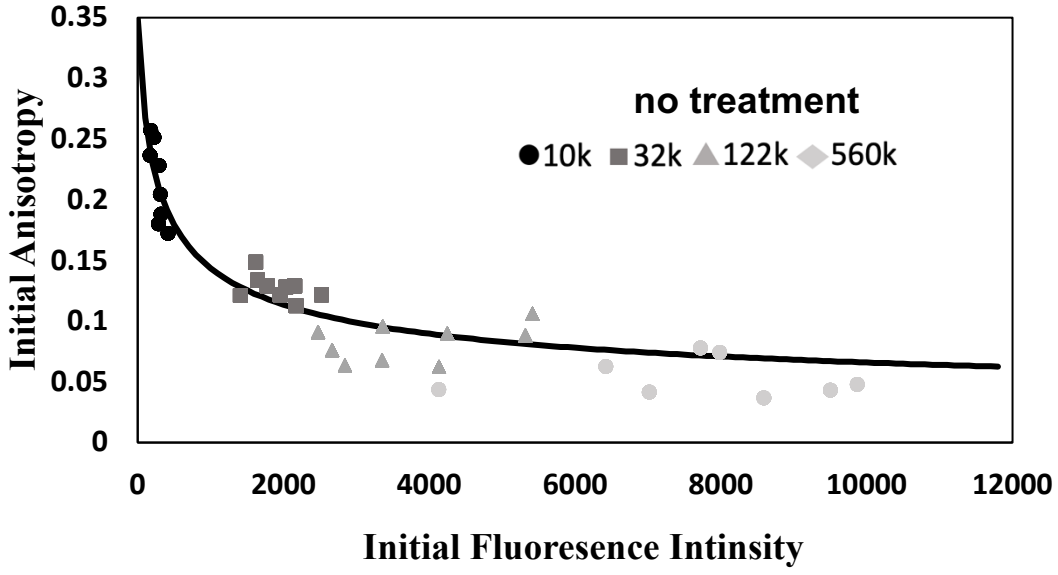

Figure 29: Correlation between initial anisotropy and initial fluorescence intensity for untreated cells. Symbols indicate **average** data for cells representing the four expression groups. This figure indicates that the oligomerization state of LHR is highly dependent on the expression level of LHR per cell. Data are presented in each point as the mean ± SEM for n = 10 measurements; the four cell lines were significantly different in one-way ANOVA and Tukey's multiple comparisons tests ($p < 0.05$).

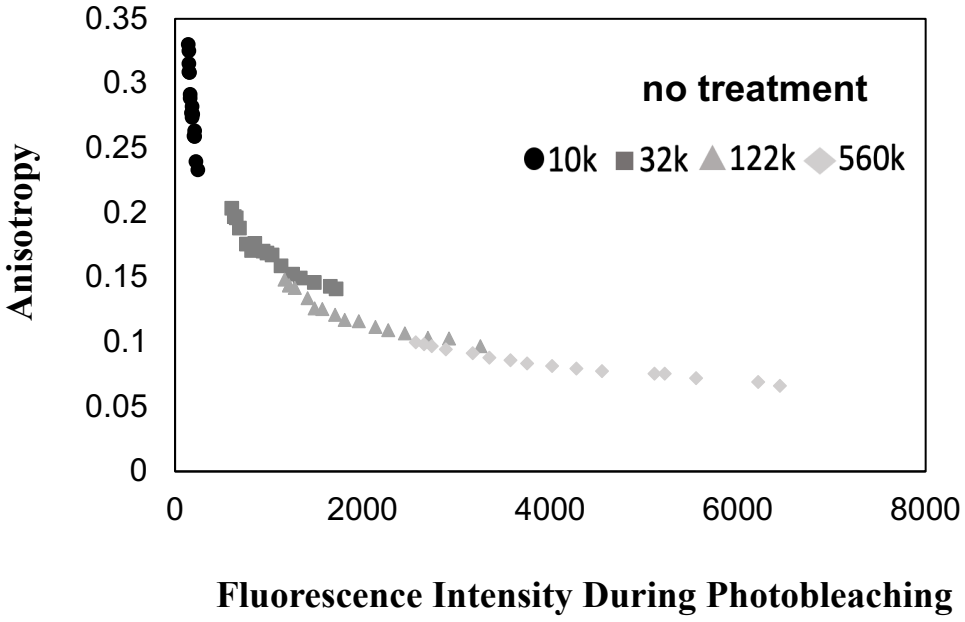

Figure 30: Correlation between anisotropy value and fluorescence intensities during photobleaching for untreated cells. Symbols indicate average data for cells representing the four expression groups. The oligomerization state of LHR is highly dependent on the expression level of LHR per cell and has curvature as above. Data are presented in each point as the mean ± SEM for n = 10 measurements; the four cell lines were significantly different in one-way ANOVA and Tukey's multiple comparisons tests ($p < 0.05$).

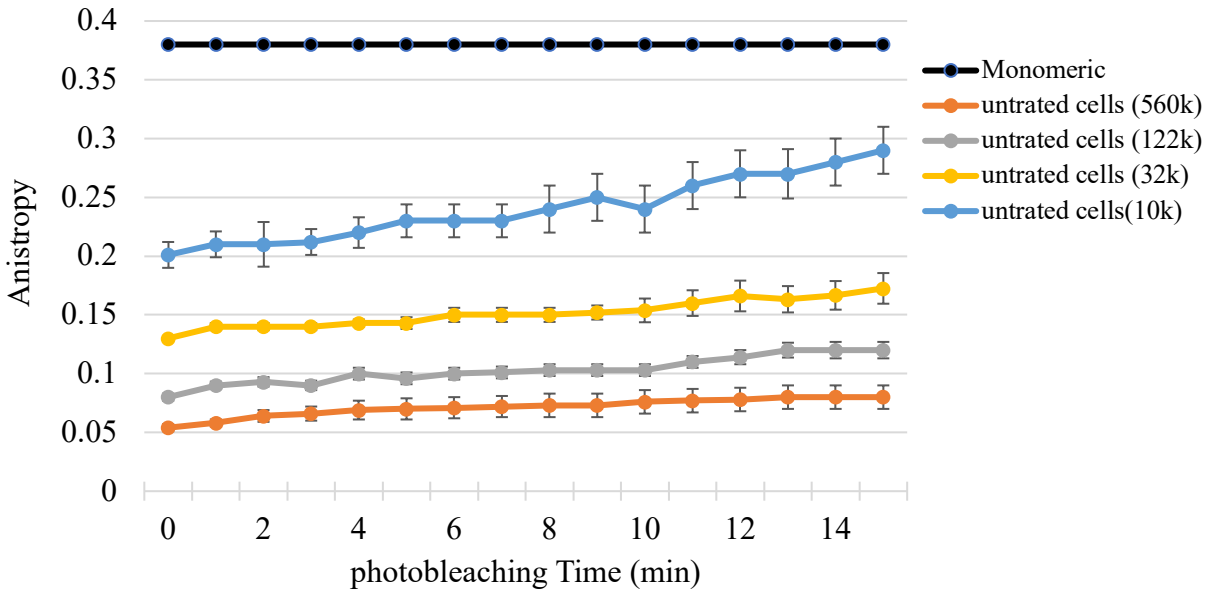

Figure 31: Fluorescence anisotropy during photobleaching for 15 minutes in cells that express hLHR at different levels. The difference between the known values for monomer anisotropy and extrapolated anisotropies for LHR expressed in CHO cells provides information on the cluster size of LHR. Data are presented as the means ± SEM for n = 30 measurements. Anisotropy values for the four cell lines were significantly different as analyzed by one-way ANOVA and Tukey's multiple comparisons tests ($p < 0.05$).

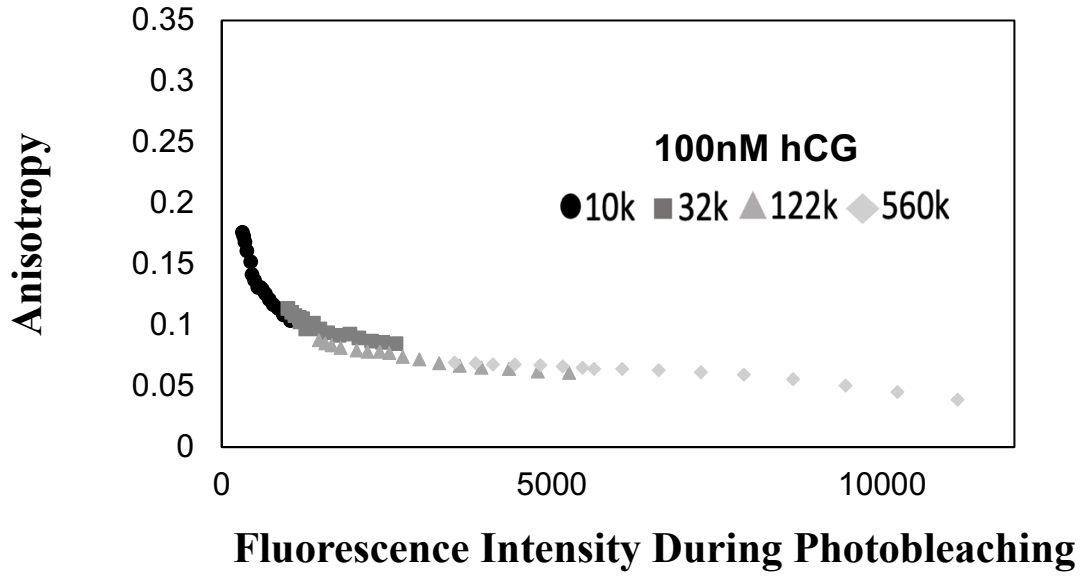

Figure 32: Correlation between anisotropy values and fluorescence intensities during photobleaching in cells treated with 100nM hCG. Symbols indicate average data for cells representing the four expression groups. The figure indicates that the oligomerization state of LHR is highly dependent on the number of LHR per cell. Data are presented in each point as the mean ± SEM. Cells expressing 10k, 32k or either 122k and 560k LHR per cell were significantly different as analyzed by one-way ANOVA and Tukey's multiple comparisons tests ($p < 0.05$). There are no significant differences between anisotropy values for cells expressing 122k or 560k in response to hCG.

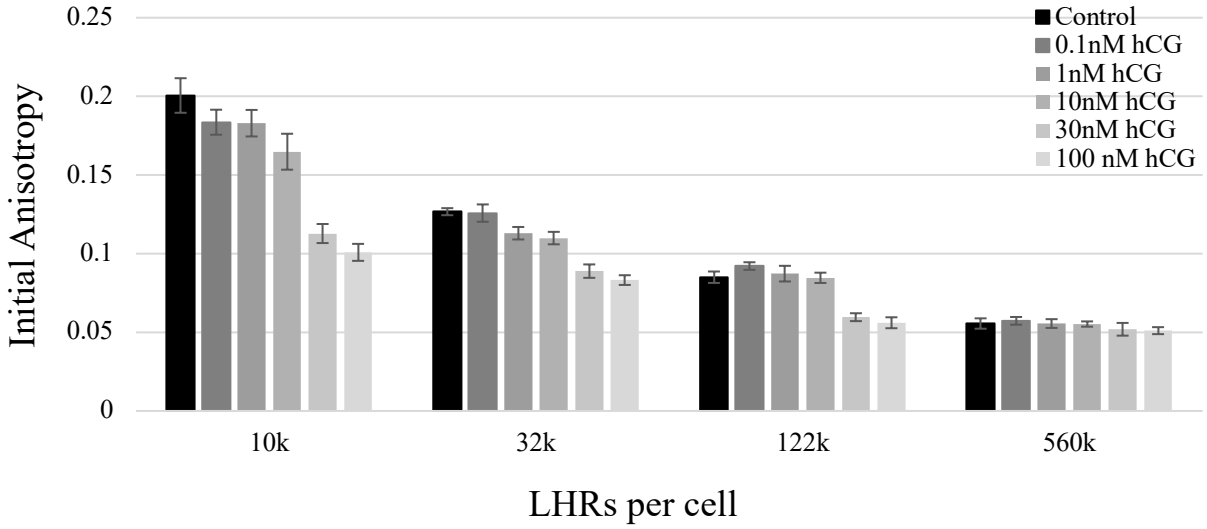

Figure 33: Average initial fluorescence anisotropy values for four cell lines in response to different hCG concentrations. The four cell lines differed in their expression levels of LHR. These results indicate that the effect of hCG on cluster size of LHR is concentration-dependent for cells expressing low numbers of LHR/cell. However, hCG treatment did not affect the LHR cluster size when cells expressed the higher value of 560k LHR per cell. Data are presented as the mean ± SEM for n = 30 measurements**.**

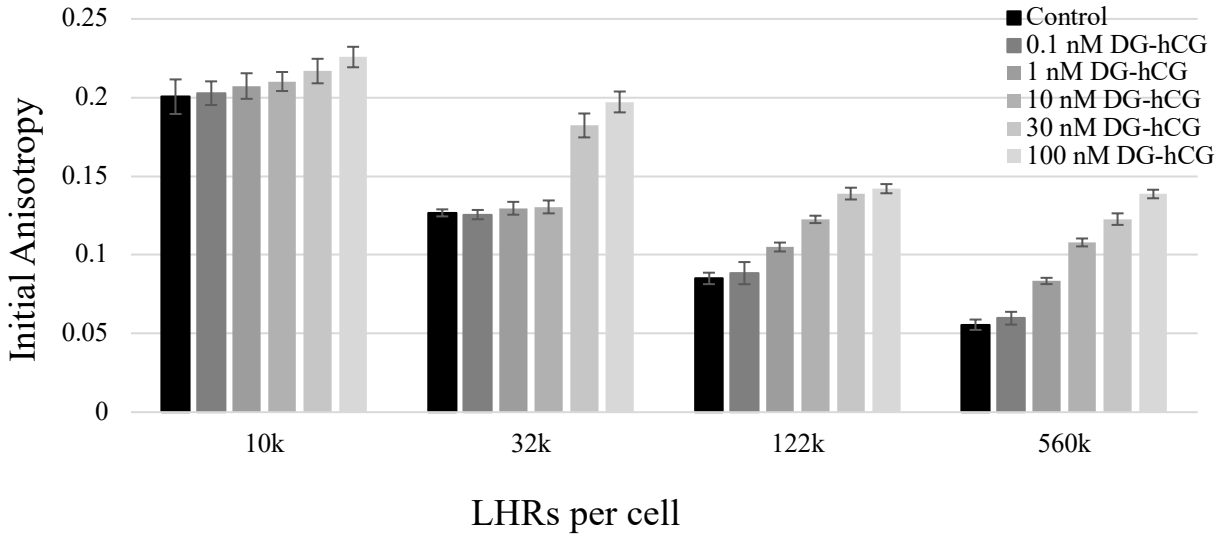

Figure 34: Average initial fluorescence anisotropy for four cell lines in response to different DG-hCG concentrations. These results indicate that DG-hCG reduces the cluster size of LHR in a concentration-dependent manner, but effects are more apparent when the expression level of LHR is high. Data are presented in each bar as the mean ± SEM for n = 30 measurements; the four groups were significantly different as analyzed by one-way ANOVA and Tukey's multiple comparisons tests ($p < 0.05$).

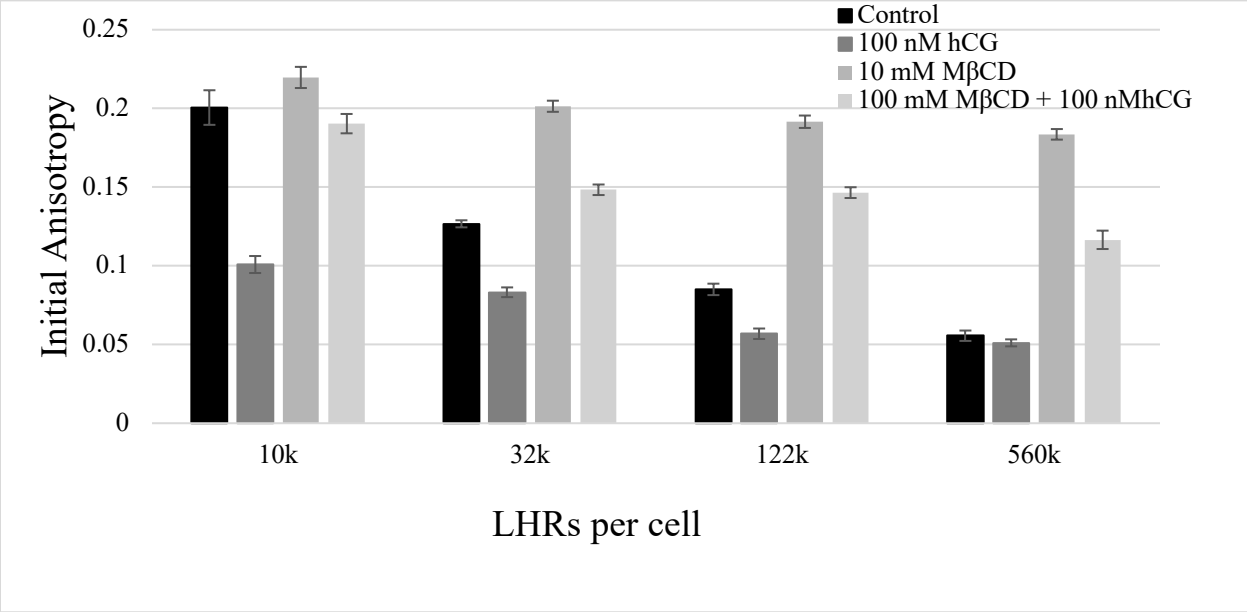

Figure 35: Average initial fluorescence anisotropy values for cells expressing various numbers of LHR per cell after treatment with MβCD. After cholesterol depletion from cell membranes using MβCD, initial anisotropies increased in otherwise untreated cells and, to a lesser extent, hCG-treated cells. Data are presented in each bar as the mean ± SEM for n = 30 measurements. There were no significant differences between effects of MβCD on cells expressing either 10k LHR per cell or 32k LHR per cell and cells expressing 122k LHR per cell or 560k LHR per cell. There were significant differences between these two groups in response to MβCD analyzed by one-way ANOVA and Tukey's multiple comparison's test ($p < 0.05$).

Table 3: Summary of fluorescence parameters for FITC and eYFP excited at 488 nm. These quantities were used to convert the flow cytometer signal from FITC bead standards to numbers of eYFP and thus numbers of LHR-eYFP present on CHO cell lines.

Fluorophore	$a(\lambda_e)$ [a] (au)	$a(\lambda_{pk})$ [b] (au)	$\varepsilon(\lambda_{pk})$ [c] (L mol^{-1}cm^{-1})	$\sum_{\lambda_d+-w_d 1\,2}^{\lambda_d+w_d 1\,2} f_\lambda$ [d]	$\sum_{0}^{\infty} f_\lambda$ [e]	$\emptyset_f$ [f]	Relative fluorescence [g] (Equation 3)
FITC	77.3	100	68,000	2981	5010	0.95	28815
eYFP	38.1	100	84,000	2723	3809	0.61	13956

[a] relative chromophore absorbance at excitation wavelength
[b] relative chromophore absorbance at peak absorption wavelength
[c] chromophore peak molar absorptivity
[d] total chromophore fluorescence within detector filter bandwidths
[e] total chromophore fluorescence over all wavelengths
[f] chromophore fluorescence quantum yield
[g] relative measured fluorescence in arbitrary units for one chromophore of the indicated type

Table 4: Summary of changes in fluorescence anisotropy upon fluorescence photobleaching for 15 minutes in unstimulated cells expressing different average numbers of hLHR-eYFP per cell.

	Mean of Anisotropy ±SEM			
#LHR/Cell (average) / time	**10k**	**32k**	**122k**	**560k**
0	0.20±0.01	0.13±0.002	0.08±0.003	0.05±0.003
1	0.21±0.01	0.14±0.003	0.09±0.003	0.06±0.003
2	0.21±0.02	0.14±0.003	0.09±0.004	0.06±0.01
3	0.21±0.01	0.14±0.003	0.09±0.004	0.07±0.01
4	0.22±0.01	0.14±0.01	0.10±0.01	0.07±0.01
5	0.23±0.01	0.14±0.01	0.10±0.01	0.07±0.01
6	0.23±0.01	0.15±0.01	0.10±0.01	0.07±0.01
7	0.23±0.01	0.15±0.01	0.10±0.01	0.07±0.01
8	0.24±0.01	0.15±0.01	0.10±0.01	0.07±0.01
9	0.25±0.02	0.15±0.01	0.10±0.01	0.07±0.01
10	0.24±0.02	0.15±0.01	0.10±0.01	0.08±0.01
11	0.26±0.02	0.16±0.01	0.11±0.01	0.08±0.01
12	0.27±0.02	0.17±0.01	0.11±0.01	0.08±0.01
13	0.27±0.02	0.163±0.01	0.12±0.01	0.08±0.01
14	0.28±0.02	0.17±0.01	0.12±0.01	0.08±0.01
15	0.29±0.02	0.17±0.01	0.12±0.01	0.08±0.01

Data are presented as means ± SEM for n=30 measurements. The four cell lines were significantly different as analyzed by one-way ANOVA and Tukey's multiple comparisons test ($p < 0.05$).

Table 5: Summary of change in initial anisotropy in cell lines expressing hLHR and variously treated with hCG and or MβCD.

	Mean of Initial Anisotropy ±SEM			
#LHR/Cell (average) / treatment	**10K**	**32K**	**122K**	**560K**
Control	0.20±0.01^{a}	0.13±0.002^{e}	0.08±0.003^{f}	0.05±0.003^{gh}
100 nM hCG	0.10±0.01^{b}	0.08±0.003^{f}	0.06±0.003^{gf}	0.05±0.002^{h}
30nM hCG	0.11±0.01^{b}	0.09±0.004^{bf}	0.06±0.003^{gf}	0.05±0.004^{h}
10nM hCG	0.17±0.01^{c}	0.11±0.004^{b}	0.09±0.003^{f}	0.06±0.002^{gh}
1nM hCG	0.18±0.01^{c}	0.11±0.004^{b}	0.09±0.005^{f}	0.06±0.003^{gh}
0.1nM hCG	0.18±0.01^{c}	0.13±0.005^{e}	0.09±0.002^{bf}	0.06±0.002^{gh}
10 mM MβCD	0.22±0.01^{ad}	0.20±0.004^{a}	0.19±0.004^{ac}	0.18±0.003^{ac}
10 mM MβCD +10nM hCG	0.22±0.01^{ad}	0.20±0.003^{a}	0.20±0.003 ^{ac}	0.17±0.03^{c}

Data are presented as means ± SEM for n = 30 measurements. Values with different superscripts were significantly different as analyzed by one-way ANOVA and Tukey's multiple comparisons test ($p < 0.05$).

Table 6: Summary of change in initial anisotropy in cell lines expressing hLHR and treated with various DG-hCG concentrations.

	Mean of Initial Anisotropy ±SEM			
#LHR/Cell (average) treatment	**10k**	**32k**	**122k**	**560k**
Control	0.20±0.01^{a}	0.13±0.002^{c}	0.08±0.003^{e}	0.05±0.003^{g}
100 nM DG-hCG	0.23±0.01^{b}	0.20±0.01^{a}	0.14±0.003^{c}	0.14±0.003^{c}
30 nM DG-hCG	0.22±0.01^{ab}	0.18±0.01^{d}	0.14±0.004^{c}	0.12±0.004^{cf}
10 nM DG-hCG	0.21±0.01^{ab}	0.13±0.004^{c}	0.12±0.002^{cf}	0.11±0.003^{f}
1 nM DG-hCG	0.21±0.01^{ab}	0.13±0.004^{c}	0.11±0.003^{f}	0.08±0.002^{ef}
0.1 nM DG-hCG	0.20±0.01^{ab}	0.13±0.003^{c}	0.09±0.01^{ef}	0.06±0.004^{efg}

Data are presented as means ± SEM for n = 30 measurements. Values with different superscripts were significantly different as analyzed by one-way ANOVA and Tukey's multiple comparisons test ($p < 0.05$).

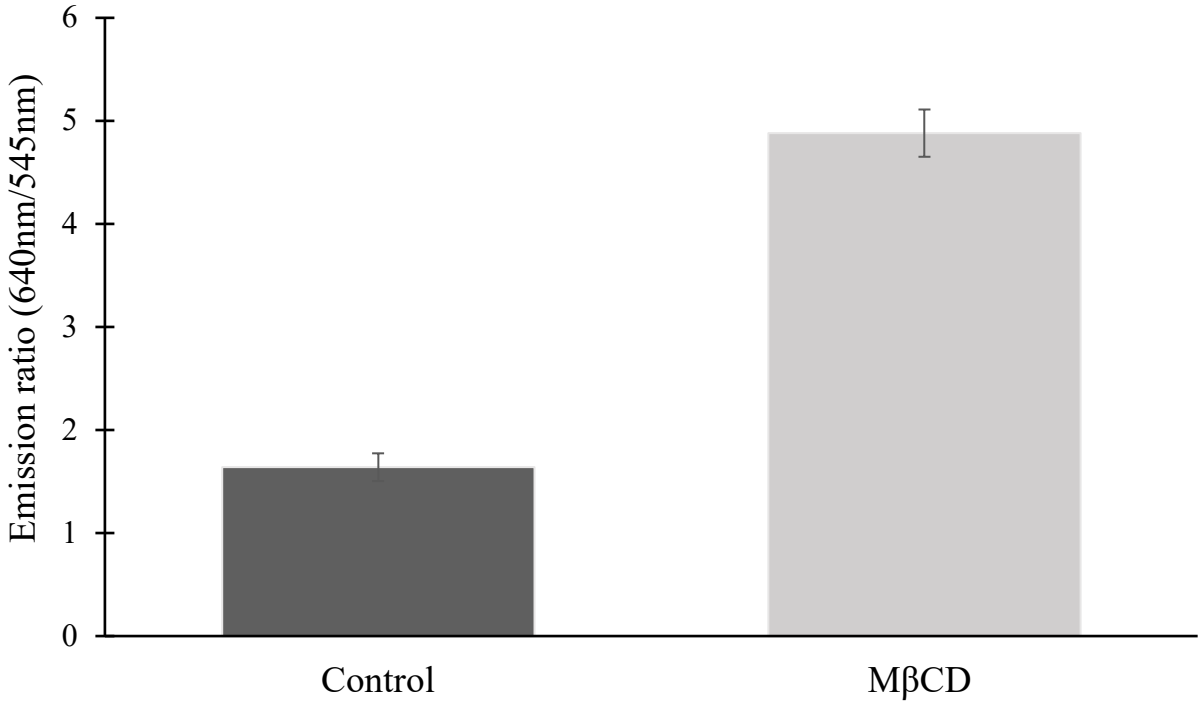

Figure 36: Fluorescence emission of Di-4-ANEPPDHQ labeled CHO cell membranes. Di-4-ANEPPDHQ fluorescence emission was measured simultaneously at 545 nm and 640 nm. The ratio of intensities at 640 nm to that at 545 nm was calculated as "Emission ratio". Control CHO have no effect on Di-4- ANEPPDHQ emission. There was, however, a significant increase in the emission ratio to a value of approximately 5 in cells treated with M$\boldsymbol{\beta}$**CD** and this indicates a significant decrease in membrane order caused by M$\boldsymbol{\beta}$**CD** treatment. Data are presented in each bar as the mean ± SEM for n=40 measurements and analyzed by one-way ANOVA and Tukey's multiple comparison's test ($p < 0.05$).

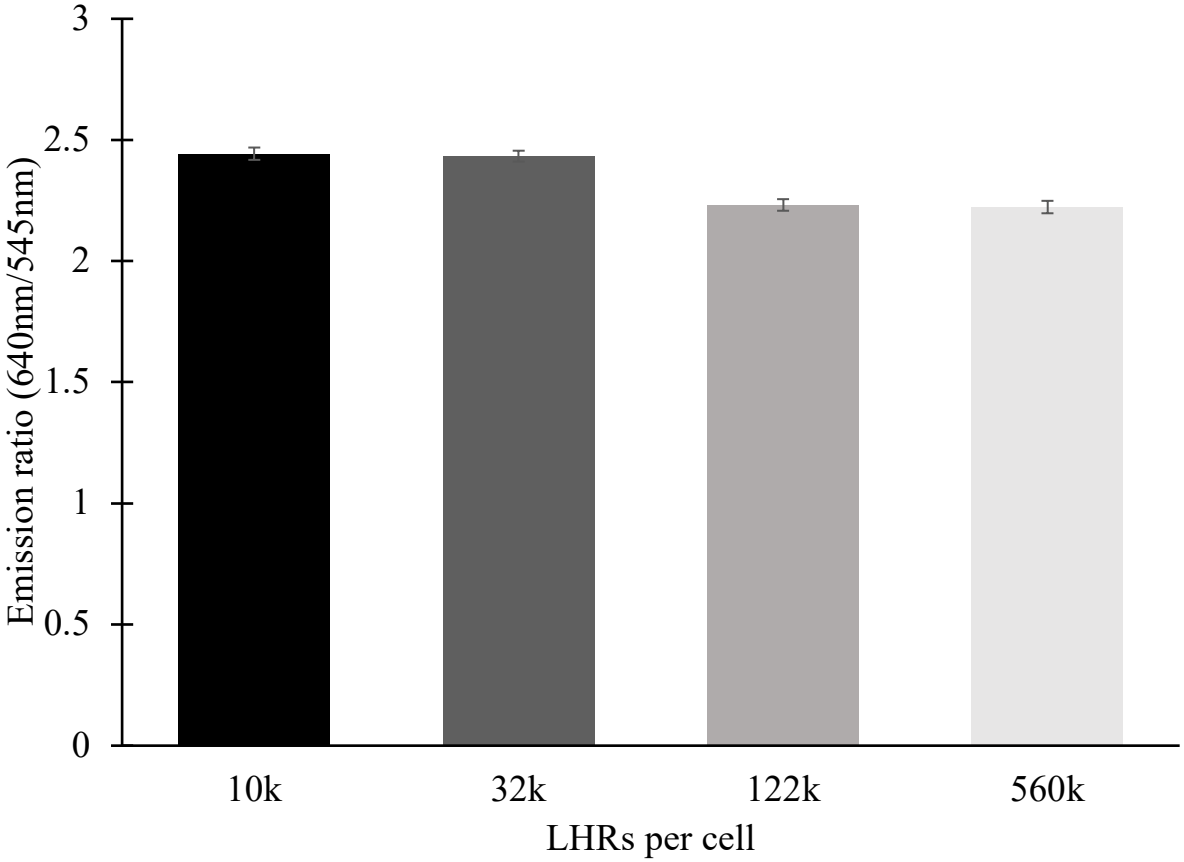

Figure 37: Fluorescence emission of Di-4-ANEPPDHQ labeled the four groups of cells expressing various average numbers of LHR per cell. Di-4-ANEPPDHQ fluorescence emission was measured simultaneously at 545 nm and 640 nm and the ratio of intensities at 640 nm to that at 545 nm calculated as "Emission ratio". Cells expressing 10k or 32k LHR per cell had significant increases in the emission ratio compared to cells with 122k or 560k LHR per cell. Data are presented in each bar as the mean ± SEM for n = 40 measurements and analyzed by one-way ANOVA and Tukey's multiple comparison's test ($p < 0.05$).

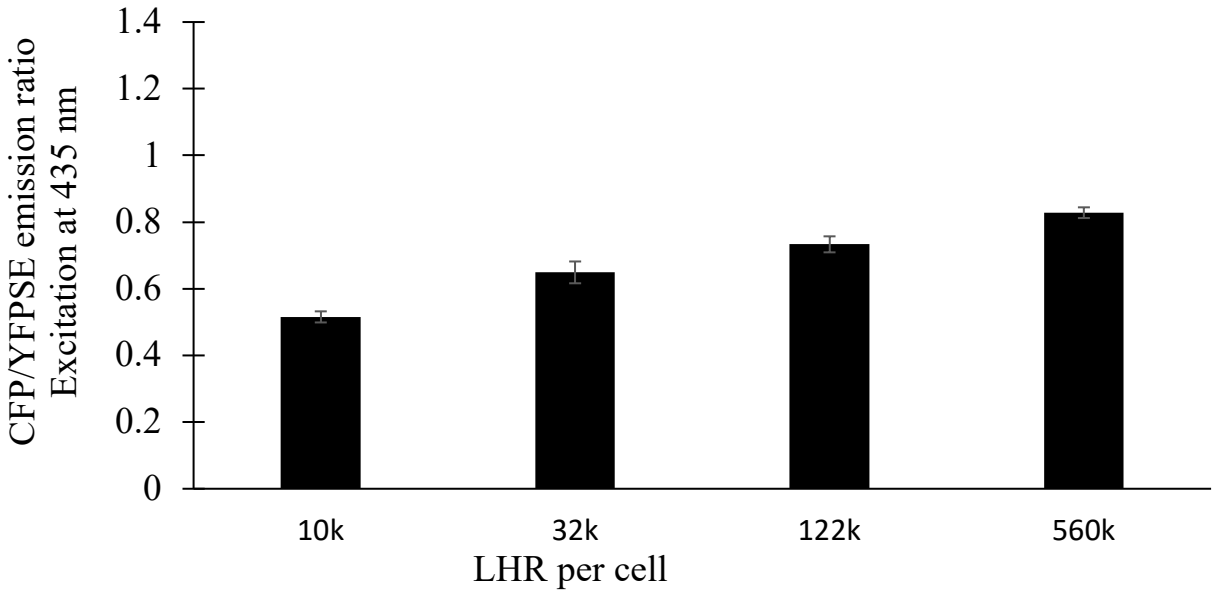

Figure 38: Relationship between numbers of LHR per cell and ICUE3 sensor reading reflecting levels of cAMP per cell in untreated cells. The ICUE3 sensor emits both CFP fluor emssion at 480 nm and YFP sensitized fluor emsission at 535 nm. Upon 435 nm excitation the ratio of CFP emission to YFP sensitized emission increases with cAMP concentration. Data are presented as the mean ± SEM for n = 15 measurements. cAMP levels were significantly different between the four cell lines as analyzed by one-way ANOVA and Tukey's multiple comparison's test ($p < 0.05$).

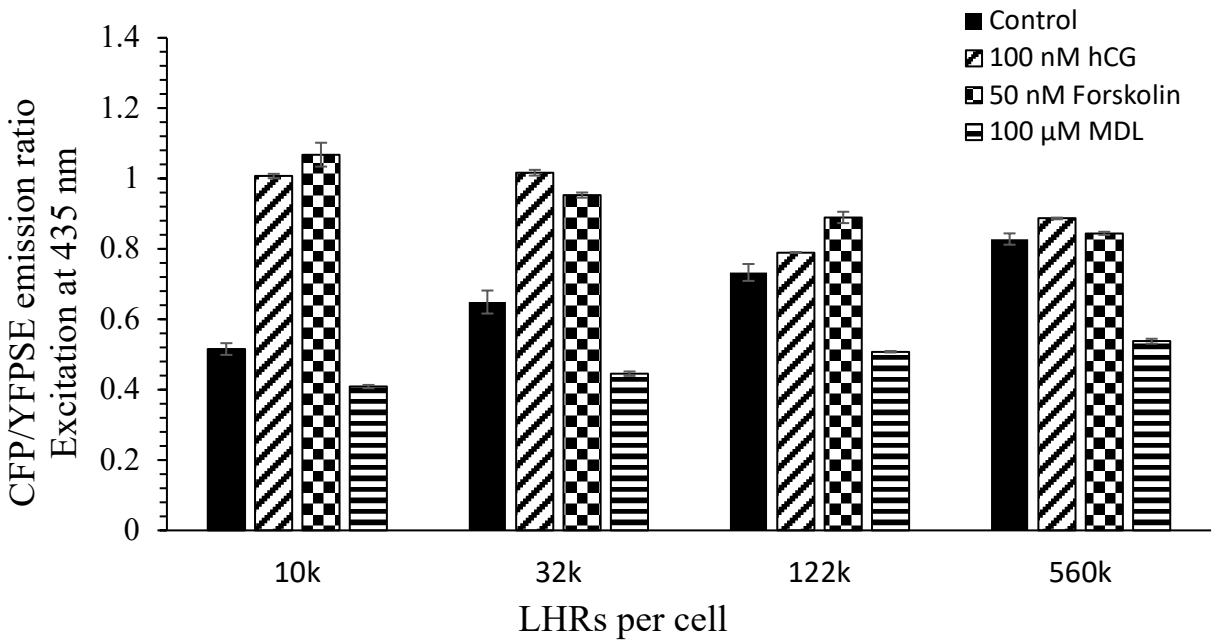

Figure 39: Effect of hCG on intracellular cAMP concentration in variously treated cells. The ICUE3 sensor emits both CFP fluor emssion at 480 nm and YFP sensitized fluor emsission at 535 nm. Upon 435 nm excitation the ratio of CFP emission to YFP sensitized emission increases with cAMP concentration. Data are presented as the mean ± SEM for n = 15 measurements and were analyzed by one-way ANOVA and Tukey's multiple comparison's test ($p < 0.05$).

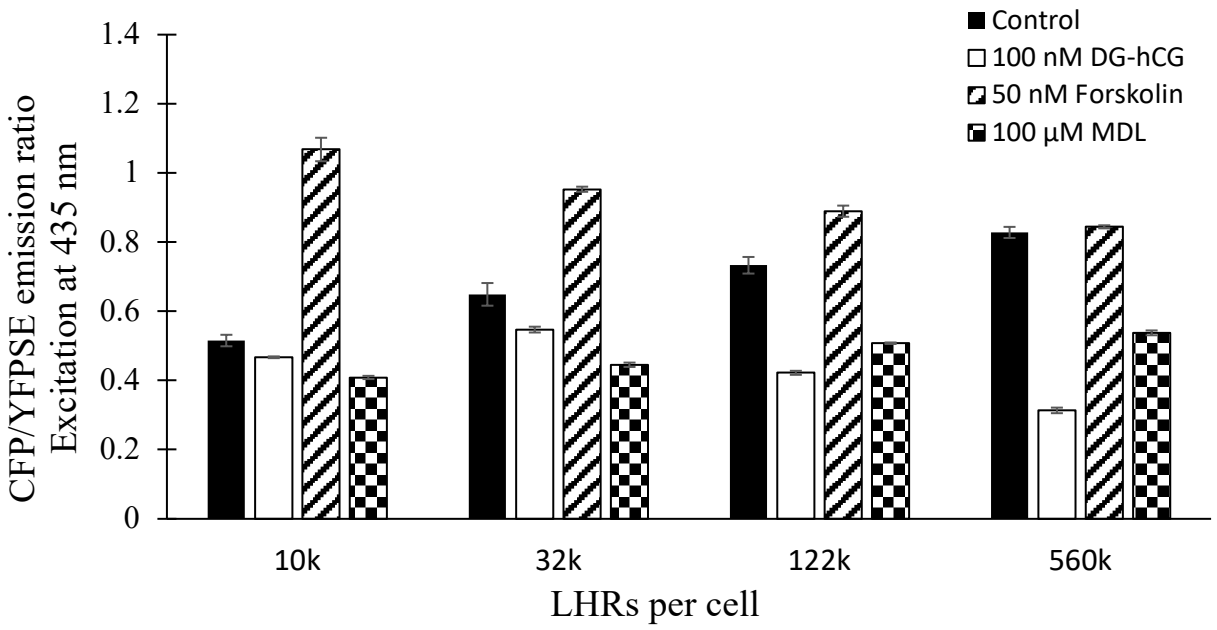

Figure 40: Effect of DG-hCG on production of cAMP in variously treated cells expressing different numbers of LHR per cell. The ICUE3 sensor emits both CFP fluor emssion at 480 nm and YFP sensitized fluor emsission at 535 nm. Upon 435 nm excitation the ratio of CFP emission to YFP sensitized emission increases with cAMP concentration. Forskolin was used as a positive control and MDL was used as a negative control. Data are presented in each bar as the mean ± SEM for n = 15 measurements and were analyzed by one-way ANOVA and Tukey's multiple comparison's test ($p < 0.05$).

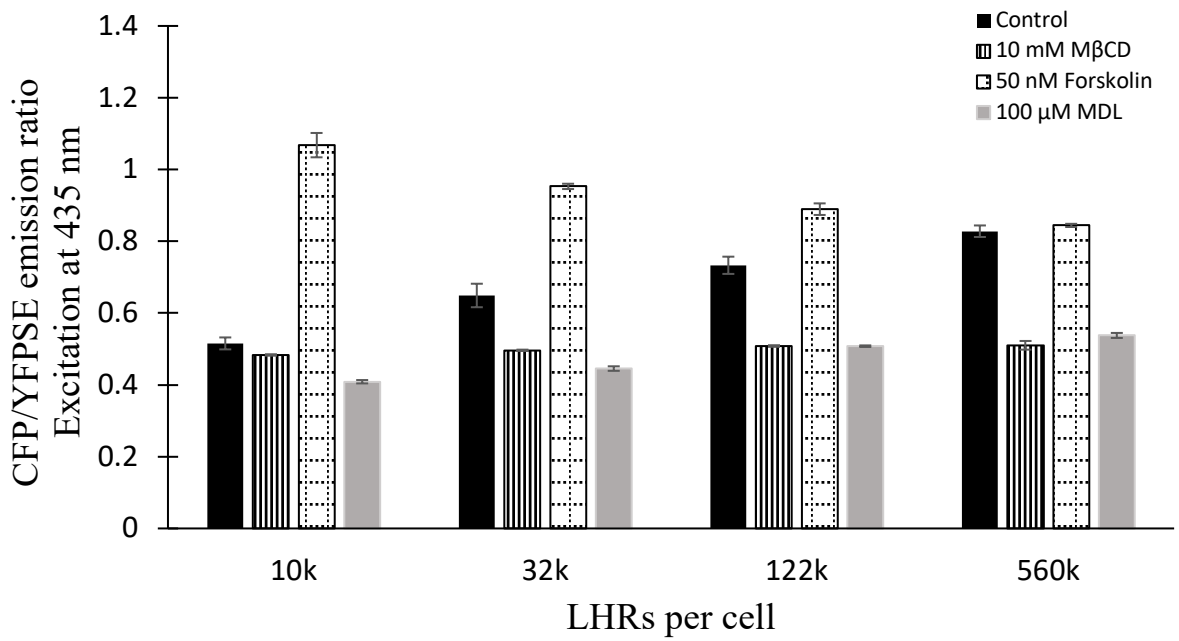

Figure 41: Effect of cholesterol depletion on production of cAMP in variously treated cells expressing different numbers of LHR per cell. The ICUE3 sensor emits both CFP fluor emssion at 480 nm and YFP sensitized fluor emsission at 535 nm. Upon 435 nm excitation the ratio of CFP emission to YFP sensitized emission increases with cAMP concentration. Data are presented in each bar as the mean ± SEM for n = 15 measurements and analyzed by one-way ANOVA and Tukey's multiple comparison's test ($p < 0.05$). Forskolin was used as a positive control and MDL-12,330a was used as a negative control.

Table 7: Summary of changes in intracellular cAMP as measured experimentally by changes in the CFP/YFPSE ratio. Measurements were made on cells expressing hLHR at different levels and treated with hCG, DG-hCG, MβCD or forskolin.

	Mean of CFP/YFPSE emission ratio at 435 nm ±SEM			
#LHR/Cell (average) treatment	**10K**	**32K**	**122K**	**560K**
Control	0.52±0.02 [a]	0.65±0.03[e]	0.73±0.02[c]	0.83±0.02 [c]
100 nM hCG	1.01±0.01[b]	1.01±0.01[b]	0.79±0.001[c]	0.93±0.003[c]
100 nM DG-hCG	0.47±0.003[d]	0.55±0.01[ad]	0.42±0.01[df]	0.31±0.01[f]
10 mM MβCD	0.51±0.03[ad]	0.53±0.02[ad]	0.53±0.01[ad]	0.42±0.003[df]
Forskolin	0.86±0.002[c]	1.06±0.01[b]	0.60±0.01[ae]	0.79±0.01 [c]
MDL-12,330a hydrochloride	0.50±0.004 [ad]	0.53±0.01[ad]	0.53±0.003[ad]	0.59±0.01[ae]

Data are presented as means ± SEM for n = 15 measurements. Differences between expression and treatment group were analyzed by one-way ANOVA and Tukey's multiple comparison's test. Different superscripts indicate significant differences ($p < 0.05$).

5. CHAPTER 5: STUDY CONCLUSIONS AND FUTURE DIRECTIONS

Development of the reproductive organs and healthy function of the reproductive system in humans is impossible without normal function of LHR. Stimulation of sperm maturation and production of testosterone in males is regulated by LHR as is embryonic development of Leydig cells needed for testosterone secretion. In females, follicular development, ovulation, estrogen secretion and function of the corpus luteum require functional LHR. During the first trimester of pregnancy, LHR are involved in maintaining progesterone secretion which, in turn, maintains the uterine lining. A better understanding of LHR function is invaluable to treating pathologic conditions related to LHR expression and function.

The expression level of LHR depends on a number of factors depending on the organ being studied. What is clear, however, is that overexpression of membrane proteins like LHR results in a higher density of proteins, *i.e*. molecular crowding, which can affect receptor signaling, desensitization and internalization [2-8]. High molecular densities may also lead to oligomerization of the proteins [10].

There are disagreements in the literature with respect to the oligomerization state of inactive LHR [149, 182]. These disagreements may arise from differences in expression levels of LHR. In this study, we assessed the role of LHR expression on initial fluorescence anisotropy of receptors using homo-FRET methods and measurements of LHR activity. Receptor fluorescence anisotropy is decreased by receptor aggregation and so provides an indispensable means of assessing receptor aggregation on intact cells. The goal of this project was to establish how expression levels for a well-characterized GPCR affect receptor function. Conclusions from these studies are illustrated in **Figures 41-44**.

These studies suggest a possible mechanism involved in receptor-receptor interactions. Receptors interact with one another under various well-defined conditions. For LHR that have not bound hCG, receptor cell surface density is a factor in receptor interactions. With increased surface density, *i.e.* higher expression, initial anisotropy values are lower, indicating that receptors are more extensively clustered. The effects of hCG depend on the extent of "pre-clustering" of the receptor prior to hormone treatment. When receptor expression levels are lower, hCG binding to the receptor recruits additional receptors to existing as pre-clusters. This produces a further decrease in initial anisotropies, receptors become more extensively clustered and intracellular cAMP increased (**Figure 41** and the left panel of **Figure 43**). When receptors are already pre-clustered at high receptor expression levels, hCG binding has modest effects, if any, on further receptor aggregation and in intracellular cAMP level (**Figure 42** and the right panel of **Figure 43**).

The relationship between receptor expression and receptor aggregation is likely to be influenced by the presence on cell membranes of membrane microdomains which appear to function as signaling platforms for LHR. LHR accumulate in these microdomains when the receptors have clustered. Thus, clusters occur either as a result of high receptor densities or, when receptor density is lower, in response to hCG binding to the receptor. In either case, the clustered receptors in microdomains have become more concentrated in comparatively small membrane areas and the receptors actively signal. Disruption of membrane microdomains by MβCD appears to disperse at least some of the receptor clusters and reduces intracellular cAMP levels.

Studies with DG-hCG, an hCG antagonist, suggest that LHR interactions, either in response to hCG or as a result of high receptor densities, result from receptor association coefficients which can be calculated. Binding of DG-hCG reduces receptor interactions and, as a result, reduces the ability of receptors to signal. This reduction become more significant as the

numbers of LHR per cell increased (**Figure 44**). Experimentally, initial anisotropy values increased in DG-hCG treated cells and intracellular cAMP levels decrease.

These results serve as an important guide to future studies. First, and most important, they provide cautionary guidance to researchers studying GPCR function by demonstrating systematically that receptor numbers affect receptor function. With respect to LHR, the receptor number per cell or, alternatively, receptor surface density in LH target tissues would provide a better understanding of the receptor's functional state. As an aside, it is probably important to specifically consider receptor density per unit cell surface area in this regard. Total numbers of receptor per cell can be similar on cell types such as large and small luteal cells, but these cells have very different sizes [266]. Thus, small cells have receptor densities that are higher while larger cells have lower receptor densities.

To better understand the relationship between expression levels of LHR and physiologic function, it would be interesting to have transgenic mouse models where LHR are expressed in tissues in higher numbers. These mouse models could provide information on a range of behavioral, phenotypic and physiologic effects resulting from receptor overexpression. One can speculate that changes in behavior such as aggression might appear in mice with higher expression levels of LHR as a result of an increase of testosterone [39, 267]. In addition, skin changes might appear since studies have found LHR in skin [34, 253]. Diseases associated with LHR such as AD [56-61] and cancers [33, 62-68] might be modeled in these mice to determine whether LHR are involved in disease progression in meaningful ways.

Pharmacologic agents could also be tested *in vivo* in mice that overexpress LHR. Transgenic mouse models expressing enhanced LHR or knockout of endogenous LHR (LuRKO) have been already generated and used successfully in experiments that mimic human disorders

related to receptor mutation [39, 51, 147]. Transgenic mouse models expressing low or high numbers of LHR per cell are needed for particularly interesting studies. One could, for example, monitor mouse behavior related to memory, of interest due to the relationship between LHR expression and development of AD, after treatment with pharmacologic agents targeting LHR. Compounds that are available or have been used previously would be of interest including thienopyridine compounds which are believed to bind to LHR receptors and increase downstream steroidogenesis [268] and deslorelin acetate which increases expression of LHR [269]. Drugs already in clinical use include triptorelin, leuprolide, goserelin and buserelin which increase LHR expression and are used in the treatment of infertility, uterine fibroids, endometriosis and sex-hormone sensitive cancers associated with low expression levels of LHR [270-272]. LH antagonists such as T-98475, cetrorelix, ganirelix, degarelix, and abarelix [33, 65, 271, 273-277] may be involved in remission of tumors that overexpress LHR. Furthermore, vanadium compounds have been found to increase the aggregation of LHR and induce its activity [278].

The receptor aggregation state would also be of interest in response to treatment of cell lines with micro RNAs. An 18-nucleotide segment of non-coding RNA, miR-112, regulates the expression of LHR by controlling the expression of LHR mRNA-binding protein. This molecule plays a role in controlling the degradation rate of mRNA for LHR [279] and might be of interest. Other studies found miR-136-3p and miR-513a-3p decrease the expression of LHR [280, 281]. Gene therapy with micro-RNAs might be useful in regulating the expression of LHR in pathologic conditions.

Finally, it might be interesting to explore ways of targeting non-gonadal tissues so that LHR could be expressed at appropriate levels. Previous studies have found that LHR are expressed in the retina and have a role in reducing visual processing. They may also affect

development of eyes in the fetus [253, 254]. Although there is no pathology associated with LHR expression in the eye, it seems likely that this may exist. LHR expressed in skin might possibly explain skin changes in menopausal women [34]. Studies using transgenic knockout LHR mice provide evidence that the absence of LHR significantly reduces amyloid beta load in brains. amyloid beta load is a problem for patients with AD [56-60]. A better understanding of the relationship between LHR expression levels and memory, vision, skin properties, *etc*. in transgenic mice and monitoring changes following treatments with available drugs may more fully elucidate the role of LHR expression levels in human health.

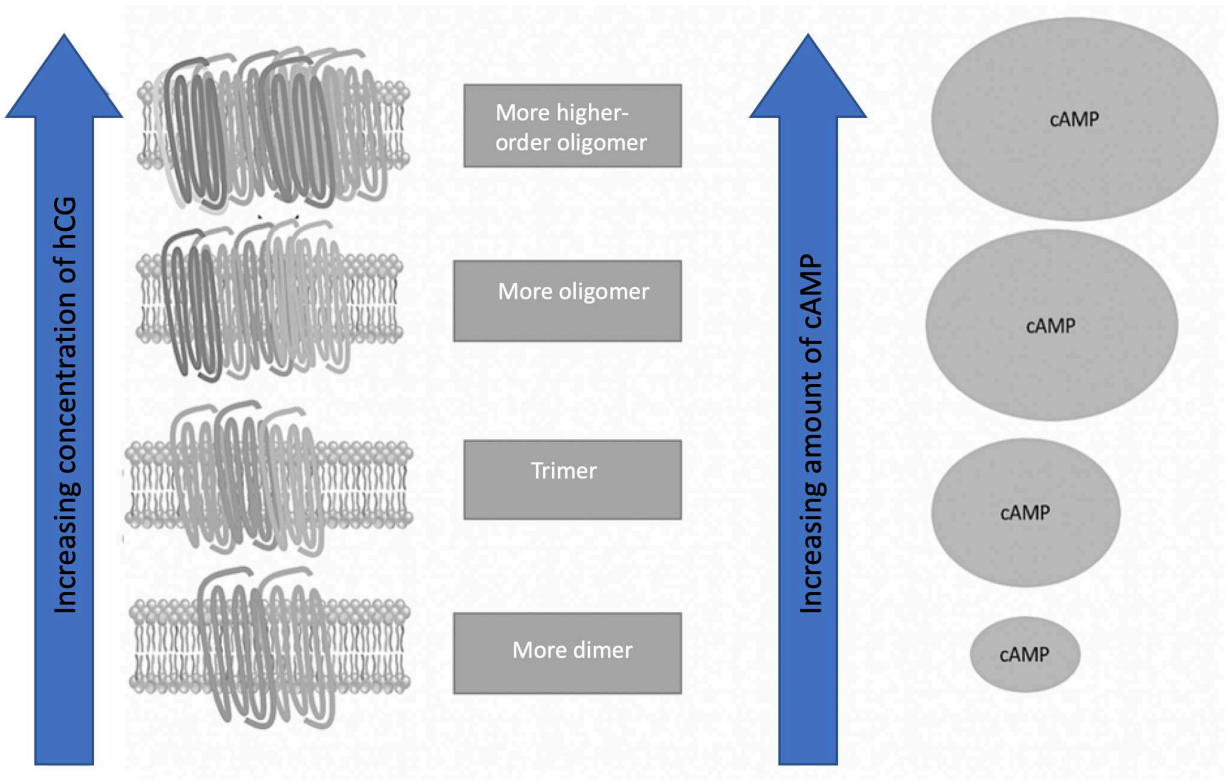

Figure 42: Relationship between the size of LHR clusters and production of cAMP in cells expressing low levels of LHR.

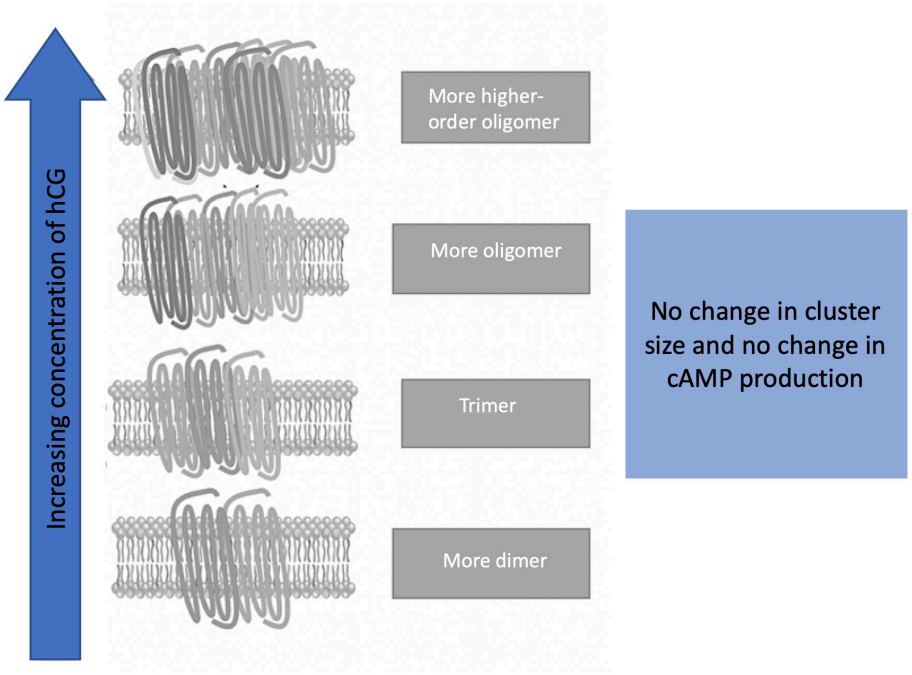

Figure 43: Relationship between the size of LHR clusters and production of cAMP in cells expressing lower numbers of LHR per cell.

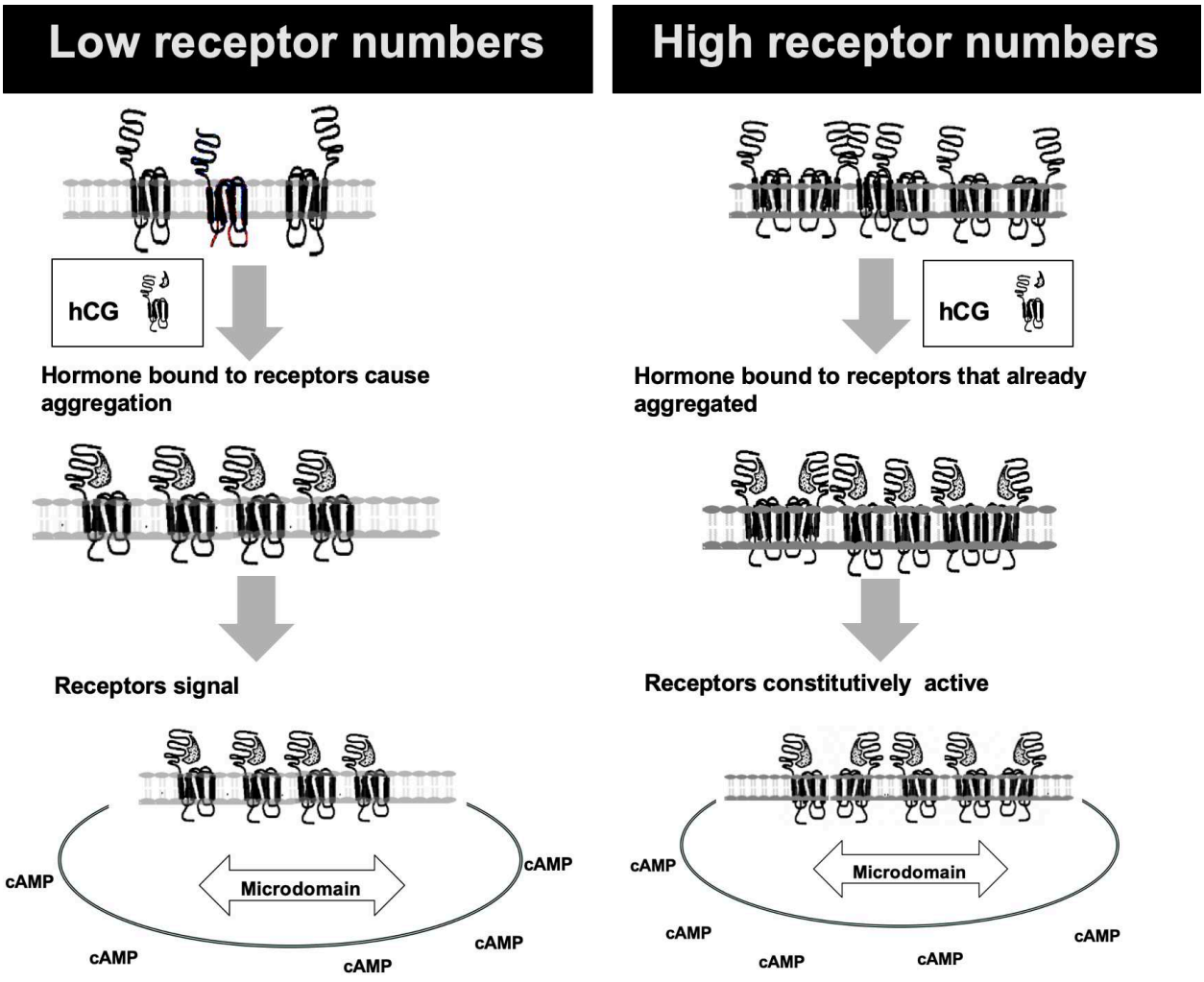

Figure 44: LHR expression levels affect the cluster size and activity of LHR in response to hCG.

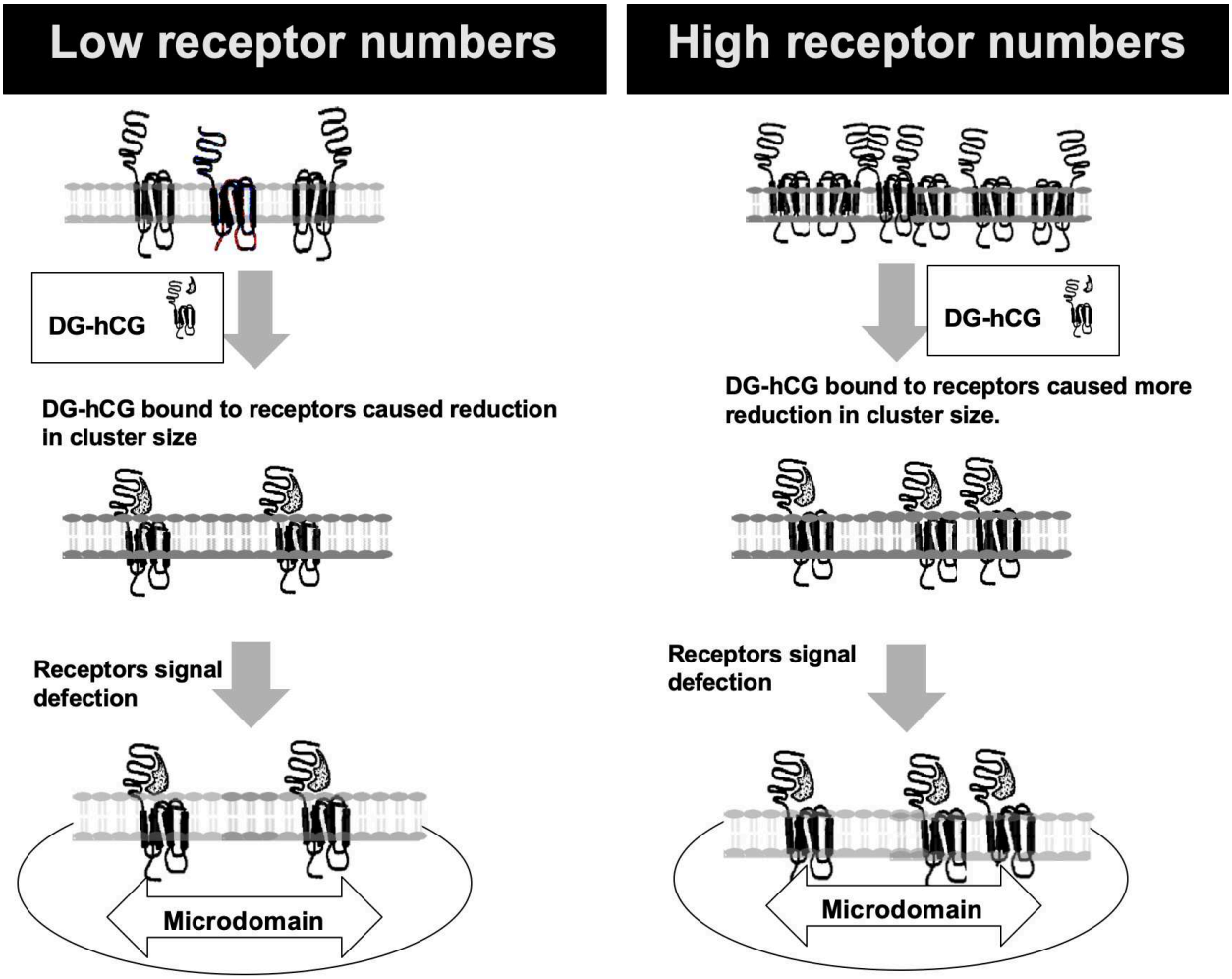

Figure 45: LHR expression levels affect the cluster size and activity of LHR in response to DG-hCG.

REFERENCES

1. Burger, K., G. Gimpl, and F. Fahrenholz, Regulation of receptor function by cholesterol. Cellular and Molecular Life Sciences CMLS, 2000. 57(11): p. 1577-1592.
2. Ascoli, M. and P. Narayan, The gonadotropin hormones and their receptors, in Yen & Jaffe's Reproductive Endocrinology. 2014, Elsevier. p. 27-44. e8.
3. Hunzicker-Dunn, M., et al., Membrane organization of luteinizing hormone receptors differs between actively signaling and desensitized receptors. Journal of Biological Chemistry, 2003. 278(44): p. 42744-42749.
4. Casarini, L., et al., Gonadotrophin Receptors. Endocrinology of the testis and male reproduction, 2017: p. 1-46.
5. Grzesik, P., et al., Differences in signal activation by LH and hCG are mediated by the LH/CG receptor's extracellular hinge region. Frontiers in endocrinology, 2015. 6: p. 140.
6. Ji, I., et al., Trans-activation of mutant follicle-stimulating hormone receptors selectively generates only one of two hormone signals. Molecular Endocrinology, 2004. 18(4): p. 968-978.
7. Grzesik, P., et al., Differences between lutropin-mediated and choriogonadotropin-mediated receptor activation. The FEBS Journal, 2014. 281(5): p. 1479-1492.
8. Horvat, R.D., B.G. Barisas, and D.A. Roess, Luteinizing hormone receptors are self-associated in slowly diffusing complexes during receptor desensitization. Molecular Endocrinology, 2001. 15(4): p. 534-542.
9. Pubchem. Cholesterol. 2019, March 27; Available from: https://pubchem.ncbi.nlm.nih.gov/compound/Cholesterol.
10. Meyer, B.H., et al., FRET imaging reveals that functional neurokinin-1 receptors are monomeric and reside in membrane microdomains of live cells. Proceedings of the National Academy of Sciences of the United States of America, 2006. 103(7): p. 2138-2143.
11. Pierce, K.L., R.T. Premont, and R.J. Lefkowitz, Signalling: seven-transmembrane receptors. Nature reviews Molecular cell biology, 2002. 3(9): p. 639.
12. Fredriksson, R., et al., The G-protein-coupled receptors in the human genome form five main families. Phylogenetic analysis, paralogon groups, and fingerprints. Molecular pharmacology, 2003. 63(6): p. 1256-1272.
13. Boron, W.F. and E.L. Boulpaep, Medical Physiology E-Book. 2016: Elsevier Health Sciences.
14. Venter, J.C., et al., The sequence of the human genome. science, 2001. 291(5507): p. 1304-1351.
15. Kobilka, B.K., G protein coupled receptor structure and activation. Biochimica et Biophysica Acta (BBA)-Biomembranes, 2007. 1768(4): p. 794-807.
16. Isberg, V., et al., GPCRdb: an information system for G protein-coupled receptors. Nucleic acids research, 2015. 44(D1): p. D356-D364.
17. Guo, H., et al., Methods used to study the oligomeric structure of G protein-coupled receptors. Bioscience Reports, 2017: p. BSR20160547.

18. Rask-Andersen, M., S. Masuram, and H.B. Schiöth, The druggable genome: evaluation of drug targets in clinical trials suggests major shifts in molecular class and indication. Annual review of pharmacology and toxicology, 2014. 54: p. 9-26.
19. Chakraborty, H. and A. Chattopadhyay, Excitements and challenges in GPCR oligomerization: molecular insight from FRET. ACS Chemical Neuroscience, 2014. 6(1): p. 199-206.
20. Chattopadhyay, A., GPCRs: lipid-dependent membrane receptors that act as drug targets. Advances in Biology, 2014. 2014.
21. Rosenbaum, D.M., S.G. Rasmussen, and B.K. Kobilka, The structure and function of G-protein-coupled receptors. Nature, 2009. 459(7245): p. 356.
22. Peng, Z.-L., J.-Y. Yang, and X. Chen, An improved classification of G-protein-coupled receptors using sequence-derived features. BMC bioinformatics, 2010. 11(1): p. 420.
23. Pitcher, J.A., N.J. Freedman, and R.J. Lefkowitz, G protein–coupled receptor kinases. 1998, Annual Reviews 4139 El Camino Way, PO Box 10139, Palo Alto, CA 94303-0139, USA.
24. W, N.A. and L. Gerald, Hormones. 1987, Academic Press.
25. Marquer, C., et al., Influence of MT7 toxin on the oligomerization state of the M1 muscarinic receptor 1. Biology of the cell, 2010. 102(7): p. 409-420.
26. Kamal, M., P. Maurice, and R. Jockers, Expanding the concept of G protein-coupled receptor (GPCR) dimer asymmetry towards GPCR-interacting proteins. Pharmaceuticals, 2011. 4(2): p. 273-284.
27. Terrillon, S. and M. Bouvier, Roles of G-protein-coupled receptor dimerization. EMBO Reports, 2004. 5(1): p. 30-34.
28. Dufau, M.L., The luteinizing hormone receptor. Current Opinion in Endocrinology, Diabetes and Obesity, 1995. 2(5): p. 365-374.
29. Camp, T.A., J.O. Rahal, and K.E. Mayo, Cellular localization and hormonal regulation of follicle-stimulating hormone and luteinizing hormone receptor messenger RNAs in the rat ovary. Molecular endocrinology, 1991. 5(10): p. 1405-1417.
30. Sullivan, M.W., et al., Ovarian Responses in Women to Recombinant Follicle-Stimulating Hormone and Luteinizing Hormone (LH): A Role for LH in the Final Stages of Follicular Maturation 1. The Journal of Clinical Endocrinology & Metabolism, 1999. 84(1): p. 228-232.
31. Qiao, J. and B. Han, Diseases caused by mutations in luteinizing hormone/chorionic gonadotropin receptor. Progress in molecular biology and translational science, 2019. 161: p. 69-89.
32. Leuschner, C., et al., Targeted destruction of androgen-sensitive and-insensitive prostate cancer cells and xenografts through luteinizing hormone receptors. The Prostate, 2001. 46(2): p. 116-125.
33. Engel, J.B. and A.V. Schally, Drug Insight: clinical use of agonists and antagonists of luteinizing-hormone-releasing hormone. Nature Reviews Endocrinology, 2007. 3(2): p. 157.
34. Pabon, J., et al., Human skin contains luteinizing hormone/chorionic gonadotropin receptors. The Journal of Clinical Endocrinology & Metabolism, 1996. 81(7): p. 2738-2741.

35. Kero, J., et al., Elevated luteinizing hormone induces expression of its receptor and promotes steroidogenesis in the adrenal cortex. The Journal of Clinical Investigation, 2000. 105(5): p. 633-641.
36. Lasley, B., et al., Identification of immunoreactive luteinizing hormone receptors in the adrenal cortex of the female rhesus macaque. Reproductive Sciences, 2016. 23(4): p. 524-530.
37. Sharpe, R.M., Pathways of endocrine disruption during male sexual differentiation and masculinisation. Best practice & research Clinical endocrinology & metabolism, 2006. 20(1): p. 91-110.
38. Troppmann, B., et al., Structural and functional plasticity of the luteinizing hormone/choriogonadotrophin receptor. Human Reproduction Update, 2013. 19(5): p. 583-602.
39. Narayan, P., Genetic models for the study of luteinizing hormone receptor function. Frontiers in endocrinology, 2015. 6: p. 152.
40. Maman, E., et al., High expression of luteinizing hormone receptors messenger RNA by human cumulus granulosa cells is in correlation with decreased fertilization. Fertility and sterility, 2012. 97(3): p. 592-598.
41. Young, J. and A.S. McNeilly, Theca: the forgotten cell of the ovarian follicle. Reproduction, 2010. 140(4): p. 489-504.
42. Pierce, J.G. and T.F. Parsons, Glycoprotein hormones: structure and function. Annual review of biochemistry, 1981. 50(1): p. 465-495.
43. Jaffee, R., P.A. Lee, and A. Midgley, Serum gonadotropins before at the inception of and following human pregnancy. Journal of Clinical Endocrinology and Metabolism, 1969. 29: p. 1281-1283.
44. Ellinwood, W., T. Nett, and G. Niswender, Maintenance of the corpus luteum of early pregnancy in the ewe. II. Prostaglandin secretion by the endometrium in vitro and in vivo. Biology of Reproduction, 1979. 21(4): p. 845-856.
45. Galet, C. and M. Ascoli, The differential binding affinities of the luteinizing hormone (LH)/choriogonadotropin receptor for LH and choriogonadotropin are dictated by different extracellular domain residues. Molecular Endocrinology, 2005. 19(5): p. 1263-1276.
46. Gębarowska, D., A.J. Zięcik, and E.L. Gregoraszczuk, Luteinizing hormone receptors on granulosa cells from preovulatory follicles and luteal cells throughout the oestrous cycle of pigs. Animal Reproduction Science, 1997. 49(2-3): p. 191-205.
47. Diagram System. Ovum female reproductive system. 2018, September 19; Available from: https://diagramsystem.net/ovum-female-reproductive-system/.
48. Williams, C.J. and G.F. Erickson, Morphology and physiology of the ovary, in Endotext [Internet]. 2012, MDText. com, Inc.
49. Empower Pharmacy. Hcg mechanism of action. 2019; Available from: https://www.empowerpharmacy.com/hormone-replacement.html.
50. Wu, S.-M., et al., Luteinizing hormone receptor mutations in disorders of sexual development and cancer. Pediatric Pathology & Molecular Medicine, 2000. 19(1): p. 21-40.
51. Zhang, F.-P., et al., Normal prenatal but arrested postnatal sexual development of luteinizing hormone receptor knockout (LuRKO) mice. Molecular endocrinology, 2001. 15(1): p. 172-183.

52. Latronico, A.C., et al., Brief Report: Testicular and Ovarian Resistance to Luteinizing Hormone Caused by Inactivating Mutations of the Luteinizing Hormone-Receptor Gene. Obstetrical & gynecological survey, 1996. 51(7): p. 416-419.
53. Davies, T., P. Laurberg, and R. Bahn, Williams textbook of endocrinology. Hyperthyroid disorders. 13th ed. India: Elsevier Publications, 2016: p. 369-415.
54. Yariz, K.O., et al., Inherited mutation of the luteinizing hormone/choriogonadotropin receptor (LHCGR) in empty follicle syndrome. Fertility and sterility, 2011. 96(2): p. e125-e130.
55. Laue, L., et al., Genetic heterogeneity of constitutively activating mutations of the human luteinizing hormone receptor in familial male-limited precocious puberty. Proceedings of the National Academy of Sciences, 1995. 92(6): p. 1906-1910.
56. Casadesus, G., et al., Luteinizing hormone modulates cognition and amyloid-β deposition in Alzheimer APP transgenic mice. Biochimica et Biophysica Acta (BBA)-Molecular Basis of Disease, 2006. 1762(4): p. 447-452.
57. Rao, C., Involvement of luteinizing hormone in Alzheimer disease development in elderly women. Reproductive Sciences, 2017. 24(3): p. 355-368.
58. Lin, J., et al., Genetic ablation of luteinizing hormone receptor improves the amyloid pathology in a mouse model of Alzheimer disease. Journal of Neuropathology & Experimental Neurology, 2010. 69(3): p. 253-261.
59. Webber, K.M., et al., The contribution of luteinizing hormone to Alzheimer disease pathogenesis. Clinical Medicine & Research, 2007. 5(3): p. 177-183.
60. Bowen, R.L., et al., Luteinizing hormone, a reproductive regulator that modulates the processing of amyloid-β precursor protein and amyloid-β deposition. Journal of Biological Chemistry, 2004. 279(19): p. 20539-20545.
61. Burnham, V.L. and J.E. Thornton, Luteinizing hormone as a key player in the cognitive decline of Alzheimer's disease. Hormones and behavior, 2015. 76: p. 48-56.
62. Lenhard, M., et al., Opposed roles of follicle-stimulating hormone and luteinizing hormone receptors in ovarian cancer survival. Histopathology, 2011. 58(6): p. 990-994.
63. Parrott, J.A., et al., Expression and actions of both the follicle stimulating hormone receptor and the luteinizing hormone receptor in normal ovarian surface epithelium and ovarian cancer. Molecular and Cellular Endocrinology, 2001. 172(1): p. 213-222.
64. Cui, J., et al., Regulation of gene expression in ovarian cancer cells by luteinizing hormone receptor expression and activation. BMC Cancer, 2011. 11(1): p. 280.
65. Emons, G. and A.V. Schally, The use of luteinizing hormone releasing hormone agonists and antagonists in gynaecological cancers. Human Reproduction, 1994. 9(7): p. 1364-1379.
66. Lojun, S., et al., Presence of functional luteinizing hormone/chorionic gonadotropin (hCG) receptors in human breast cell lines: implications supporting the premise that hCG protects women against breast cancer. Biology of reproduction, 1997. 57(5): p. 1202-1210.
67. Meduri, G., et al., Luteinizing hormone/human chorionic gonadotropin receptors in breast cancer. Cancer Research, 1997. 57(5): p. 857-864.
68. Kwok, C., et al., Receptors for luteinizing hormone-releasing hormone (GnRH) as therapeutic targets in triple negative breast cancers (TNBC). Targeted oncology, 2015. 10(3): p. 365-373.

69. Peters, C.A. and P.C. Walsh, The effect of nafarelin acetate, a luteinizing-hormone–releasing hormone agonist, on benign prostatic hyperplasia. New England Journal of Medicine, 1987. 317(10): p. 599-604.
70. Halmos, G., et al., High incidence of receptors for luteinizing hormone-releasing hormone (LHRH) and LHRH receptor gene expression in human prostate cancers. The Journal of urology, 2000. 163(2): p. 623-629.
71. Sipos, E., et al., Characterization of luteinizing hormone-releasing hormone receptor type I (LH-RH-I) as a potential molecular target in OCM-1 and OCM-3 human uveal melanoma cell lines. OncoTargets and therapy, 2018. 11: p. 933.
72. Nagy, A. and A.V. Schally, Targeting of cytotoxic luteinizing hormone-releasing hormone analogs to breast, ovarian, endometrial, and prostate cancers. Biology of reproduction, 2005. 73(5): p. 851-859.
73. Rönnberg, L., A. Kauppila, and H. Rajaniemi, Luteinizing hormone receptor disorder in endometriosis. Fertility and Sterility, 1984. 42(1): p. 64-68.
74. Lin, J., et al., Increased expression of luteinizing hormone/human chorionic gonadotropin receptor gene in human endometrial carcinomas. The Journal of Clinical Endocrinology & Metabolism, 1994. 79(5): p. 1483-1491.
75. Zou, J., et al., Association of luteinizing hormone/choriogonadotropin receptor gene polymorphisms with polycystic ovary syndrome risk: a meta-analysis. Gynecological Endocrinology, 2019. 35(1): p. 81-85.
76. Thathapudi, S., et al., Association of luteinizing hormone chorionic gonadotropin receptor gene polymorphism (rs2293275) with polycystic ovarian syndrome. Genetic testing and molecular biomarkers, 2015. 19(3): p. 128-132.
77. Gonzalez-Barcena, D., et al., Treatment of uterine leiomyomas with luteinizing hormone-releasing hormone antagonist Cetrorelix. Human reproduction (Oxford, England), 1997. 12(9): p. 2028-2035.
78. Lacroix, A., et al., Cushing's syndrome variants secondary to aberrant hormone receptors. Trends in Endocrinology & Metabolism, 2004. 15(8): p. 375-382.
79. Saner-Amigh, K., et al., Elevated expression of luteinizing hormone receptor in aldosterone-producing adenomas. The Journal of Clinical Endocrinology & Metabolism, 2006. 91(3): p. 1136-1142.
80. Kunal, S.B., A. Killivalavan, and R. Medhamurthy, Involvement of Src family of kinases and cAMP phosphodiesterase in the luteinizing hormone/chorionic gonadotropin receptor-mediated signaling in the corpus luteum of monkey. Reproductive Biology and Endocrinology, 2012. 10(1): p. 25.
81. Bird, J., et al., Luteinizing hormone and human chorionic gonadotropin decrease type 2 5α-reductase and androgen receptor protein levels in women's skin. The Journal of Clinical Endocrinology & Metabolism, 1998. 83(5): p. 1776-1782.
82. Rao, C.V. An overview of the past, present, and future of nongonadal LH/hCG actions in reproductive biology and medicine. in Seminars in reproductive medicine. 2001. Copyright© 2001 by Thieme Medical Publishers, Inc., 333 Seventh Avenue, New ….
83. Dufau, M.L., The luteinizing hormone receptor 1. Annual Review of Physiology, 1998. 60(1): p. 461-496.
84. Ascoli, M., F. Fanelli, and D.L. Segaloff, The lutropin/choriogonadotropin receptor, a 2002 perspective. Endocrine Reviews, 2002. 23(2): p. 141-174.

85. Borgbo, T., et al., The polymorphic insertion of the luteinizing hormone receptor “insLQ” show a negative association to LHR gene expression and to the follicular fluid hormonal profile in human small antral follicles. Molecular and cellular endocrinology, 2018. 460: p. 57-62.
86. Müller, T., J.r. Gromoll, and M. Simoni, Absence of exon 10 of the human luteinizing hormone (LH) receptor impairs LH, but not human chorionic gonadotropin action. The Journal of Clinical Endocrinology & Metabolism, 2003. 88(5): p. 2242-2249.
87. Vischer, H.F., et al., Ligand Selectivity of Gonadotropin Receptors Role of the β-strands of extracellular leucine-rich repeats 3 and 6 of the human luteinizing hormone receptor. Journal of Biological Chemistry, 2003. 278(18): p. 15505-15513.
88. Smits, G., et al., Glycoprotein hormone receptors: determinants in leucine-rich repeats responsible for ligand specificity. The EMBO journal, 2003. 22(11): p. 2692-2703.
89. Dhar, N., et al., Dissecting the structural and functional features of the Luteinizing hormone receptor using receptor specific single chain fragment variables. Molecular and cellular endocrinology, 2016. 427: p. 1-12.
90. Puett, D., et al., The luteinizing hormone receptor: insights into structure–function relationships and hormone-receptor-mediated changes in gene expression in ovarian cancer cells. Molecular and cellular endocrinology, 2010. 329(1-2): p. 47-55.
91. Kleinau, G. and G. Krause, Thyrotropin and homologous glycoprotein hormone receptors: structural and functional aspects of extracellular signaling mechanisms. Endocrine reviews, 2009. 30(2): p. 133-151.
92. The National Center for Biotechnology Information. Glycoprotein hormones, alpha polypeptide [homo sapiens (human)]. 2019, September 18; Available from: https://www.ncbi.nlm.nih.gov/gene/1081.
93. Sequence Structure Function Analysis of Glycoprotein Hormone Receptors. Scheme of GPHRs. 2017, Jan 17; Available from: http://www.ssfa-gphr.de/scheme.php.
94. Riccetti, L., et al., Human luteinizing hormone and chorionic gonadotropin display biased agonism at the LH and LH/CG receptors. Scientific reports, 2017. 7(1): p. 940.
95. Casarini, L., et al., LH and hCG action on the same receptor results in quantitatively and qualitatively different intracellular signalling. PloS One, 2012. 7(10): p. e46682.
96. Segaloff, D.L. and M. Ascoli, The lutropin/choriogonadotropin receptor… 4 years later. Endocrine Reviews, 1993. 14(3): p. 324-347.
97. Strauss, J.F. and R.L. Barbieri, Yen & Jaffe's reproductive endocrinology E-book: physiology, pathophysiology, and clinical management (Expert Consult-Online and Print). 2013: Elsevier Health Sciences.
98. Cole, L.A., Human chorionic gonadotropin (hCG). 2014: Elsevier.
99. Lapthorn, A., et al., Crystal structure of human chorionic gonadotropin. Nature, 1994. 369(6480): p. 455.
100. Wu, H., et al., Structure of human chorionic gonadotropin at 2.6 Å resolution from MAD analysis of the selenomethionyl protein. Structure, 1994. 2(6): p. 545-558.
101. Ogiwara, K., et al., Characterization of luteinizing hormone and luteinizing hormone receptor and their indispensable role in the ovulatory process of the medaka. PLoS One, 2013. 8(1): p. e54482.
102. Riccetti, L., et al., Human LH and hCG stimulate differently the early signalling pathways but result in equal testosterone synthesis in mouse Leydig cells in vitro. Reproductive Biology and Endocrinology, 2017. 15(1): p. 2.

103. Huhtaniemi, I.T. and K.J. Catt, Differential binding affinities of rat testis luteinizing hormone (LH) receptors for human chorionic gonadotropin, human LH, and ovine LH. Endocrinology, 1981. 108(5): p. 1931-1938.
104. Rivero-Müller, A., et al., Rescue of defective G protein–coupled receptor function in vivo by intermolecular cooperation. Proceedings of the National Academy of Sciences, 2010. 107(5): p. 2319-2324.
105. Trehan, A., et al., Rescue of Defective G Protein-Coupled Receptor Function by Intermolecular Cooperation, in G Protein-Coupled Receptor Genetics. 2014, Springer. p. 239-255.
106. Lee, C., et al., Two defective heterozygous luteinizing hormone receptors can rescue hormone action. Journal of Biological Chemistry, 2002. 277(18): p. 15795-15800.
107. Lee, C., Cis-and Trans-activation of Hormone Receptors: The LH Receptor. 2003.
108. Ji, I., et al., Cis-and trans-activation of hormone receptors: the LH receptor. Molecular Endocrinology, 2002. 16(6): p. 1299-1308.
109. Osuga, Y., et al., Co-expression of defective luteinizing hormone receptor fragments partially reconstitutes ligand-induced signal generation. Journal of Biological Chemistry, 1997. 272(40): p. 25006-25012.
110. Rahman, N.A. and C. Rao, Recent progress in luteinizing hormone/human chorionic gonadotrophin hormone research. Molecular human reproduction, 2009. 15(11): p. 703-711.
111. Minegishi, T., K. Nakamura, and Y. Ibuki, Structure and Reguration of LH/CG Recepter. Endocrine Journal, 1993. 40(3): p. 275-287.
112. Keutmann, H.T., et al., Chemically deglycosylated human chorionic gonadotropin subunits: characterization and biological properties. Biochemistry, 1983. 22(13): p. 3067-3072.
113. Morell, A.G., et al., The role of sialic acid in determining the survival of glycoproteins in the circulation. Journal of Biological Chemistry, 1971. 246(5): p. 1461-1467.
114. Dunkel, L., et al., Circulating luteinizing hormone receptor inhibitor (s) in boys with chronic renal failure. Kidney international, 1997. 51(3): p. 777-784.
115. Wolf-Ringwall, A.L., et al., Restricted lateral diffusion of luteinizing hormone receptors in membrane microdomains. Journal of Biological Chemistry, 2011. 286(34): p. 29818-29827.
116. Roess, D.A. and S.M. Smith, Self-association and raft localization of functional luteinizing hormone receptors. Biology of Reproduction, 2003. 69(6): p. 1765-1770.
117. Huhtaniemi, I.T., et al., The murine luteinizing hormone and follicle-stimulating hormone receptor genes: transcription initiation sites, putative promoter sequences and promoter activity. Molecular and cellular endocrinology, 1992. 88(1-3): p. 55-66.
118. Roess, D.A., et al., Luteinizing Hormone Receptors Are Self-Associated in the Plasma Membrane 1. Endocrinology, 2000. 141(12): p. 4518-4523.
119. Casarini, L., et al., 'Spare'Luteinizing Hormone Receptors: Facts and Fiction. Trends in Endocrinology & Metabolism, 2018. 29(4): p. 208-217.
120. The National Center for Biotechnology Information. Chorionic gonadotropin subunit beta [homo sapiens (human)]. 2019, September 18; Available from: https://www.ncbi.nlm.nih.gov/gene/114335.
121. The National Center for Biotechnology Information, Luteinizing hormone subunit beta [homo sapiens (human)]. 2019, September 18.

122. Fares, F., The role of O-linked and N-linked oligosaccharides on the structure–function of glycoprotein hormones: development of agonists and antagonists. Biochimica et Biophysica Acta (BBA)-General Subjects, 2006. 1760(4): p. 560-567.
123. Keutmann, H.T., L. Johnson, and R.J. Ryan, Evidence for a conformational change in deglycosylated glycoprotein hormones. FEBS letters, 1985. 185(2): p. 333-338.
124. Edge, A.S., et al., Deglycosylation of glycoproteins by trifluoromethanesulfonic acid. Analytical biochemistry, 1981. 118(1): p. 131-137.
125. Kalyan, N.K. and O.P. Bahl, Effect of deglycosylation on the subunit interactions and receptor binding activity of human chorionic gonadotropin. Biochemical and biophysical research communications, 1981. 102(4): p. 1246-1253.
126. Matzuk, M. and I. Boime, Site-specific mutagenesis defines the intracellular role of the asparagine-linked oligosaccharides of chorionic gonadotropin beta subunit. Journal of Biological Chemistry, 1988. 263(32): p. 17106-17111.
127. Dunkel, L., et al., Deglycosylated human chorionic gonadotropin (hCG) antagonizes hCG stimulation of 3', 5'-cyclic adenosine monophosphate accumulation through a noncompetitive interaction with recombinant human luteinizing hormone receptors. Endocrinology, 1993. 132(2): p. 763-769.
128. Browne, E.S., et al., Is deglycosylated human chorionic gonadotropin an antagonist to human chorionic gonadotropin? Characterization of deglycosylated human chorionic gonadotropin action in two testicular interstitial cell fractions. Biochimica et Biophysica Acta (BBA)-General Subjects, 1990. 1033(3): p. 226-234.
129. Sairam, M., Role of carbohydrates in glycoprotein hormone signal transduction. The FASEB Journal, 1989. 3(8): p. 1915-1926.
130. Richardson, M., G. Masson, and M. Sairam, Inhibitory action of chemically deglycosylated human chorionic gonadotrophin on hormone-induced steroid production by dispersed cells from human corpus luteum. Journal of endocrinology, 1984. 101(3): p. 327-332.
131. Watson, J. and J. Raeburn, Progesterone production by human ovarian tissues in response to deglycosylated human chorionic gonadotrophin. European Journal of Obstetrics & Gynecology and Reproductive Biology, 1984. 17(5): p. 315-320.
132. Patton, P.E., et al., The effect of deglycosylated human chorionic gonadotropin on corpora luteal function in healthy women. Fertility and sterility, 1988. 49(4): p. 620-625.
133. LIU, L., et al., Stimulation of testosterone production in the cynomolgus monkey in vivo by deglycosylated and desialylated human choriogonadotropin. Endocrinology, 1989. 124(1): p. 175-180.
134. Cho, N., et al., Discovery of a novel, potent, and orally active nonpeptide antagonist of the human luteinizing hormone-releasing hormone (LHRH) receptor. Journal of medicinal chemistry, 1998. 41(22): p. 4190-4195.
135. Palmer, B.F., Sexual dysfunction in men and women with chronic kidney disease and end-stage kidney disease. Advances in renal replacement therapy, 2003. 10(1): p. 48-60.
136. Kalyani, R.R., S. Gavini, and A.S. Dobs, Male hypogonadism in systemic disease. Endocrinology and metabolism clinics of North America, 2007. 36(2): p. 333-348.
137. Jonas, K.C., et al., G protein-coupled receptor transactivation: from molecules to mice, in Methods in cell biology. 2013, Elsevier. p. 433-450.
138. Kanamarlapudi, V., U.D. Gordon, and A.L. Bernal, Luteinizing hormone/chorionic gonadotrophin receptor overexpressed in granulosa cells from polycystic ovary syndrome ovaries is functionally active. Reproductive biomedicine online, 2016. 32(6): p. 635-641.

139. Stocco, D.M., et al., Multiple signaling pathways regulating steroidogenesis and steroidogenic acute regulatory protein expression: more complicated than we thought. Molecular endocrinology, 2005. 19(11): p. 2647-2659.
140. Jonas, K.C., et al., Single molecule analysis of functionally asymmetric G protein-coupled receptor (GPCR) oligomers reveals diverse spatial and structural assemblies. Journal of Biological Chemistry, 2015. 290(7): p. 3875-3892.
141. Breen, S.M., et al., Ovulation involves the luteinizing hormone-dependent activation of Gq/11 in granulosa cells. Molecular endocrinology, 2013. 27(9): p. 1483-1491.
142. Veldhuis, J.D., W. MAY, and D. Juchter, Mechanisms subserving hormone action in the ovary: role of calcium ions as assessed by steady state calcium exchange in cultured swine granulosa cells. Endocrinology, 1987. 120(2): p. 445-449.
143. Casarini, L., et al., Follicle-stimulating hormone potentiates the steroidogenic activity of chorionic gonadotropin and the anti-apoptotic activity of luteinizing hormone in human granulosa-lutein cells in vitro. Molecular and cellular endocrinology, 2016. 422: p. 103-114.
144. Davis, J.S., et al., Luteinizing hormone stimulates the formation of inositol trisphosphate and cyclic AMP in rat granulosa cells. Evidence for phospholipase C generated second messengers in the action of luteinizing hormone. Biochemical Journal, 1986. 238(2): p. 597-604.
145. Davis, J.S., et al., Human chorionic gonadotropin activates the inositol 1, 4, 5-trisphosphate-Ca2+ intracellular signalling system in bovine luteal cells. FEBS letters, 1986. 208(2): p. 287-291.
146. Gavi, S., et al., G-protein-coupled receptors and tyrosine kinases: crossroads in cell signaling and regulation. Trends in Endocrinology & Metabolism, 2006. 17(2): p. 48-54.
147. Hai, L., et al., Constitutive luteinizing hormone receptor signaling causes sexual dysfunction and Leydig cell adenomas in male mice. Biology of reproduction, 2017. 96(5): p. 1007-1018.
148. Hunzicker-Dunn, M., et al., ARF6: a newly appreciated player in G protein-coupled receptor desensitization. FEBS letters, 2002. 521(1-3): p. 3-8.
149. Crenshaw, S.A., Role of homotropic association of luteinizing hormone receptors in hormone mediated signaling. 2012, Colorado State University: Fort Collins, Colorado.
150. Tranchant, T., et al., Preferential β-arrestin signalling at low receptor density revealed by functional characterization of the human FSH receptor A189 V mutation. Molecular and cellular endocrinology, 2011. 331(1): p. 109-118.
151. Lamm, M. and M. Hunzicker-Dunn, Phosphorylation-independent desensitization of the luteinizing hormone/chorionic gonadotropin receptor in porcine follicular membranes. Molecular Endocrinology, 1994. 8(11): p. 1537-1546.
152. Lamm, M., et al., The effect of protein kinases on desensitization of the porcine follicular membrane luteinizing hormone/chorionic gonadotropin-sensitive adenylyl cyclase. Endocrinology, 1994. 134(4): p. 1745-1754.
153. Zhu, X., et al., A luteinizing hormone receptor with a severely truncated cytoplasmic tail (LHR-ct628) desensitizes to the same degree as the full-length receptor. Journal of Biological Chemistry, 1993. 268(3): p. 1723-1728.
154. Mukherjee, S., et al., A direct role for arrestins in desensitization of the luteinizing hormone/choriogonadotropin receptor in porcine ovarian follicular membranes. Proceedings of the National Academy of Sciences, 1999. 96(2): p. 493-498.

155. Ekstrom, R.C. and M. Hunzicker-Dunn, Homologous desensitization of ovarian luteinizing hormone/human chorionic gonadotropin-responsive adenylyl cyclase is dependent upon GTP. Endocrinology, 1989. 124(2): p. 956-963.
156. Wang, Z., R.W. Hipkin, and M. Ascoli, Progressive cytoplasmic tail truncations of the lutropin-choriogonadotropin receptor prevent agonist-or phorbol ester-induced phosphorylation, impair agonist-or phorbol ester-induced desensitization, and enhance agonist-induced receptor down-regulation. Molecular Endocrinology, 1996. 10(6): p. 748-759.
157. Wang, Z., X. Liu, and M. Ascoli, Phosphorylation of the lutropin/choriogonadotropin receptor facilitates uncoupling of the receptor from adenylyl cyclase and endocytosis of the bound hormone. Molecular Endocrinology, 1997. 11(2): p. 183-192.
158. Minton, A.P., Influence of excluded volume upon macromolecular structure and associations in 'crowded" media. Current opinion in biotechnology, 1997. 8(1): p. 65-69.
159. Hirakawa, T., C. Galet, and M. Ascoli, MA-10 cells transfected with the human lutropin/choriogonadotropin receptor (hLHR): a novel experimental paradigm to study the functional properties of the hLHR. Endocrinology, 2002. 143(3): p. 1026-1035.
160. Ellis, R.J., Macromolecular crowding: obvious but underappreciated. Trends in biochemical sciences, 2001. 26(10): p. 597-604.
161. Rao, M. and S. Mayor, Use of Forster's resonance energy transfer microscopy to study lipid rafts. Biochimica et Biophysica Acta (BBA)-Molecular Cell Research, 2005. 1746(3): p. 221-233.
162. Zhu, S., et al., A conjugate of methotrexate and an analog of luteinizing hormone releasing hormone shows increased efficacy against prostate cancer. Scientific reports, 2016. 6: p. 33894.
163. Saxena, R. and A. Chattopadhyay, Membrane cholesterol stabilizes the human serotonin1A receptor. Biochimica et Biophysica Acta (BBA)-Biomembranes, 2012. 1818(12): p. 2936-2942.
164. Paila, Y.D. and A. Chattopadhyay, The function of G-protein coupled receptors and membrane cholesterol: specific or general interaction? Glycoconjugate journal, 2009. 26(6): p. 711.
165. Simons, K. and E. Ikonen, Functional rafts in cell membranes. nature, 1997. 387(6633): p. 569.
166. Chattopadhyay, A., et al., Role of cholesterol in ligand binding and G-protein coupling of serotonin 1A receptors solubilized from bovine hippocampus. Biochemical and Biophysical Research Communications, 2005. 327(4): p. 1036-1041.
167. Pucadyil, T.J. and A. Chattopadhyay, Role of cholesterol in the function and organization of G-protein coupled receptors. Progress in lipid research, 2006. 45(4): p. 295-333.
168. Gimpl, G., K. Burger, and F. Fahrenholz, Cholesterol as modulator of receptor function. Biochemistry, 1997. 36(36): p. 10959-10974.
169. Yao, Z. and B. Kobilka, Using synthetic lipids to stabilize purified b2 adrenoceptor in detergent micelles. Anal. Biochem, 2005. 343: p. 344-346.
170. Cherezov, V., et al., High-resolution crystal structure of an engineered human β2-adrenergic G protein–coupled receptor. science, 2007. 318(5854): p. 1258-1265.
171. Ganguly, S., A.H. Clayton, and A. Chattopadhyay, Organization of higher-order oligomers of the serotonin 1A receptor explored utilizing homo-FRET in live cells. Biophysical Journal, 2011. 100(2): p. 361-368.

172. Hanson, M.A., et al., A specific cholesterol binding site is established by the 2.8 Å structure of the human β2-adrenergic receptor. Structure, 2008. 16(6): p. 897-905.
173. Saxena, R. and A. Chattopadhyay, Membrane cholesterol stabilizes the human serotonin 1A receptor. Biochimica et Biophysica Acta (BBA)-Biomembranes, 2012. 1818(12): p. 2936-2942.
174. Nguyen, D.H. and D. Taub, CXCR4 function requires membrane cholesterol: implications for HIV infection. The Journal of Immunology, 2002. 168(8): p. 4121-4126.
175. Pucadyil, T.J. and A. Chattopadhyay, Cholesterol modulates ligand binding and G-protein coupling to serotonin1A receptors from bovine hippocampus. Biochimica et Biophysica Acta (BBA)-Biomembranes, 2004. 1663(1-2): p. 188-200.
176. Albert, A.D. and K. Boesze-Battaglia, The role of cholesterol in rod outer segment membranes. Progress in lipid research, 2005. 44(2-3): p. 99-124.
177. Oates, J. and A. Watts, Uncovering the intimate relationship between lipids, cholesterol and GPCR activation. Current opinion in structural biology, 2011. 21(6): p. 802-807.
178. Jafurulla, M., S. Tiwari, and A. Chattopadhyay, Identification of cholesterol recognition amino acid consensus (CRAC) motif in G-protein coupled receptors. Biochemical and biophysical research communications, 2011. 404(1): p. 569-573.
179. Sengupta, D., G.A. Kumar, and A. Chattopadhyay, Interaction of membrane cholesterol with GPCRs: Implications in receptor oligomerization, in G-Protein-Coupled Receptor Dimers. 2017, Springer. p. 415-429.
180. Jones, O.T. and M.G. McNamee, Annular and nonannular binding sites for cholesterol associated with the nicotinic acetylcholine receptor. Biochemistry, 1988. 27(7): p. 2364-2374.
181. Smith, S.M., et al., Luteinizing hormone receptors translocate to plasma membrane microdomains after binding of human chorionic gonadotropin. Endocrinology, 2006. 147(4): p. 1789-1795.
182. Lei, Y., et al., Constitutively-active human LH receptors are self-associated and located in rafts. Molecular and Cellular Endocrinology, 2007. 260: p. 65-72.
183. Sanchez, S.A., et al., Methyl-β-cyclodextrins preferentially remove cholesterol from the liquid disordered phase in giant unilamellar vesicles. The Journal of membrane biology, 2011. 241(1): p. 1-10.
184. Li, R., et al., Analytical characterization of methyl-β-cyclodextrin for pharmacological activity to reduce lysosomal cholesterol accumulation in Niemann-Pick disease type C1 cells. Assay and drug development technologies, 2017. 15(4): p. 154-166.
185. Rodal, S.K., et al., Extraction of cholesterol with methyl-β-cyclodextrin perturbs formation of clathrin-coated endocytic vesicles. Molecular biology of the cell, 1999. 10(4): p. 961-974.
186. Horvath, G. and G.E. Seidel Jr, Vitrification of bovine oocytes after treatment with cholesterol-loaded methyl-β-cyclodextrin. Theriogenology, 2006. 66(4): p. 1026-1033.
187. McGraw, C., et al., Membrane cholesterol depletion reduces downstream signaling activity of the adenosine A2A receptor. Biochimica et Biophysica Acta (BBA)-Biomembranes, 2019. 1861(4): p. 760-767.
188. Ganguly, S. and A. Chattopadhyay, Cholesterol depletion mimics the effect of cytoskeletal destabilization on membrane dynamics of the serotonin 1A receptor: a zFCS study. Biophysical journal, 2010. 99(5): p. 1397-1407.

189. Varma, R. and S. Mayor, GPI-anchored proteins are organized in submicron domains at the cell surface. Nature, 1998. 394(6695): p. 798.
190. Zheng, H., et al., Palmitoylation and membrane cholesterol stabilize μ-opioid receptor homodimerization and G protein coupling. BMC cell biology, 2012. 13(1): p. 6.
191. Milligan, G., G protein-coupled receptor dimerisation: molecular basis and relevance to function. Biochimica et Biophysica Acta (BBA)-Biomembranes, 2007. 1768(4): p. 825-835.
192. Guan, R., et al., Bioluminescence resonance energy transfer studies reveal constitutive dimerization of the human lutropin receptor and a lack of correlation between receptor activation and the propensity for dimerization. Journal of Biological Chemistry, 2009. 284(12): p. 7483-7494.
193. Tao, Y.-X., N.B. Johnson, and D.L. Segaloff, Constitutive and agonist-dependent self-association of the cell surface human lutropin receptor. Journal of Biological Chemistry, 2004. 279(7): p. 5904-5914.
194. Horvat, R.D., et al., Intrinsically fluorescent luteinizing hormone receptor demonstrates hormone-driven aggregation. Biochemical and Biophysical Research Communications, 1999. 255(2): p. 382-385.
195. Luborsky, J., W. Slater, and H. Behrman, Luteinizing Hormone (LH) Receptor Aggregation: Modification of Ferritin-LH Binding and Aggregation by Prostaglandin F2 α and Ferritin-LH. Endocrinology, 1984. 115(6): p. 2217-2226.
196. Althumairy, D.A., Evaluating levels of luteinizing hormone receptor dimers and oligomers. 2015, Colorado State University. Libraries.
197. Bader, A.N., et al., Homo-FRET imaging enables quantification of protein cluster sizes with subcellular resolution. Biophysical journal, 2009. 97(9): p. 2613-2622.
198. Segaloff, D.L., H. Wang, and J.S. Richards, Hormonal regulation of luteinizing hormone/chorionic gonadotropin receptor mRNA in rat ovarian cells during follicular development and luteinization. Molecular endocrinology, 1990. 4(12): p. 1856-1865.
199. Martín-Sánchez, F., V. Compan, and P. Pelegrín, Measuring NLR Oligomerization III: Detection of NLRP3 Complex by Bioluminescence Resonance Energy Transfer. NLR Proteins: Methods and Protocols, 2016: p. 159-168.
200. Li, X., et al., Quantification of membrane protein dynamics and interactions in plant cells by fluorescence correlation spectroscopy. Molecular plant, 2016. 9(9): p. 1229-1239.
201. Ciccotosto, G.D., et al., Aggregation distributions on cells determined by photobleaching image correlation spectroscopy. Biophysical journal, 2013. 104(5): p. 1056-1064.
202. Zhang, X.-E., Z. Cui, and D. Wang, Sensing of biomolecular interactions using fluorescence complementing systems in living cells. Biosensors and Bioelectronics, 2016. 76: p. 243-250.
203. Cevheroğlu, O., et al., The yeast Ste2p G protein-coupled receptor dimerizes on the cell plasma membrane. Biochimica et Biophysica Acta (BBA)-Biomembranes, 2017.
204. Lalonde, S., et al., Molecular and cellular approaches for the detection of protein–protein interactions: latest techniques and current limitations. The Plant Journal, 2008. 53(4): p. 610-635.
205. Martínez-Muñoz, L., J.M. Rodríguez-Frade, and M. Mellado, Use of Resonance Energy Transfer Techniques for In Vivo Detection of Chemokine Receptor Oligomerization. Chemotaxis: Methods and Protocols, 2016: p. 341-359.

206. Forster, T., Energiewanderung und fluoreszenz. Naturwissenschaften, 1946. 33(6): p. 166-175.
207. Chan, F.T., C.F. Kaminski, and G.S. Kaminski Schierle, HomoFRET Fluorescence Anisotropy Imaging as a Tool to Study Molecular Self-Assembly in Live Cells. ChemPhysChem, 2011. 12(3): p. 500-509.
208. Bader, A.N., et al., Homo-FRET imaging as a tool to quantify protein and lipid clustering. ChemPhysChem, 2011. 12(3): p. 475-483.
209. Runnels, L.W. and S.F. Scarlata, Theory and application of fluorescence homotransfer to melittin oligomerization. Biophysical journal, 1995. 69(4): p. 1569-1583.
210. Bajar, B., et al., A guide to fluorescent protein FRET pairs. Sensors, 2016. 16(9): p. 1488.
211. Jafurulla, M. and A. Chattopadhyay, Application of Quantitative Fluorescence Microscopic Approaches to Monitor Organization and Dynamics of the Serotonin1A Receptor, in Fluorescent Methods to Study Biological Membranes. 2012, Springer. p. 417-437.
212. Lidke, K.A., et al., The role of photon statistics in fluorescence anisotropy imaging. IEEE Transactions on Image Processing, 2005. 14(9): p. 1237-1245.
213. Tramier, M., et al., [25] Homo-FRET versus hetero-FRET to probe homodimers in living cells, in Methods in enzymology. 2003, Elsevier. p. 580-597.
214. Clayton, A.H. and A. Chattopadhyay, Taking care of bystander FRET in a crowded cell membrane environment. Biophysical journal, 2014. 106(6): p. 1227.
215. Oomen, M., Homo-FRET detection in wide-field, steady-state microscopy, with mCherry as labeling fluorophore. 2014.
216. Beyeler, K., Detect clustering in cells using Homo-FRET. 2015.
217. Saha, S., R. Raghupathy, and S. Mayor, Homo-FRET imaging highlights the nanoscale organization of cell surface molecules, in Advanced Fluorescence Microscopy. 2015, Springer. p. 151-173.
218. Gautier, I., et al., Homo-FRET microscopy in living cells to measure monomer-dimer transition of GFP-tagged proteins. Biophysical Journal, 2001. 80(6): p. 3000-3008.
219. Warren, S., et al., Homo-FRET based biosensors and their application to multiplexed imaging of signalling events in live cells. International journal of molecular sciences, 2015. 16(7): p. 14695-14716.
220. Kagie, N., Homo-FRET Detection by Fluorescence Polarization Anisotropy in Wide-field Microscopy. 2013.
221. Xia, Z. and Y. Liu, Reliable and global measurement of fluorescence resonance energy transfer using fluorescence microscopes. Biophysical journal, 2001. 81(4): p. 2395-2402.
222. Szabó, Á., J. Szöllősi, and P. Nagy, Coclustering of ErbB1 and ErbB2 revealed by FRET-sensitized acceptor bleaching. Biophysical journal, 2010. 99(1): p. 105-114.
223. Yeow, E.K. and A.H. Clayton, Enumeration of oligomerization states of membrane proteins in living cells by homo-FRET spectroscopy and microscopy: theory and application. Biophysical journal, 2007. 92(9): p. 3098-3104.
224. Blackman, S.M., D.W. Piston, and A.H. Beth, Oligomeric state of human erythrocyte band 3 measured by fluorescence resonance energy homotransfer. Biophysical journal, 1998. 75(2): p. 1117-1130.
225. Warren, S.C., et al., Homo-FRET based biosensors and their application to multiplexed imaging of signalling events in live cells. International Journal of Molecular Sciences, 2015. 16(7): p. 14695-14716.

226. Shi, X., et al., Anomalous negative fluorescence anisotropy in yellow fluorescent protein (YFP 10C): quantitative analysis of FRET in YFP dimers. Biochemistry, 2007. 46(50): p. 14403-14417.
227. Jameson, D.M. and G. Mocz, Fluorescence polarization/anisotropy approaches to study protein-ligand interactions, in Protein-Ligand Interactions. 2005, Springer. p. 301-322.
228. Tramier, M. and M. Coppey-Moisan, Fluorescence anisotropy imaging microscopy for homo-FRET in living cells. Methods in cell biology, 2008. 85: p. 395-414.
229. Piston, D.W. and M.A. Rizzo, FRET by fluorescence polarization microscopy. Methods in cell biology, 2008. 85: p. 415-430.
230. Borst, J.W., et al., Effects of refractive index and viscosity on fluorescence and anisotropy decays of enhanced cyan and yellow fluorescent proteins. Journal of fluorescence, 2005. 15(2): p. 153-160.
231. DiPilato, L.M. and J. Zhang, The role of membrane microdomains in shaping β2-adrenergic receptor-mediated cAMP dynamics. Molecular Biosystems, 2009. 5(8): p. 832-837.
232. Börner, S., et al., FRET measurements of intracellular cAMP concentrations and cAMP analog permeability in intact cells. Nature Protocols, 2011. 6(4): p. 427-438.
233. Nikolaev, V.O. and M.J. Lohse, Monitoring of cAMP synthesis and degradation in living cells. Physiology, 2006. 21(2): p. 86-92.
234. Mazina, O., et al., Determination of biological activity of gonadotropins hCG and FSH by Förster resonance energy transfer based biosensors. Scientific reports, 2017. 7: p. 42219.
235. Klarenbeek, J.B., et al., A mTurquoise-based cAMP sensor for both FLIM and ratiometric read-out has improved dynamic range. PloS one, 2011. 6(4): p. e19170.
236. Gorshkov, K. and J. Zhang, Visualization of cyclic nucleotide dynamics in neurons. 2014.
237. DiPilato, L.M., X. Cheng, and J. Zhang, Fluorescent indicators of cAMP and Epac activation reveal differential dynamics of cAMP signaling within discrete subcellular compartments. Proceedings of the National Academy of Sciences of the United States of America, 2004. 101(47): p. 16513-16518.
238. Ponsioen, B., et al., Detecting cAMP-induced Epac activation by fluorescence resonance energy transfer: Epac as a novel cAMP indicator. EMBO reports, 2004. 5(12): p. 1176-1180.
239. Mazina, O., et al., cAMP assay for GPCR ligand characterization: application of BacMam expression system, in G Protein-Coupled Receptor Screening Assays. 2015, Springer. p. 65-77.
240. Hadhoud, G.E., Evaluating Luteinizing Hormone Receptor Signaling Using the Cyclic AMP Reporter ICUE3. 2018, Colorado State University.
241. Zhang, D., Rotational motion and organization studies of cell membrane proteins. 2016, Colorado State University.
242. Jiang, L.I., et al., Use of a cAMP BRET sensor to characterize a novel regulation of cAMP by the sphingosine 1-phosphate/G13 pathway. Journal of Biological Chemistry, 2007. 282(14): p. 10576-10584.
243. Ghigo, A. and D. Mika, cAMP/PKA signaling compartmentalization in cardiomyocytes: Lessons from FRET-based biosensors. Journal of Molecular and Cellular Cardiology, 2019.
244. Patterson, G.H., D.W. Piston, and B.G. Barisas, Förster distances between green fluorescent protein pairs. Analytical biochemistry, 2000. 284(2): p. 438-440.

245. FPbase. Fluorescent protein properties 2019; Available from: https://www.fpbase.org.
246. Rekas, A., et al., Crystal structure of venus, a yellow fluorescent protein with improved maturation and reduced environmental sensitivity. Journal of biological chemistry, 2002. 277(52): p. 50573-50578.
247. Shaner, N.C., P.A. Steinbach, and R.Y. Tsien, A guide to choosing fluorescent proteins. Nature methods, 2005. 2(12): p. 905.
248. Goedhart, J., et al., Bright cyan fluorescent protein variants identified by fluorescence lifetime screening. Nature methods, 2010. 7(2): p. 137.
249. Karges, B., et al., Zero-length cross-linking reveals that tight interactions between the extracellular and transmembrane domains of the luteinizing hormone receptor persist during receptor activation. Molecular Endocrinology, 2005. 19(8): p. 2086-2098.
250. Minegishi, T., et al., Regulation of human luteinizing hormone receptor in the ovary. Reproductive medicine and biology, 2008. 7(1): p. 11-16.
251. Chambers, A.E., et al., Circulating LH/hCG receptor (LHCGR) may identify pre-treatment IVF patients at risk of OHSS and poor implantation. Reproductive Biology and Endocrinology, 2011. 9(1): p. 161.
252. Sorbi, F., et al., Luteinizing Hormone/Human Chorionic Gonadotropin Receptor Immunohistochemical Score Associated with Poor Prognosis in Endometrial Cancer Patients. BioMed research international, 2018. 2018.
253. Movsas, T.Z., et al., Confirmation of luteinizing hormone (LH) in living human vitreous and the effect of LH receptor reduction on murine electroretinogram. Neuroscience, 2018. 385: p. 1-10.
254. Movsas, T.Z., R. Sigler, and A. Muthusamy, Elimination of signaling by the luteinizing hormone receptor reduces ocular VEGF and retinal vascularization during mouse eye development. Current eye research, 2018. 43(10): p. 1286-1289.
255. Urizar, E., et al., Glycoprotein hormone receptors: link between receptor homodimerization and negative cooperativity. The EMBO Journal, 2005. 24(11): p. 1954-1964.
256. Zhang, D., et al., Fluorescence Observation of Single-Cell cAMP Signaling by G Protein-Coupled Receptors. Journal of fluorescence, 2019. 29(1): p. 53-60.
257. Piston, D.W. and G.-J. Kremers, Fluorescent protein FRET: the good, the bad and the ugly. Trends in biochemical sciences, 2007. 32(9): p. 407-414.
258. Ganguly, S., R. Saxena, and A. Chattopadhyay, Reorganization of the actin cytoskeleton upon G-protein coupled receptor signaling. Biochimica et Biophysica Acta (BBA)-Biomembranes, 2011. 1808(7): p. 1921-1929.
259. Jacobson, K.A., New paradigms in GPCR drug discovery. Biochemical pharmacology, 2015. 98(4): p. 541-555.
260. Chandra, A.K., et al., Protection against vanadium-induced testicular toxicity by testosterone propionate in rats. Toxicology mechanisms and methods, 2010. 20(6): p. 306-315.
261. Winter, P.W., et al., The anti-diabetic bis (maltolato) oxovanadium (IV) decreases lipid order while increasing insulin receptor localization in membrane microdomains. Dalton Transactions, 2012. 41(21): p. 6419-6430.
262. Jin, L., et al., Characterization and application of a new optical probe for membrane lipid domains. Biophysical journal, 2006. 90(7): p. 2563-2575.

263. Demchenko, A.P., et al., Monitoring biophysical properties of lipid membranes by environment-sensitive fluorescent probes. Biophysical journal, 2009. 96(9): p. 3461-3470.
264. Dinic, J., et al., Laurdan and di-4-ANEPPDHQ do not respond to membrane-inserted peptides and are good probes for lipid packing. Biochimica et Biophysica Acta (BBA)-Biomembranes, 2011. 1808(1): p. 298-306.
265. Samama, P., et al., A mutation-induced activated state of the beta 2-adrenergic receptor. Extending the ternary complex model. Journal of Biological Chemistry, 1993. 268(7): p. 4625-4636.
266. Fitz, T., et al., Characterization of two steroidogenic cell types in the ovine corpus luteum. Biology of Reproduction, 1982. 27(3): p. 703-711.
267. Batrinos, M.L., Testosterone and aggressive behavior in man. International journal of endocrinology and metabolism, 2012. 10(3): p. 563.
268. Derkach, K., et al., In vitro and in vivo studies of functional activity of new low molecular weight agonists of the luteinizing hormone receptor. Biochemistry (Moscow) Supplement Series A: Membrane and Cell Biology, 2016. 10(4): p. 294-300.
269. Maia, V.N., et al., Expression of angiogenic factors and luteinizing hormone receptors in the corpus luteum of mares induced to ovulate with deslorelin acetate. Theriogenology, 2016. 85(3): p. 461-465.
270. Schally, A.V., Luteinizing hormone-releasing hormone analogs: their impact on the control of tumorigenesis☆. Peptides, 1999. 20(10): p. 1247-1262.
271. Schally, A.V., et al., Hypothalamic hormones and cancer. Frontiers in neuroendocrinology, 2001. 22(4): p. 248-291.
272. Emons, G., et al., High affinity binding and direct antiproliferative effects of LHRH analogues in human ovarian cancer cell lines. Cancer Research, 1993. 53(22): p. 5439-5446.
273. Nicholson, R. and K. Walker, Use of LH-RH agonists in the treatment of breast disease. Proceedings of the Royal Society of Edinburgh, Section B: Biological Sciences, 1989. 95: p. 271-281.
274. Schally, A.V. and A.M. Comaru-Schally, Rational use of agonists and antagonists of luteinizing hormone-releasing hormone (LH-RH) in the treatment of hormone-sensitive neoplasms and gynaecologic conditions. Advanced drug delivery reviews, 1997. 28(1): p. 157-169.
275. Beer, T.M., et al., Phase II study of abarelix depot for androgen independent prostate cancer progression during gonadotropin-releasing hormone agonist therapy. The Journal of urology, 2003. 169(5): p. 1738-1741.
276. Group, A.S., et al., A phase 3, multicenter, open label, randomized study of abarelix versus leuprolide plus daily antiandrogen in men with prostate cancer. The Journal of urology, 2002. 167(4): p. 1670-1674.
277. Sarma, P., et al., Peptidomimetic GnRH receptor antagonists for the treatment of reproductive and proliferative diseases. Expert Opinion on Therapeutic Patents, 2006. 16(6): p. 733-751.
278. Althumairy, D., et al., Effects of vanadium(iv) compounds on plasma membrane lipids leads to G protein-coupled receptor signal transduction. Journal of Inorganic Biochemistry, in press.

279. Menon, K., B. Menon, and T. Gulappa, Regulation of Luteinizing Hormone Receptor mRNA Expression in the Ovary: The Role of miR-122, in Vitamins and hormones. 2018, Elsevier. p. 67-87.
280. Kitahara, Y., et al., Role of microRNA-136-3p on the expression of luteinizing hormone-human chorionic gonadotropin receptor mRNA in rat ovaries. Biology of reproduction, 2013. 89(5): p. 114, 1-10.
281. Troppmann, B., et al., MicroRNA miR-513a-3p acts as a co-regulator of luteinizing hormone/chorionic gonadotropin receptor gene expression in human granulosa cells. Molecular and cellular endocrinology, 2014. 390(1-2): p. 65-72.

APPENDIX: DATA ANALYSIS FOR CALCULATING RECEPTOR NUMBER PER CELL

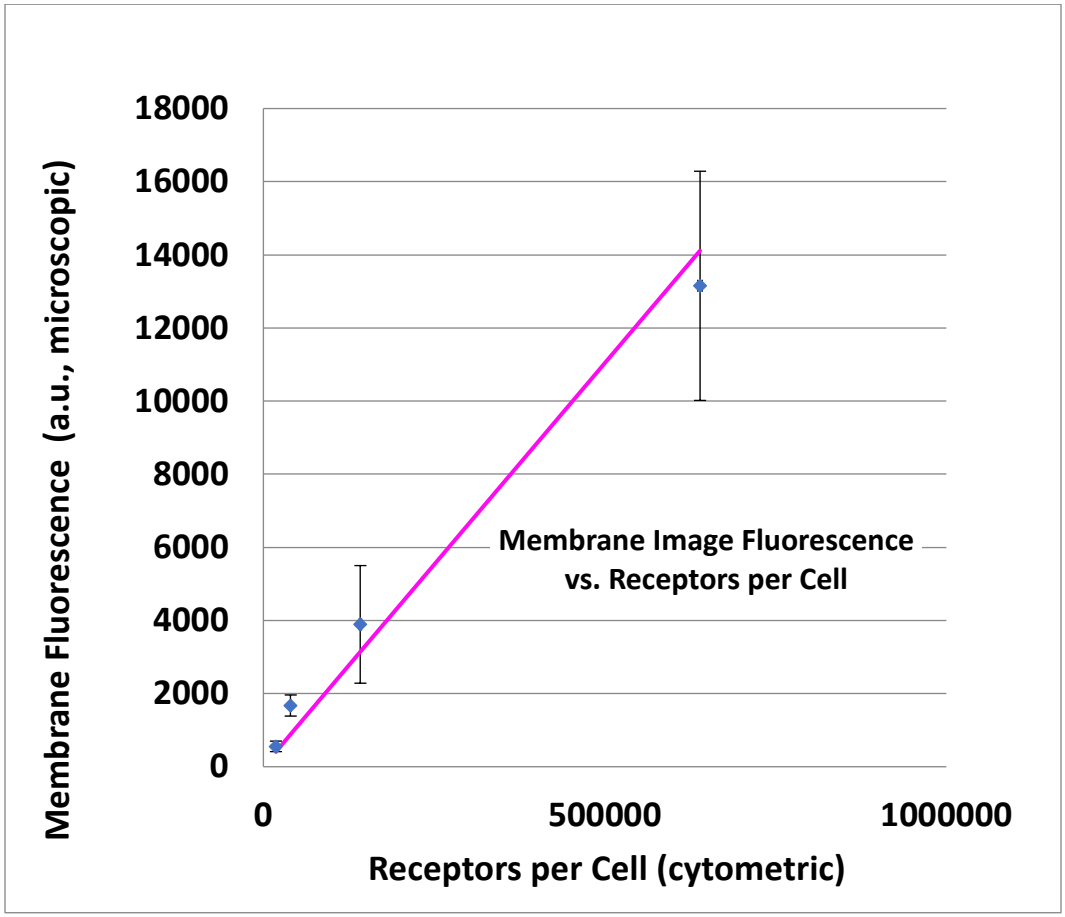

Figure A1: Calibration curve for conversion the receptors number per cell in flow cytometry to numbers of receptor per cell in fluorescence microscope.

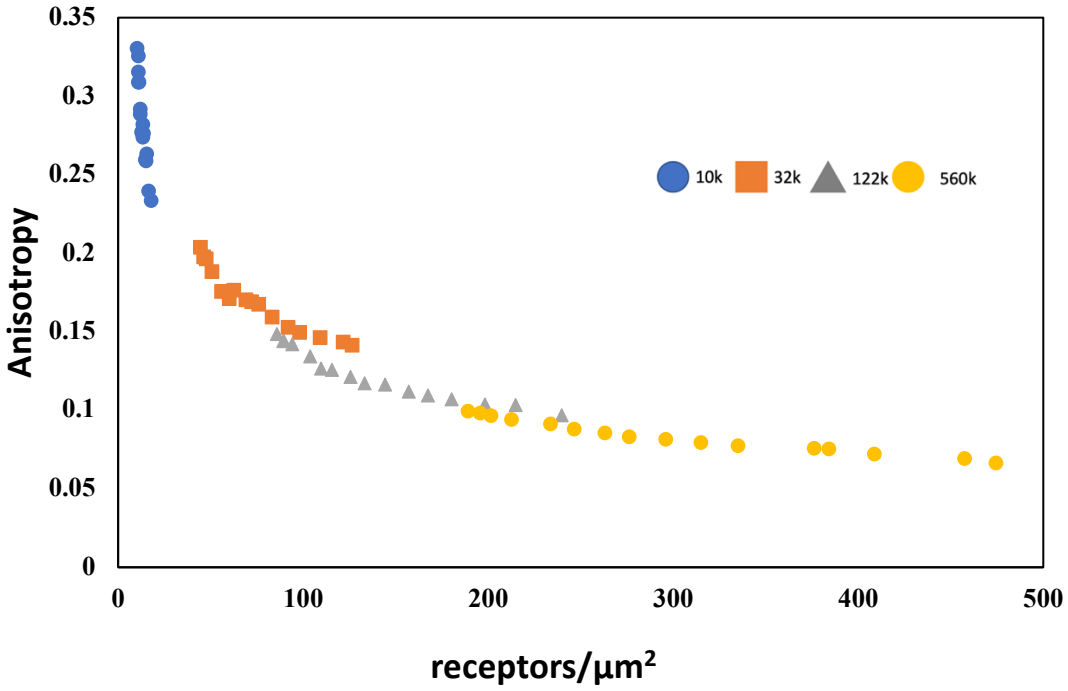

Figure A2: The correlation between anisotropy and receptors number per μm^2 during photobleaching in untreated cells. Symbols indicate average data for cells representing the four expression groups. This figure indicates that the oligomerization state of LHR is highly dependent on the receptors number of LHR per cell. Data are presented in each point as the mean ± SEM for n=10 measurements; The four cell lines were significantly different in one-way ANOVA and Tukey's multiple comparisons tests ($p < 0.05$)

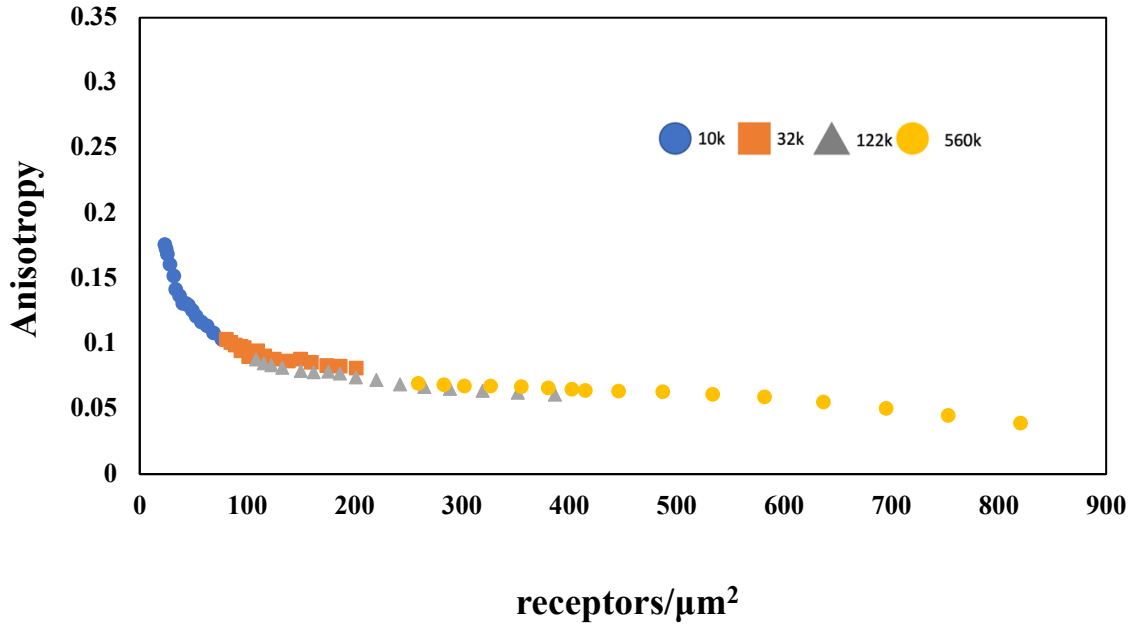

Figure A3: The correlation between anisotropy and receptors number per μm^2 during photobleaching in cells treated with hCG. Symbols indicate average data for cells representing the four expression groups. This figure indicates that the oligomerization state of LHR is highly dependent on the receptors number of LHR per cell. Data are presented in each point as the mean ± SEM for n=10 measurements; The four cell lines were significantly different in one-way ANOVA and Tukey's multiple comparisons tests ($p < 0.05$)

LIST OF ABBREVIATIONS

GPCR	G protein-coupled receptors
LHR	Luteinizing hormone receptors
LH	Luteinizing hormone
hCG	Human chorionic gonadotropin
DG-hCG	Deglycosylated human chorionic gonadotropin
T2R	Taste receptors
7TM	Seven hydrophobic transmembrane
GTP	Guanosine triphosphate
GDP	Guanosine diphosphate
AC	Adenylyl cyclase
α	Alpha
γ	Gamma
β	Beta
ATP	Adenosine triphosphate
cAMP	Cyclic adenosine monophosphate
PDE	Phosphodiesterase
cGMP	Cyclic guanosine monophosphate
GMP	Guanosine monophosphate
PLC	Phospholipase C
PIP_2	Phosphatidylinositol 4,5-bisphosphate
DAG	Diacylglycerol
PKC	Protein kinase C
IP_3	Inositol triphosphate
Ca^{+2}	Calcium ion
K^+	Potassium
CL	Corpus luteum
FSH	Follicle stimulating hormone
GnRH	Gonadotropin releasing hormone

RPKM	Reads Per Kilobase Million
LCH	Leydig cell hypoplasia
FMPP	Familial male-limited precocious puberty
AD	Alzheimer disease
Aβ	B-amyloid peptide
GPHRs	Glycoprotein hormone receptors
ECD	Extracellular domain
LRRs	Leucine rich repeats
ECLs	Three extracellular loops
ICLs	Intracellular loops
ICD	Intracellular domain
hLH	Humane luteinizing hormone
Da	Dalton
PKB	Protein kinase B
ERK	Extracellular signal-regulated kinases
HF	Hydrogen fluoride
TFMS	Trifluoromethanesulfonic acid
LHR^{cAMP-}	Luteinizing hormone receptor unable to signal
LHR^{LH-}	Luteinizing hormone receptor unable to bind hormone
PKA	Protein kinase A
EPAC	Exchange protein directly activated by camp
CREB	Camp-response element-binding protein
P38 MAPK	P38 mitogen-activated protein kinases
STAR	Steroidogenic acute regulatory
P450scc	P450 cholesterol side chain cleavage enzyme
mTORC1	Rapamycin complex 1
PKB	Protein kinase B
EGFRs	Epidermal growth factor receptors
IGF-I	Insulin-like growth factor 1 receptors
ERK1/2	Extracellular signal-regulated kinases 1 and 2
SFKs	Src family of kinases

ARNO	Arf nucleotide binding site opener
ARF6	ADP ribosylation factor 6
MβCD	Methyl-β-cyclodextrin
GPI	Glycosyl phosphatidyl inositol
FCCS	Fluorescence cross-correlation spectroscopy
homo-FRET	Homo-transfer fluorescence resonance energy transfer
hetero-FRET	Hetero-transfer fluorescence resonance energy transfer
BRET	Bioluminescence resonance energy transfer
PD-PALM	Dual-color photoactivatable dyes and localization microscopy
FPR	Fluorescence photobleaching recovery
BiFC	Bimolecular fluorescence complementation
Å	Angstroms
R_0	Förster distance
E	Efficiency of FRET
HSV-1	Herpes simplex virus
TK	Thymidine kinase
I	Intensity
v	Vertical
h	Horizontal
G	G factor
RG6	Rhodamine 6G
eYFP	Enhanced yellow fluorescent protein
θ	Rotation correlation
τ_D	Fluorescence lifetime
RIA	Radioimmunoassay
ECLIA	Electrochemiluminescence immunoassays
ELISA	Enzyme-linked immunosorbent assays
HTRF	Homogeneous time-resolved fluorescence
CAMYEL	Camp sensor using YFP-Epac-rluc
ICUE	Indicator of camp Using Epac
eCFP	Enhanced cyan fluorescence protein

cpV-L194	Circularly permuted Venus at lysine 194 of eyfp
IVF	*In vitro* fertilization
IVM	*In vitro* maturation
CHO	Chinese hamster ovary
DMEM	Dulbecco's Modified Eagle medium
G418	Genticin
FBS	Fetal bovine serum
P/S	Penicillin/streptomycin
EDTA	Ethylenediaminetetraacetic acid
GFP	Green fluorescence protein
PVDF	Polyvinylidene fluoride or polyvinylidene difluoride
TBST	Tris Buffered Saline with Tween
PBS	Phosphate-buffered saline
MDL-12,330a hydrochloride	*Cis*-N-(2-Phenylcyclopentyl)-azacyclotridec-1-en-2-amine Hydrochloride
FITC	Fluorescein isothiocyanate
MESF	Molecules of equivalent soluble fluorophores
r_0	Fundamental anisotropy
YFPSE	YFP sensitized emission
SEM	Standard error of the mean
LuRK0	Transgenic mouse knockout of endogenous LHR